



RESEARCH ARTICLE

Tropical Fock–Goncharov coordinates for SL_3 -webs on surfaces I: construction

Daniel C. Douglas¹ and Zhe Sun²

¹Department of Mathematics, Virginia Tech, 225 Stanger Street, Blacksburg, VA 24061, USA; E-mail: dcdouglas@vt.edu.

²Key Laboratory of Wu Wen-Tsun Mathematics, Chinese Academy of Sciences; School of Mathematical Sciences, University of Science and Technology of China, 96 Jinzhai Road, 230026 Hefei, Anhui, China; E-mail: sunz@ustc.edu.cn.

Received: 23 April 2023; Revised: 11 October 2023; Accepted: 9 November 2023

Abstract

For a finite-type surface \mathfrak{S} , we study a preferred basis for the commutative algebra $\mathbb{C}[\mathcal{R}_{SL_3(\mathbb{C})}(\mathfrak{S})]$ of regular functions on the $SL_3(\mathbb{C})$ -character variety, introduced by Sikora–Westbury. These basis elements come from the trace functions associated to certain trivalent graphs embedded in the surface \mathfrak{S} . We show that this basis can be naturally indexed by nonnegative integer coordinates, defined by Knutson–Tao rhombus inequalities and modulo 3 congruence conditions. These coordinates are related, by the geometric theory of Fock and Goncharov, to the tropical points at infinity of the dual version of the character variety.

Contents

1	Introduction	2
2	Global webs	4
2.1	Topological setting	4
2.2	Webs	5
2.3	Faces	6
2.4	Nonelliptic webs	6
3	Local webs	7
3.1	Ideal polygons	7
3.2	Local webs	7
3.3	External faces	7
3.4	Combinatorial identity	8
3.5	Nonellipticity	8
3.6	Essential and rungless local webs	9
3.7	Ladder-webs in ideal biangles	10
3.8	Honeycomb-webs in ideal triangles	13
4	Good position of a global web	15
4.1	Generic isotopies	15
4.2	Minimal position	15
4.3	Split ideal triangulations	16
4.4	Good position	17
5	Global coordinates for nonelliptic webs	19
5.1	Dotted ideal triangulations	19

5.2	Local coordinate functions	19
5.3	Local coordinates from Fock–Goncharov theory	21
5.4	Global coordinates from local coordinate functions	21
6	Knutson–Tao cone	23
6.1	Integer cones	24
6.2	Local Knutson–Tao cone	24
6.3	Global Knutson–Tao cone	29
7	Main result: global coordinates	30
7.1	Inverse mapping	30
7.2	Inverse mapping: ladder gluing construction	30
7.3	Inverse mapping: resolving an elliptic web	32
7.4	Inverse mapping: definition	33
8	Proof of the main lemma	34
8.1	Preparation: web pictures on the surface	34
8.2	Preparation: sequences	35
8.3	Preparation: edge-sequences and the fellow traveler lemma	36
8.4	Preparation: shared-routes	37
8.5	Preparation: oriented shared-routes	40
8.6	Proof of the main lemma: intersection points	41
8.7	Proof of the main lemma: finishing the argument	42
8.8	Proof of the main lemma: proof of Lemma 8.14	43
9	Webs on surfaces-with-boundary	47
9.1	Essential webs	47
9.1.1	Surfaces-with-boundary	47
9.1.2	Essential webs	47
9.2	Rungless essential webs; first version of the boundary result	48
9.2.1	Rungless essential webs	48
9.2.2	Knutson–Tao cone associated to an ideal triangulation	48
9.2.3	Coordinates for rungless essential webs	48
9.3	Application: geometry and topology of $SL_3(\mathbb{C})$ -character varieties	49
9.4	Boundary-fixed essential webs; second version of the boundary result	50
9.4.1	Boundary-fixed essential webs	50
9.4.2	Boundary-fixed Knutson–Tao cone	52
9.4.3	Coordinates for boundary-fixed essential webs	52
9.5	Application: representation theory of the Lie group $SL_3(\mathbb{C})$	53

1. Introduction

For a finitely generated group Γ and a suitable Lie group G , a primary object of study in low-dimensional geometry and topology is the character variety

$$\mathcal{R}_G(\Gamma) = \{\rho : \Gamma \longrightarrow G\} // G$$

consisting of group homomorphisms ρ from Γ to G , considered up to conjugation. Here, the quotient is taken in the algebraic geometric sense of geometric invariant theory [MFK94]. Character varieties can be explored using a wide variety of mathematical skill sets. Some examples include the Higgs bundle approach of Hitchin [Hit92], the dynamics approach of Labourie [Lab06] and the representation theory approach of Fock–Goncharov [FG06].

We are interested in the case where the group G is the special linear group $SL_n(\mathbb{C})$. Adopting the viewpoint of algebraic geometry, one can study the $SL_n(\mathbb{C})$ -character variety $\mathcal{R}_{SL_n(\mathbb{C})}(\Gamma)$ by means of its commutative algebra of regular functions $\mathbb{C}[\mathcal{R}_{SL_n(\mathbb{C})}(\Gamma)]$. An example of a regular function is the

trace function $\text{Tr}_\gamma : \mathcal{R}_{\text{SL}_n(\mathbb{C})}(\Gamma) \rightarrow \mathbb{C}$ associated to an element $\gamma \in \Gamma$, sending a representation ρ to the trace $\text{Tr}(\rho(\gamma)) \in \mathbb{C}$ of the matrix $\rho(\gamma) \in \text{SL}_n(\mathbb{C})$. A theorem of Procesi [Pro76] implies that the trace functions Tr_γ generate the algebra of functions $\mathbb{C}[\mathcal{R}_{\text{SL}_n(\mathbb{C})}(\Gamma)]$ as an algebra and also identifies all of the relations.

Sikora [Sik01] provided a more refined description of Procesi's result in the case where $\Gamma = \pi_1(\mathfrak{X})$ is the fundamental group of a topological space \mathfrak{X} ; see also the earlier work of Bullock [Bul97] for the case $G = \text{SL}_2(\mathbb{C})$. Sikora extended the notion of a trace function to include functions $\text{Tr}_W \in \mathbb{C}[\mathcal{R}_{\text{SL}_n(\mathbb{C})}(\mathfrak{X})]$ on the character variety $\mathcal{R}_{\text{SL}_n(\mathbb{C})}(\mathfrak{X}) := \mathcal{R}_{\text{SL}_n(\mathbb{C})}(\pi_1(\mathfrak{X}))$ that are associated to homotopy classes of certain (ciliated) oriented n -valent graphs W , called webs, in the space \mathfrak{X} . The trace functions Tr_W span the algebra of functions $\mathbb{C}[\mathcal{R}_{\text{SL}_n(\mathbb{C})}(\mathfrak{X})]$ as a vector space, and the relations are described pictorially in terms of the associated graphs.

In this article, we restrict attention to the case where the Lie group is $\text{SL}_3(\mathbb{C})$ and the space $\mathfrak{X} = \mathfrak{S}$ is a punctured finite-type surface. Sikora–Westbury [SW07] proved that the collection of trace functions Tr_W associated to nonelliptic webs W , which are certain webs embedded in the surface \mathfrak{S} , forms a linear basis for the algebra of functions $\mathbb{C}[\mathcal{R}_{\text{SL}_3(\mathbb{C})}(\mathfrak{S})]$.

An analogous result [HP93] in the case of $\text{SL}_2(\mathbb{C})$ says that the collection of trace functions Tr_γ associated to essential multicurves γ embedded in the surface \mathfrak{S} forms a linear basis for the algebra of functions $\mathbb{C}[\mathcal{R}_{\text{SL}_2(\mathbb{C})}(\mathfrak{S})]$. A well-known topological-combinatorial fact says that if the punctured surface \mathfrak{S} is equipped with an ideal triangulation λ , then the geometric intersection numbers $\iota(\gamma, E)$ of a curve γ with the edges E of λ furnish an explicit system of nonnegative integer coordinates on the collection of essential multicurves γ . These coordinates can be characterized by finitely many triangle inequalities and parity conditions.

The present work is part of a series of two papers, whose goal is to generalize these SL_2 -properties to the case $n = 3$. The main result of the current paper is the following.

Theorem 1.1. *For a punctured finite-type surface \mathfrak{S} equipped with an ideal triangulation λ , the Sikora–Westbury SL_3 -web basis for the algebra of functions $\mathbb{C}[\mathcal{R}_{\text{SL}_3(\mathbb{C})}(\mathfrak{S})]$ admits an explicit system of nonnegative integer coordinates, which can be characterized by finitely many Knutson–Tao rhombus inequalities [KT99] and modulo 3 congruence conditions.*

In the companion article [DS20b], we prove that the web coordinates from Theorem 1.1 are natural with respect to the action of the mapping class group of the surface \mathfrak{S} .

Theorem 1.2 [DS20b]. *If another ideal triangulation λ' of \mathfrak{S} is chosen, then the induced coordinate transformation takes the form of a tropicalized \mathcal{A} -coordinate cluster transformation (as opposed to \mathcal{X} -coordinate) in the language of Fock–Goncharov [FG06, FZ02].*

Strictly speaking, Theorems 1.1 and 1.2 have been stated assuming that the punctured surface \mathfrak{S} has empty boundary. In §9, we give two different, but related, generalizations (Theorems 9.1 and 9.8) of Theorem 1.1 valid in the boundary setting, $\partial\mathfrak{S} \neq \emptyset$; see also [Kim20]. There, we also provide applications to the geometry and topology of $\text{SL}_3(\mathbb{C})$ -character varieties, as well as to the representation theory of the Lie group $\text{SL}_3(\mathbb{C})$. In the companion article [DS20b], we likewise provide a version of Theorem 1.2 valid in the boundary setting.

This work drew much inspiration from papers of Xie [Xie13], Kuperberg [Kup96] and Goncharov–Shen [GS15].

At its heart, Theorem 1.1 simply describes how to assign tuples of numbers to pictures. We have motivated these web pictures W by their association with trace functions Tr_W . As such, it is desirable to tie directly the coordinates to the trace functions. Such a relationship is well known for $\text{SL}_2(\mathbb{C})$; see [FG07a], for instance. In that case, the trace functions Tr_γ for curves γ can be expressed as Laurent polynomials $\text{Tr}_\gamma = \text{Tr}_\gamma(X_i)$ in variables X_i where there is one variable per coordinate (that is, per edge E_i of λ). Moreover, the coordinates of a curve γ can be read off as the exponents of the highest term of the trace polynomial $\text{Tr}_\gamma(X_i)$, demonstrating the tropical geometric nature of these coordinates.

There is a similar story for $\mathrm{SL}_3(\mathbb{C})$ and conjecturally for $\mathrm{SL}_n(\mathbb{C})$. The Fock–Goncharov theory tells us how to express the trace functions Tr_W for webs W as Laurent polynomials $\mathrm{Tr}_W(X_i)$. Here, the number of variables X_i (called Fock–Goncharov coordinates) increases with n . In the case $n = 3$, Kim [Kim20], building on [Dou20], showed that the tropical coordinates of Theorem 1.1 appear as the exponents of the highest term of the Fock–Goncharov trace polynomial $\mathrm{Tr}_W(X_i)$. This idea was Xie’s [Xie13] point of departure, and these coordinates were constructed following his lead.

Kuperberg’s landmark paper [Kup96] influenced [SW07] and laid the topological foundation for the present work as well. He proved that a certain collection of web pictures drawn on an ideal polygon \mathfrak{D}_k indexes a linear basis for the subspace of $\mathrm{SL}_3(\mathbb{C})$ -invariant tensors in a k -fold tensor product of finite-dimensional irreducible representations of $\mathrm{SL}_3(\mathbb{C})$. Along the way, he showed how the pictures for the ideal polygon \mathfrak{D}_k can be obtained by gluing together the more basic pictures for an ideal triangle \mathfrak{D}_3 . We apply Kuperberg’s local pictorial ideas in order to analyze global web pictures drawn on a triangulated surface (\mathfrak{S}, λ) .

Motivated by the Fock–Goncharov duality conjecture [FG06] (see also [GHKK18, GS18]), Goncharov–Shen [GS15] developed a theory by which bases of algebras of functions on moduli spaces, defined abstractly via the geometric Satake correspondence, can be indexed by positive integral tropical points, namely the preimage points mapping to $\mathbb{Z}_{>0}$ under a tropicalized potential function. They showed that, for an ideal triangle \mathfrak{D}_3 equipped with a general linear symmetry group, the positive integral tropical points correspond to solutions of the Knutson–Tao rhombus inequalities. In the SL_3 -setting of this article, Theorem 1.1 also makes use of these inequalities in order to assign positive integer coordinates to webs. We think of this result as a manifestation of Goncharov–Shen’s ideas about duality; see [DS20b] for a further discussion. (For another geometric application of the Goncharov–Shen potential function, see [HS23].)

Frohman–Sikora [FS22] independently constructed coordinates for the same SL_3 -web basis as that appearing in Theorem 1.1. While their topological strategy is the same, their coordinates are different from ours. They do not characterize by inequalities the values taken by their coordinates, and they do not address the question of naturality under changing the triangulation. Their proof is algebraic, as it uses the Sikora–Westbury theorem (discussed above) saying that the nonelliptic webs are linearly independent, which ultimately relies on the diamond lemma from noncommutative algebra. On the other hand, we give a purely topological-combinatorial proof of Theorem 1.1, which does not require using this linear independence. Moreover, we give an alternative geometric proof of this Sikora–Westbury theorem, by using Theorem 1.1 together with the SL_3 -quantum trace map [Dou20, Kim20]. (Ishibashi–Kano [IK22] mimicked the construction and proof strategy of Theorem 1.1 to define shearing coordinates for unbounded SL_3 -laminations.)

As another application, Kim [Kim20, Kim21] used Theorems 1.1 and 1.2 to study a classical and quantum SL_3 -version of Fock–Goncharov duality, generalizing the SL_2 -case [FG06, AK17].

For the underlying SL_3 -geometry, see [FG07b, CTT20].

We are also interested in comparing our methods to other approaches to studying webs and related objects, falling under the umbrella of so-called ‘higher laminations’. In addition to webs [Sik05, Fon12, CKM14], this includes cluster algebras [FP16, IY23], buildings [FKK13, Le16, Mar19] and spectral networks [GMN13, NY22].

2. Global webs

We introduce the primary topological objects of study.

2.1. Topological setting

Let \mathfrak{S} be an oriented *punctured surface* of finite topological type, namely \mathfrak{S} is diffeomorphic to the space obtained by removing a finite subset P , called the set of *punctures*, from a closed oriented surface \mathfrak{S} . In particular, note that \mathfrak{S} has empty boundary, $\partial\mathfrak{S} = \emptyset$. We require that there is at least one puncture

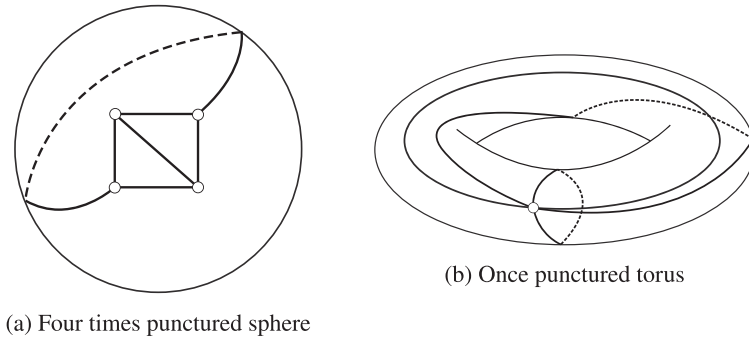


Figure 1. Ideal triangulations.

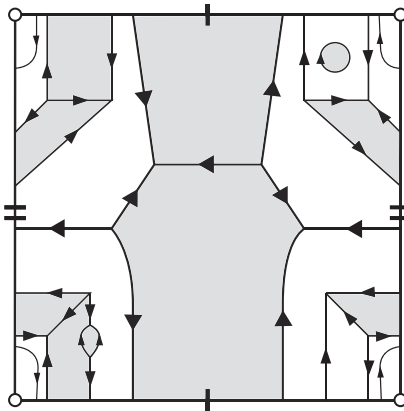


Figure 2. Web.

and that the Euler characteristic $\chi(\mathfrak{S})$ of the punctured surface \mathfrak{S} is strictly less than zero, $\chi(\mathfrak{S}) < 0$. These topological conditions guarantee the existence of an *ideal triangulation* λ of the punctured surface \mathfrak{S} , namely a triangulation $\bar{\lambda}$ of the closed surface $\bar{\mathfrak{S}}$ whose vertex set is equal to the set of punctures P . See Figure 1 for some examples of ideal triangulations.

To simplify the exposition, we always assume that λ does not contain any *self-folded triangles*, meaning that each triangle \mathfrak{T} of λ has three distinct edges. Such a λ always exists. Our results should generalize, essentially without change, to allow for self-folded triangles.

2.2. Webs

Definition 2.1. An *immersed curve*, or just *curve*, γ in any surface (possibly with boundary) $\widehat{\mathfrak{S}}$ is an immersion into $\widehat{\mathfrak{S}}$ of the circle S^1 or the compact interval I . In other words, a curve is either an oriented *loop* (that is, a closed curve) or an oriented *arc*, possibly with self-intersections.

We will often be working with *embedded curves*, where there are no self-intersections.

Definition 2.2. An *embedded global web*, or just *global web* or *web*, $W = \{w_i\}_i$ on the surface \mathfrak{S} is a finite collection of closed connected oriented trivalent (finite) graphs or closed curves w_i embedded in \mathfrak{S} such that the (images of the) components w_i are mutually disjoint and such that each vertex of w_i is either a *source* or a *sink*, namely the orientations either go all in or all out, respectively. Note that the web W has empty boundary, $\partial W = \emptyset$.

For an example, in Figure 2 we show a web on the once punctured torus, which has four components consisting of two trivalent graphs and two curves.

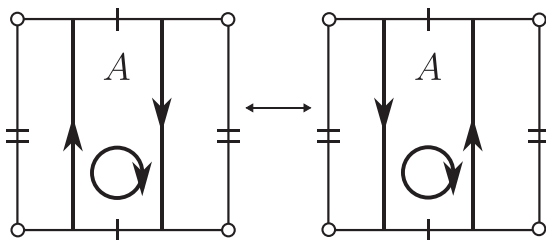


Figure 3. Global parallel-move.

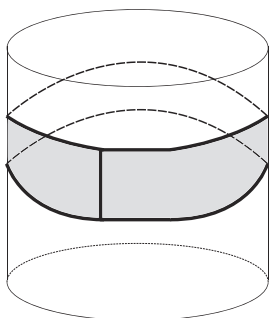


Figure 4. Prohibited square-face.

Definition 2.3. Two webs W and W' on the surface \mathfrak{S} are *parallel equivalent* if W can be taken to W' , preserving orientation, by a sequence of moves of the following two types:

1. an *isotopy* of the web, namely a smoothly varying family of webs;
2. a *global parallel-move*, exchanging two loops that together form the boundary of an embedded annulus A in the surface \mathfrak{S} ; see Figure 3.

In this case, we say that W and W' belong to the same *parallel equivalence class* $[W] = [W']$.

Intuitively, we think of parallel equivalent as meaning homotopic on the surface.

2.3. Faces

Definition 2.4. A *face* D of a web W on the surface \mathfrak{S} is a contractible component of the complement $W^c \subseteq \mathfrak{S}$ of the web. A n -*face* D_n is a face with n sides, counted with multiplicity. An alternative name for a zero-face D_0 , two-face D_2 , four-face D_4 and six-face D_6 is a *disk-, bigon-, square- and hexagon-face*, respectively.

For an example, the web shown in Figure 2 above has one disk-face, one bigon-face, two square-faces and two hexagon-faces; these faces are shaded in the figure. Notice that one of the hexagon-faces consists of five edges of the web, one edge being counted twice.

By orientation considerations, faces must have an even number of sides.

Bigon- and square-faces always consist of exactly two and four edges, respectively, of W . See Figure 4. In figures, we often omit the web orientations, as in Figure 5.

2.4. Nonelliptic webs

Definition 2.5. A web W on the surface \mathfrak{S} is called *nonelliptic* if it has no disk-, bigon- or square-faces. Otherwise, W is called *elliptic*.

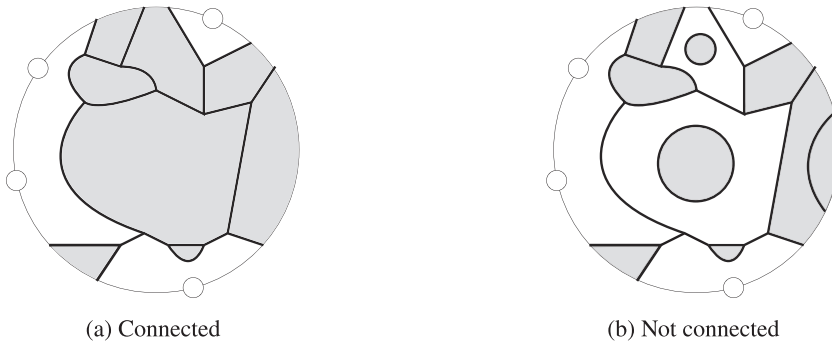


Figure 5. Local webs.

If W is nonelliptic and if W' is parallel equivalent to W , then W' is nonelliptic. Denote the set of nonelliptic webs by $\mathcal{W}_{\mathcal{E}}$, and the set of parallel equivalence classes of nonelliptic webs by $[\mathcal{W}_{\mathcal{E}}]$. The empty web $W = \emptyset$ represents a class with one element in $[\mathcal{W}_{\mathcal{E}}]$.

3. Local webs

As a technical device, we study webs-with-boundary in the disk.

3.1. Ideal polygons

For a nonnegative integer $k \geq 0$, an ideal k -polygon \mathfrak{D}_k is the surface $\mathfrak{D}_0 - P$ obtained by removing k punctures $P \subseteq \partial\mathfrak{D}_0$ from the boundary of the closed disk \mathfrak{D}_0 .

Observe that, when $k > 0$, the boundary $\partial\mathfrak{D}_k$ of the ideal polygon consists of k ideal arcs.

3.2. Local webs

Recall the notion of a curve (Definition 2.1).

Definition 3.1. An embedded local web, or just local web, $W = \{w_i\}_i$ in an ideal polygon \mathfrak{D}_k is a finite collection of connected oriented trivalent graphs or curves w_i embedded in \mathfrak{D}_k such that the components w_i are mutually disjoint and such that each vertex of w_i is either a source or sink. Note that the local web W may have boundary, in which case we require $\partial W = W \cap \partial\mathfrak{D}_k$ and we consider each point $v \in \partial W$ to be a monovalent vertex.

For some examples of local webs, see Figure 5. There, $k = 4$.

3.3. External faces

Definition 3.2. A face D of a local web W in an ideal polygon \mathfrak{D}_k ($k \geq 0$) is a contractible component of the complement $W^c \subseteq \mathfrak{D}_k$ of W that is puncture-free, meaning that D does not limit to any punctures $p \in P$. A n -face D_n is a face with n sides. Here, a maximal segment $\alpha \subseteq (\partial\mathfrak{D}_k) \cap D_n$ of the boundary $\partial\mathfrak{D}_k$ contained in the face D_n is counted as a side, called a boundary side. An external face D^{ext} (resp. internal face D^{int}) of the local web W is a face having at least one (resp. no) boundary side.

In contrast to internal faces, external faces can have an odd number of sides. An alternative name for an external two-face D_2^{ext} , three-face D_3^{ext} , four-face D_4^{ext} with one boundary side and five-face D_5^{ext} with one boundary side is a cap-, fork-, H - and half-hexagon-face, respectively; see Figure 6. Also, as for global webs (see Definition 2.4), an alternative name for an internal zero-face D_0^{int} , two-face D_2^{int} , four-face D_4^{int} and six-face D_6^{int} is a disk-, bigon-, square- and hexagon-face.

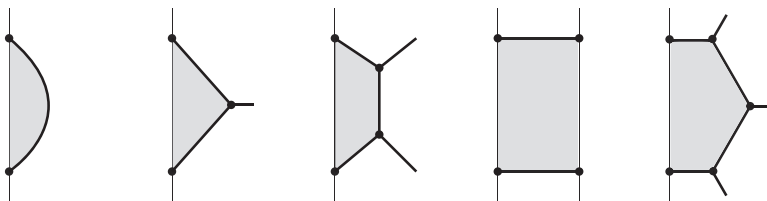


Figure 6. Cap-, fork-, H-, external four-, and half-hexagon-face.

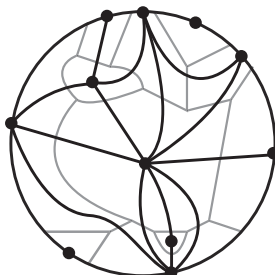


Figure 7. Tiling the closed disk with the dual graph of a local web.

For example, the connected local web in Figure 5a has one fork-face, two H-faces, one half-hexagon-face, one external six-face, one bigon-face, one square-face and one internal eight-face. Also, the disconnected local web in Figure 5b has one cap-face, one fork-face, one H-face, one half-hexagon-face, one external six-face, two disk-faces, one bigon-face and one square-face.

3.4. Combinatorial identity

Proposition 3.3 (compare [Kup96, §6.1]). *Let W be a connected local web in the closed disk \mathfrak{D}_0 with nonempty boundary $\partial W \neq \emptyset$. Then,*

$$2\pi = \sum_{\text{internal faces } D_n^{\text{int}}} \left(2\pi - \frac{\pi}{3}n\right) + \sum_{\text{external faces } D_n^{\text{ext}}} \left(\pi - \frac{\pi}{3}(n-2)\right).$$

Proof. Since W is connected, its complement $W^c \subseteq \mathfrak{D}_0$ contains at most one annulus, which faces the boundary $\partial \mathfrak{D}_0$. Such an annulus does not exist, since $\partial W \neq \emptyset$. Thus, every component D of W^c is contractible, and of course puncture-free, so D is a face.

It follows that the closed disk \mathfrak{D}_0 can be tiled by the dual graph of W . More precisely, the vertices of the dual graph are the faces of W , and the complement of the dual graph consists of triangles. In Figure 7, we demonstrate this tiling procedure for the local web W that we saw in Figure 5a above (after forgetting the punctures).

This triangular tiling gives rise to a flat Riemannian metric with conical singularities and piecewise-geodesic boundary on the closed disk \mathfrak{D}_0 , by requiring that each triangle is Euclidean equilateral. Apply the Gauss–Bonnet theorem to this singular flat surface. □

3.5. Nonellipticity

Definition 3.4. As for global webs, a local web W in an ideal polygon \mathfrak{D}_k is *nonelliptic* if W has no disk-, bigon-, or square-faces. Otherwise, W is called *elliptic*; see Figure 8.

Lemma 3.5. *Let W be a nonelliptic local web in the closed disk \mathfrak{D}_0 such that W is connected, has nonempty boundary $\partial W \neq \emptyset$ and has at least one trivalent vertex. Then W has at least three fork- and/or H-faces.*

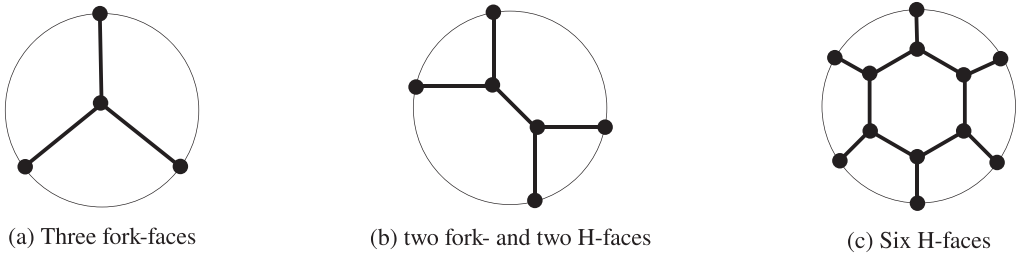


Figure 8. Nonelliptic local webs in the closed disk.

Proof. We apply the formula of Proposition 3.3. For each internal face D_n^{int} of W , the internal angle $2\pi - (\pi/3)n \leq 0$ is nonpositive since $n \geq 6$ by nonellipticity. For each external face D_n^{ext} , necessarily $n \geq 2$, and the external angle $\pi - (\pi/3)(n - 2) \leq 0$ is nonpositive if and only if $n \geq 5$. By hypothesis, W has no cap-faces (else W would be an arc). So, those external faces D_n^{ext} with a positive contribution satisfy $n = 3, 4$. The result follows since fork- and H -faces contribute $2\pi/3$ and $\pi/3$, respectively, in the formula. \square

Lemma 3.6. *Nonelliptic local webs $W (\neq \emptyset)$ in an ideal polygon $\mathfrak{D}_k (k \geq 0)$ having empty boundary $\partial W = \emptyset$ do not exist.*

Proof. Suppose otherwise. We may assume W is connected. Since W is nonelliptic, W is not a loop (this uses that \mathfrak{D}_k is contractible). Then, the outer rim of W forms the boundary of a smaller closed disk $\mathfrak{D}'_0 \subseteq \mathfrak{D}_k$ containing a subweb $W' \subseteq W$ that has nonempty boundary $\partial W' \neq \emptyset$. By nonellipticity, W' does not have a cap-face, so W' has a trivalent vertex. Applying Lemma 3.5 to connected components of W' , an analysis of innermost components leads to the fact that W' has at least one fork- or H -face. By nonellipticity, W' does not have an H -face, and it does not have a fork-face by orientation considerations applied to W . \square

Lemma 3.6 plus a small argument allows us to relax the hypotheses of Lemma 3.5 as follows.

Proposition 3.7. *Let W be a nonelliptic local web in the closed disk \mathfrak{D}_0 such that W is connected and has at least one trivalent vertex. Then W has at least three fork- and/or H -faces. If, in addition, W is assumed not to have any cap-faces, then the connectedness hypothesis above is superfluous.* \square

3.6. Essential and rungless local webs

Definition 3.8. A local web W in an ideal polygon $\mathfrak{D}_k (k \geq 0)$ is *essential* if:

1. the local web W is nonelliptic;
2. the web W is *taut*: for any compact arc α embedded in \mathfrak{D}_k whose boundary $\partial\alpha$ lies in a component E of the boundary $\partial\mathfrak{D}_k$ (and is disjoint from W), the number of intersection points $\iota(W, \overline{E})$ of W with the segment $\overline{E} \subseteq E$ delimited by $\partial\alpha$ does not exceed the number of intersection points $\iota(W, \alpha)$ of W with α , that is $\iota(W, \overline{E}) \leq \iota(W, \alpha)$; see Figures 9 and 10.

Note that essential local webs cannot have any cap- or fork-faces but can have H -faces. Later, we will need the operation of adding or removing an H -face, depicted in Figure 11.

Definition 3.9. A local web W in an ideal polygon $\mathfrak{D}_k (k \geq 0)$ is *rungless* if it does not have any H -faces; see Figure 12.

Remark 3.10.

1. A consequence of Proposition 3.7, which we will not use, is that (nonempty) essential local webs in the closed disk \mathfrak{D}_0 or ideal monoangle \mathfrak{D}_1 do not exist.

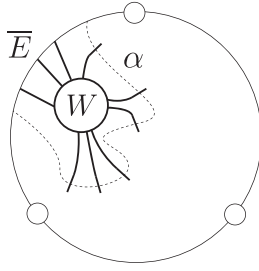


Figure 9. Tautness condition for an essential local web.

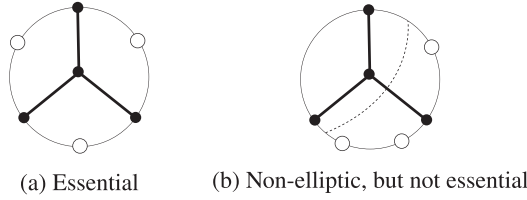


Figure 10. More nonelliptic webs.

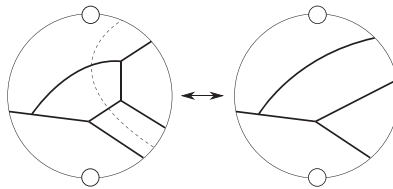


Figure 11. Adding or removing an H-face.

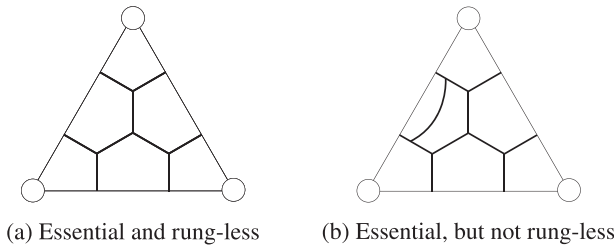


Figure 12. More essential webs.

2. Kuperberg [Kup96, §4, 6.1] says ‘(core of a) nonconvex nonelliptic web in the k -clasped web space’ for our ‘(rungless) essential local web in the ideal k -polygon’.

3.7. Ladder-webs in ideal biangles

Another name for an ideal two-polygon \mathfrak{D}_2 is an *ideal biangle* or just *biangle*, denoted by \mathfrak{B} . The boundary $\partial\mathfrak{B}$ consists of two ideal arcs E' and E'' , called the *boundary edges* of the biangle. We want to characterize essential local webs W in the biangle \mathfrak{B} ; compare (1) in Remark 3.10.

Definition 3.11. For any surface $\widehat{\mathfrak{S}}$, possibly with boundary, an *immersed multicurve*, or just *multicurve*, $\Gamma = \{\gamma_i\}$ on $\widehat{\mathfrak{S}}$ is a finite collection of connected oriented curves (Definition 2.1) γ_i immersed in $\widehat{\mathfrak{S}}$ such that $\partial\gamma_i = \gamma_i \cap \partial\widehat{\mathfrak{S}}$. Note that γ_i and γ_j might intersect in $\widehat{\mathfrak{S}}$ for any i and j . Note also that a component γ_i may be either a loop or an arc.

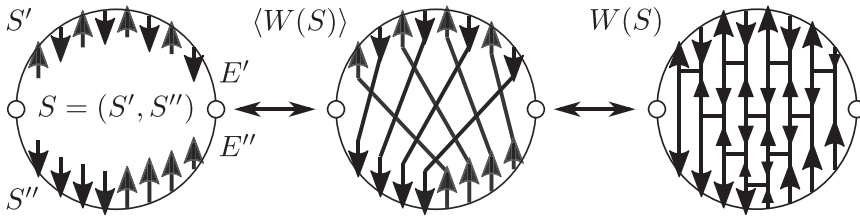


Figure 13. Construction of a ladder-web.

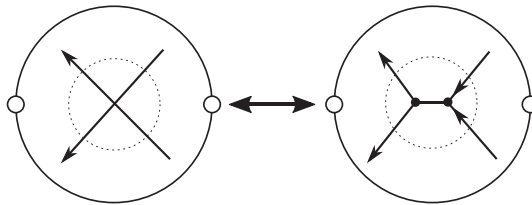


Figure 14. Replacing a local crossing with an H (also called a rung).

In the current section, components γ_i of a multicurve Γ will always be embedded, but different components might intersect. This will not be the case later on in §8.

A pair of arcs γ_1 and γ_2 each intersecting both boundary edges in \mathfrak{B} are *oppositely oriented* if γ_1 and γ_2 go into (resp. out of) and out of (resp. into) E' , respectively. Similarly, the arcs γ_1 and γ_2 are *same-oriented* if γ_1 and γ_2 both go into (resp. out of) E' , respectively.

Definition 3.12. A *symmetric strand-set pair* $S = (S', S'')$ for the biangle \mathfrak{B} is a pair of finite collections $S = (S', S'') = (\{s'\}, \{s''\})$ of disjoint oriented *strands* located on the boundary $\partial\mathfrak{B} = E' \cup E''$ such that the strands s' (resp. s'') lie on the boundary edge E' (resp. E'') and such that the number of *in-strands* (resp. *out-strands*) on E' is equal to the number of out-strands (resp. in-strands) on E'' ; see the leftmost picture in Figure 13.

Given a symmetric strand-set pair $S = (S', S'')$, in the following definition we associate to S a multicurve in the biangle \mathfrak{B} , denoted $\langle W(S) \rangle$.

Definition 3.13. The *local picture* $\langle W(S) \rangle$ associated to a symmetric strand-set pair $S = (S', S'')$ is the multicurve in the biangle \mathfrak{B} obtained by connecting the strands on E' to the strands on E'' with arcs, in an order preserving and minimally intersecting way, loosely speaking, as illustrated in the middle picture in Figure 13. Here, order preserving means in a way such that no same-oriented arcs intersect.

Observe, in the local picture $\langle W(S) \rangle$, that γ_1 and γ_2 intersect if and only if (1) they are oppositely oriented, and (2) they intersect exactly once. We denote by $\mathcal{P}(S) \subseteq \mathfrak{B}$ the set of intersection points p of pairs of oppositely oriented arcs in the local picture $\langle W(S) \rangle$.

Finally, we say how to associate a local web $W(S)$ in \mathfrak{B} to a symmetric pair $S = (S', S'')$.

Definition 3.14. The *ladder-web* $W(S)$ in the biangle \mathfrak{B} obtained from a symmetric strand-set pair $S = (S', S'')$ is the unique (up to ambient isotopy of \mathfrak{B}) local web obtained by resolving each intersection point $p \in \mathcal{P}(S)$ into two vertices connected by a horizontal edge, relative to the biangle, called a *rung*; see Figures 13 and 14.

The following statement is implicit in [Kup96, Lemma 6.7] and also appears in [FS22, §8].

Proposition 3.15. *The ladder-web $W(S)$ is essential. Conversely, given an essential local web W in the biangle \mathfrak{B} , there exists a unique symmetric strand-set pair $S = (S', S'')$ such that $W = W(S)$. Thus, W is a ladder-web.*

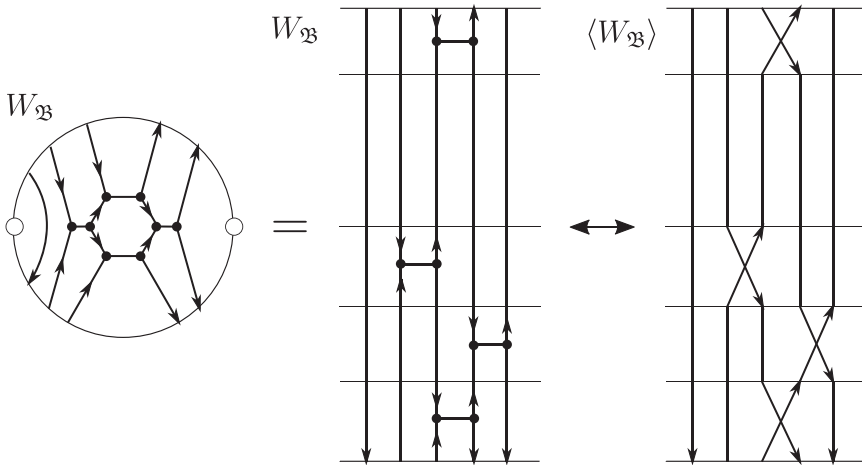


Figure 15. Essential local web $W_{\mathfrak{B}}$ in the biangle, and its corresponding local picture $\langle W_{\mathfrak{B}} \rangle$.

Proof. For the first statement, the nonellipticity of $W(S)$ follows because two oppositely oriented curves in the local picture $\langle W(S) \rangle$ do not cross more than once (if there were a square-face, a pair of curves would cross twice), and the tautness of $W(S)$ is immediate.

Conversely, let W be an essential local web in \mathfrak{B} . The collection of ends of W located on the boundary edges $E' \cup E''$ determines a strand-set pair $S = (S', S'')$. We show that S is symmetric and $W = W(S)$. In particular, S is uniquely determined.

If W has a trivalent vertex, let \overline{W} denote the induced local web in the closed disk \mathfrak{D}_0 underlying \mathfrak{B} , obtained by filling in the two punctures of \mathfrak{B} . Applying Proposition 3.7 to \overline{W} guarantees that \overline{W} (possibly minus some arc components) has at least three fork- and/or H-faces. At most two of these faces can straddle the two punctures of \mathfrak{B} , so we gather W has one fork- or H-face D^{ext} lying on E' or E'' . Since W is taut, D^{ext} is an H-face.

We can then remove this H-face from \mathfrak{B} (recall Figure 11), obtaining a local web W_1 that is essential and has strictly fewer trivalent vertices than W . Repeating this process, we obtain a sequence of essential local webs $W = W_0, W_1, \dots, W_n$ such that W_n has no trivalent vertices and is obtained from W by removing finitely many H-faces. By nonellipticity, W_n consists of a collection of arcs $\gamma_i^{(n)}$ (as opposed to loops), and since W_n is taut, each arc $\gamma_i^{(n)}$ connects to both boundary edges E' and E'' of the biangle \mathfrak{B} .

Replacing the removed H-faces with local crossings (Figure 14), we obtain a multicurve Γ in \mathfrak{B} consisting of arcs $\gamma_i^{(0)}$, each intersecting both edges E' and E'' , such that only oppositely oriented arcs $\gamma_i^{(0)}$ intersect; see Figure 15. In particular, the pair (S', S'') is symmetric.

We claim Γ is the local picture $\langle W(S) \rangle$. Since only oppositely oriented arcs intersect, Γ is order preserving (Definition 3.13). It remains to show Γ is minimally intersecting, namely that no arcs intersect more than once. Suppose they did. Then, because only oppositely oriented arcs intersect, there would be an embedded bigon B in the complement $\Gamma^c \subseteq \mathfrak{B}$; see the right side of Figure 16. Such an embedded bigon B corresponds in the local web W to a square-face, violating the nonellipticity of W . We gather $\Gamma = \langle W(S) \rangle$, as claimed.

By definition of the multicurve Γ and the local web $W(S)$, it follows that $W = W(S)$. □

For technical reasons, in §8 we will need the following concept.

Definition 3.16. The local picture $\langle W_{\mathfrak{B}} \rangle$ associated to an essential local web $W_{\mathfrak{B}}$ in the biangle \mathfrak{B} is the local picture $\langle W(S) \rangle$ (Definition 3.13) corresponding to the unique symmetric strand-set pair $S = (S', S'')$ such that $W_{\mathfrak{B}} = W(S)$; see Figure 15.

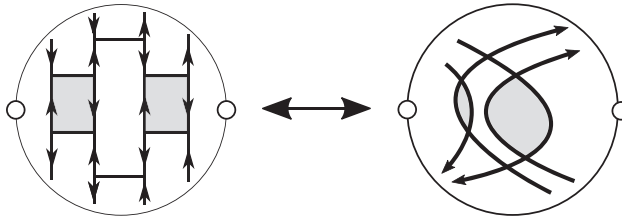


Figure 16. Prohibited ladder-webs and local pictures.

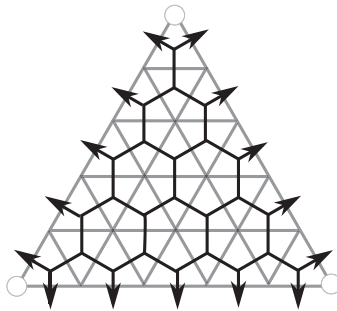


Figure 17. Honeycomb-web.

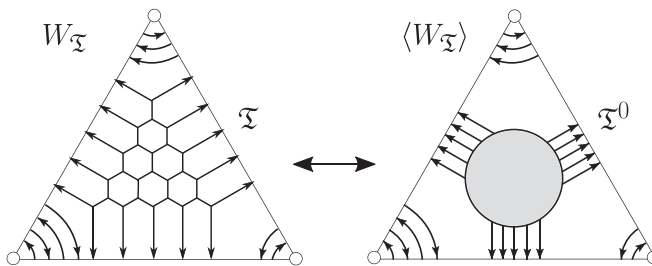


Figure 18. Rungless essential local web $W_{\mathfrak{T}}$ in the triangle and its corresponding local picture $\langle W_{\mathfrak{T}} \rangle$ in the holed triangle.

3.8. Honeycomb-webs in ideal triangles

Another name for an ideal three-polygon \mathfrak{D}_3 is an *ideal triangle* \mathfrak{T} . We want to characterize rungless essential local webs W in triangles \mathfrak{T} .

Definition 3.17. For a positive integer $n > 0$, the *n -out-honeycomb-web* H_n^{out} (resp. *n -in-honeycomb-web* H_n^{in}) in the triangle \mathfrak{T} is the local web H_n dual to the n -triangulation of \mathfrak{T} , where the orientation of H_n is such that all the arrows go out of (resp. into) the triangle \mathfrak{T} .

For example, in Figure 17 we show the five-out-honeycomb-web H_5^{out} .

The following statement is implicit in [Kup96, Lemma 6.8] and also appears in [FS22, §9].

Proposition 3.18. *A honeycomb-web H_n in the triangle \mathfrak{T} is rungless and essential. Conversely, given a connected rungless essential local web W in \mathfrak{T} having at least one trivalent vertex, there exists a unique honeycomb-web $H_n = H_n^{\text{out}}$ or $= H_n^{\text{in}}$ such that $W = H_n$. Consequently, a (possibly disconnected) rungless essential local web W in \mathfrak{T} consists of a unique (possibly empty) honeycomb H_n together with a collection of disjoint oriented arcs located on the corners of \mathfrak{T} ; see the left-hand side of Figure 18.*

Proof. The first statement is immediate.

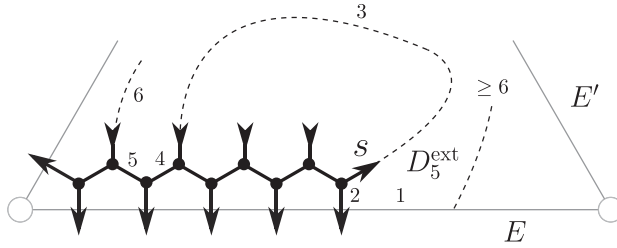


Figure 19. Laying down a honeycomb: 1 of 2.

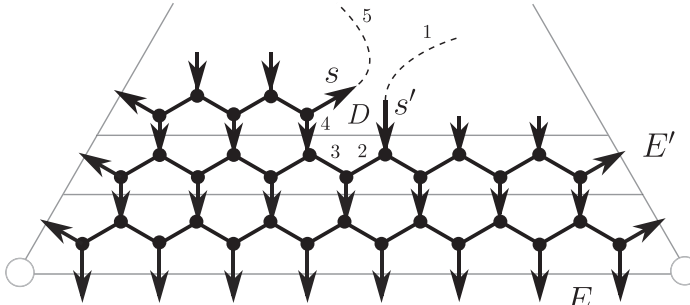


Figure 20. Laying down a honeycomb: 2 of 2.

Step 1. Let W be as in the second statement. Just like the proof of Proposition 3.15, applying Proposition 3.7 to the induced web \bar{W} in the underlying closed disk \mathfrak{D}_0 guarantees that \bar{W} has at least three fork- and/or H-faces, at most three of which can straddle the three punctures of \mathfrak{T} . Since W is taut and rungless, W has no fork- or H-faces. Thus, \bar{W} has exactly three fork- and/or H-faces, each of which straddles a puncture. Since these three faces are the only ones with a positive contribution in the formula of Proposition 3.3, they must be fork-faces. Moreover, since the total contribution of these three fork-faces is 2π , every other face has exactly zero contribution. We gather that each interior face of W is a hexagon-face and each external face of W is a half-hexagon-face.

Step 2. To prove that W is a honeycomb-web H_n , we argue by induction on n , showing that the triangle \mathfrak{T} can be tiled by W face-by-face, starting from a corner of \mathfrak{T} .

(2.a) Assume inductively that some number of half-hexagon-faces have been laid down as part of the bottom layer of faces sitting on the bottom edge E , illustrated in Figure 19.

The strand labeled s either: (1) ends on the right edge E' of the triangle \mathfrak{T} , thereby creating a fork straddling the rightmost puncture and completing the bottom layer of faces; (2) ends at a vertex disjoint from the vertices previously laid, hence the strand s is part of the boundary of the next half-hexagon-face; (3) ends at one of the vertices previously laid.

If (1), we continue to the next step of the induction, which deals with laying down the middle layers. If (2), we repeat the current step. Lastly, we argue (3) cannot occur. Indeed, suppose it did. The strand s is part of the boundary of the next half-hexagon-face D_5^{ext} . But, as can be seen from the figure, the external face D_5^{ext} has \geq six sides, which is a contradiction.

(2.b) Assume inductively that the bottom layer and some number of middle layers have been laid down and moreover that some number of faces have been laid down as part of the current layer, illustrated in Figure 20. Consider the next face D shown in the figure.

The face D is either external or internal. If it is internal, then D is a hexagon-face. In this case, the strands s and s' end at the fifth and sixth vertices of the hexagon-face, and we repeat the current step. Otherwise, D is external, so it is a half-hexagon-face, $D = D_5^{\text{ext}}$. However, we see from the figure that in this case D_5^{ext} has \geq six sides, which is a contradiction.

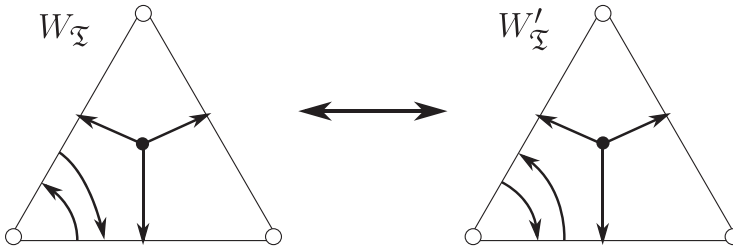


Figure 21. Local parallel-move.

To finish the induction, we repeat this step until the strand s' does not exist, in which case the strand s is part of a nonexternal side of a half-hexagon-face lying on the boundary edge E' .

Step 3. The last statement of the proposition follows since each honeycomb-web H_n attaches to all three boundary edges of the triangle \mathfrak{T} . □

Later, in order to assign coordinates to webs, we will need to consider rungless essential local webs $W_{\mathfrak{T}}$ in a triangle \mathfrak{T} up to a certain equivalence relation. Say that a *local parallel-move* applied to $W_{\mathfrak{T}}$ is a move swapping two arcs on the same corner of \mathfrak{T} ; see Figure 21.

Definition 3.19. Let $\mathcal{W}_{\mathfrak{T}}$ denote the collection of rungless essential local webs in the triangle \mathfrak{T} . We say that two local webs $W_{\mathfrak{T}}$ and $W'_{\mathfrak{T}}$ in $\mathcal{W}_{\mathfrak{T}}$ are *equivalent up to corner-ambiguity* if they are related by local parallel-moves. The corner-ambiguity equivalence class of a local web $W_{\mathfrak{T}} \in \mathcal{W}_{\mathfrak{T}}$ is denoted by $[W_{\mathfrak{T}}]$, and the set of corner-ambiguity classes is denoted $[\mathcal{W}_{\mathfrak{T}}]$.

For technical reasons, in §8 we will need the following concept.

Definition 3.20. Given a triangle \mathfrak{T} , a *holed triangle* \mathfrak{T}^0 is the triangle minus an open disk $\mathfrak{D}_0 = \mathfrak{T} - \text{Int}(\mathfrak{D}_0)$; see the right-hand side of Figure 18 above. Let $W_{\mathfrak{T}}$ be a rungless essential local web in \mathfrak{T} , which by Proposition 3.18 consists of a honeycomb-web H_n together with a collection of disjoint oriented corner arcs $\{\gamma_i\}$. The *local picture* $\langle W_{\mathfrak{T}} \rangle$ associated to $W_{\mathfrak{T}}$ is the multicurve (Definition 3.11) in the holed triangle \mathfrak{T}^0 consisting of the corner arcs γ_i together with $3n$ oriented arcs $\{\gamma'_j\}$ disjoint from each other and from the γ_i and going either all out of or all into the boundary $\partial\mathfrak{D}_0$ of the removed disk, such that for each boundary edge E of the triangle \mathfrak{T} there are n arcs γ'_j ending on E ; see again Figure 18.

4. Good position of a global web

Using the technical results about local webs from §3, we continue studying global webs W on the surface \mathfrak{S} . We assume \mathfrak{S} is equipped with an ideal triangulation λ ; see §2.1.

4.1. Generic isotopies

Definition 4.1. A web W on \mathfrak{S} is *generic* with respect to the ideal triangulation λ if none of its vertices intersect the edges E of λ , and if in addition W intersects λ transversally.

Two generic webs W and W' are *generically isotopic* if they are isotopic through generic webs; see Definition 2.3.

Whenever there is an ideal triangulation λ present, we always assume that ‘web’ means ‘generic web’. However, we distinguish between isotopies and generic isotopies.

4.2. Minimal position

Recall the notion of two parallel equivalent webs; see Definition 2.3.

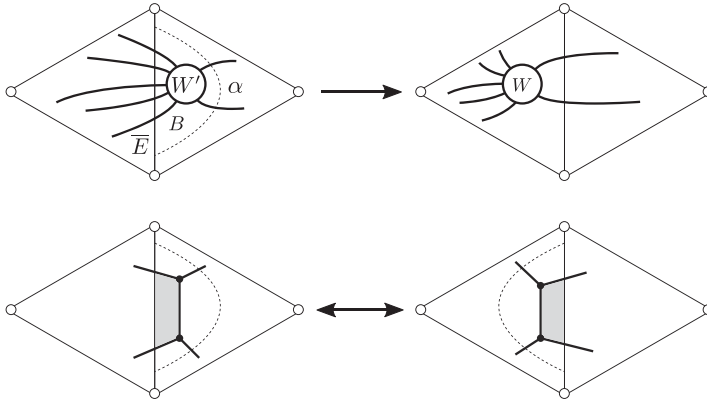


Figure 22. Tightening- and H-moves.

Definition 4.2. Given a web W on the surface \mathfrak{S} and given an edge E of the ideal triangulation λ , the local geometric intersection number of the web W with the edge E is

$$I(W, E) = \min_{W'}(\iota(W', E)) \in \mathbb{Z}_{\geq 0} \quad (W' \text{ is parallel equivalent to } W),$$

where $\iota(W', E)$ is the number of intersection points of W' with E .

The web W is in *minimal position with respect to the ideal triangulation λ* if

$$\iota(W, E) = I(W, E) \in \mathbb{Z}_{\geq 0} \quad (\text{for all edges } E \text{ of } \lambda).$$

(If this is the case, W minimizes the intersection number $\iota(W, \lambda)$ with the ideal triangulation λ .)

Let W' be a web, let \mathfrak{T} be a triangle in the ideal triangulation λ , and let $W'_\mathfrak{T} = W' \cap \mathfrak{T}$ be the *restriction* of W' to \mathfrak{T} . Suppose that the local web $W'_\mathfrak{T}$ is not taut; see Definition 3.8. Then there is an edge E of λ and a compact arc α ending on E such that $\iota(W', E) > \iota(W', \alpha)$; see Figure 22. We can then isotope the part of W' that is inside the *bigon* B , which is bounded by α and the segment \bar{E} of E delimited by $\partial\alpha$, into the adjacent triangle, resulting in a new web W . This is called a *tightening-move*. Similarly, if the restriction $W'_\mathfrak{T}$ has an H-face, then we may apply an *H-move* to push the H into the adjacent triangle; see again Figure 22.

Note that tightening- and H-moves can be achieved with an isotopy of the web but not a generic isotopy. Also, by definition, in order to apply an H-move, we assume that the shaded region shown at the bottom of Figure 22 is *empty*, namely it does not intersect the web.

We borrow the following result from [FS22, §6] (and give essentially the same proof in the arXiv version [DS20a] of this article).

Proposition 4.3. *If W' is a nonelliptic web on the surface \mathfrak{S} , then (by applying tightening-moves) there exists a nonelliptic web W that is isotopic (in particular, parallel equivalent) to W' and that is in minimal position with respect to the ideal triangulation λ ; see Definition 2.5.*

Moreover, given any two parallel equivalent nonelliptic webs W and W' in minimal position, then W can be taken to W' by a sequence of H-moves, global parallel-moves and generic isotopies; see Definition 2.3. \square

4.3. Split ideal triangulations

A *split ideal triangulation* $\widehat{\lambda}$ with respect to the ideal triangulation λ is a collection of bi-infinite arcs obtained by doubling every edge E of λ . In other words, we fatten each edge E into a *biangle* \mathfrak{B} ; see Figure 23.

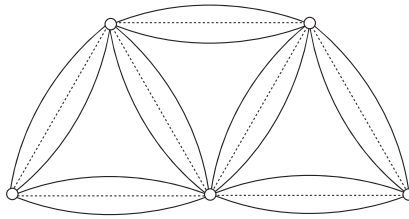


Figure 23. Split ideal triangulation.

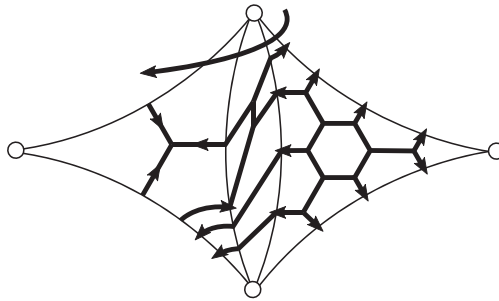


Figure 24. (Part of) a web in good position.

The notions of generic web and generic isotopy for webs with respect to the split ideal triangulation $\widehat{\lambda}$ are the same as those for webs with respect to the ideal triangulation λ . We always assume that webs are generic with respect to $\widehat{\lambda}$.

To avoid cumbersome notation, we identify the triangles \mathfrak{T} of the ideal triangulation λ to the triangles \mathfrak{T} of the split ideal triangulation $\widehat{\lambda}$.

Remark 4.4. For a related usage of split ideal triangulations, in the SL_2 -case, see [BW11].

4.4. Good position

Definition 4.5. For a fixed split ideal triangulation $\widehat{\lambda}$, a web W on \mathfrak{S} is in *good position* with respect to $\widehat{\lambda}$ if the restriction $W_{\mathfrak{B}} = W \cap \mathfrak{B}$ (resp. $W_{\mathfrak{T}} = W \cap \mathfrak{T}$) of W to each biangle \mathfrak{B} (resp. triangle \mathfrak{T}) of $\widehat{\lambda}$ is an essential (resp. rungless essential) local web; see Figure 24.

Note that for a web W in good position, each restriction $W_{\mathfrak{B}}$ to a biangle \mathfrak{B} of $\widehat{\lambda}$ is a ladder-web; see Definition 3.14, Proposition 3.15 and Figures 13 and 15. Also, each restriction $W_{\mathfrak{T}}$ to a triangle \mathfrak{T} of $\widehat{\lambda}$ is a (possibly empty) honeycomb-web H_n together with a collection of disjoint oriented corner arcs; see Definition 3.17, Proposition 3.18 and Figures 17 and 18.

If W is a web in good position, then a *modified H-move* carries an H-face in a biangle \mathfrak{B} to an H-face in an adjacent biangle \mathfrak{B}' , thereby replacing W with a new web W' ; see Figure 25. If, in addition, W is nonelliptic, then W' is also in good position. The nonelliptic condition for W is required to ensure that the new local web restriction $W'_{\mathfrak{B}'}$ is nonelliptic.

Remark 4.6. Of importance will be that the effect in the intermediate triangle \mathfrak{T} of a modified H-move is to swap two parallel oppositely oriented corner arcs; see again Figure 25.

Once more, the following result is implicit in [Kup96, Lemma 6.5 and the proof of Theorem 6.2, pp. 139-140] (in the setting of an ideal k -polygon \mathfrak{D}_k) and also appears in [FS22, §10].

Proposition 4.7. *If W' is a nonelliptic web on the surface \mathfrak{S} , then there exists a nonelliptic web W that is isotopic (in particular, parallel equivalent) to W' and that is in good position with respect to the split ideal triangulation $\widehat{\lambda}$.*

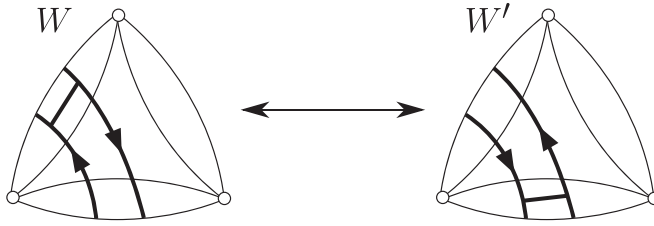


Figure 25. *Modified H-move.*

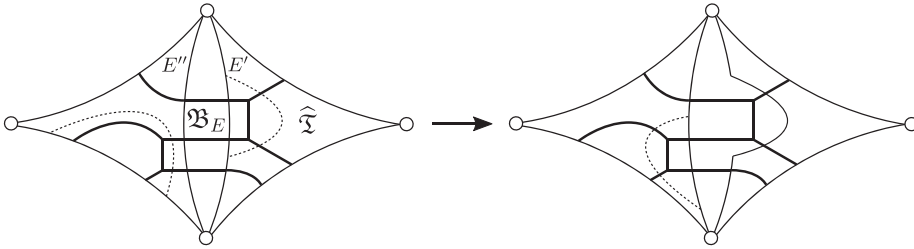


Figure 26. *Enlarging a biangle.*

Moreover, given any two parallel equivalent nonelliptic webs W and W' in good position, then W can be taken to W' by a sequence of modified H-moves, global parallel-moves and generic isotopies.

Proof. We will keep track of isotopies by moving the split triangulation $\widehat{\lambda}$ instead of webs.

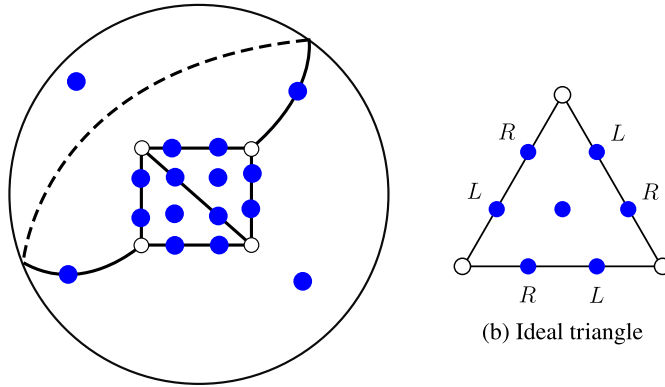
By Proposition 4.3, we can replace W' with a nonelliptic web W that is isotopic to W' and that is in minimal position with respect to the ideal triangulation λ . We proceed to construct the split ideal triangulation $\widehat{\lambda}$.

Let us begin by splitting each edge E of λ into two edges E' and E'' that are very close to E . These split edges form a preliminary split ideal triangulation $\widehat{\lambda}$, whose triangles (resp. biangles) are denoted by $\widehat{\mathfrak{T}}$ (resp. \mathfrak{B}_E); see the left-hand side of Figure 26.

By definition of minimal position, the restriction $W_{\widehat{\mathfrak{T}}}$ of W to a triangle $\widehat{\mathfrak{T}}$ of the ideal triangulation λ is taut. Since, in addition, W is nonelliptic, we have that $W_{\widehat{\mathfrak{T}}}$ is essential. If the preliminary split ideal triangulation $\widehat{\lambda}$ is sufficiently close to λ , then the restriction $W_{\widehat{\mathfrak{T}}}$ of W to the triangle $\widehat{\mathfrak{T}} \subseteq \mathfrak{T}$ associated to $\widehat{\mathfrak{T}}$ is also an essential local web. If all of the local webs $W_{\widehat{\mathfrak{T}}}$ are rungless, then W is in good position with respect to $\widehat{\lambda}$.

Otherwise, assume $W_{\widehat{\mathfrak{T}}}$ has an H-face on an edge of $\widehat{\lambda}$, say the edge E' . Then by isotopy we can enlarge the biangle \mathfrak{B}_E until it just envelops this H-face. In other words, we can isotope the edge E' so that it cuts out this H-face from the triangle $\widehat{\mathfrak{T}}$; see Figure 26. The result of this step is a new split ideal triangulation $\widehat{\lambda}$, retaining the property that the local web restrictions $W_{\widehat{\mathfrak{T}}}$ are essential. Repeating this process until all of the local webs $W_{\widehat{\mathfrak{T}}}$ are rungless, we obtain the desired split ideal triangulation $\widehat{\lambda}$. Notice it might be the case that there is more than one biangle into which an H-face can be moved; see again Figure 26.

For the second statement of the proposition, note that if a nonelliptic web W is in good position with respect to $\widehat{\lambda}$, then W is minimal with respect to the ideal triangulation λ (which, for the sake of argument, we can take to be contained in $\widehat{\lambda}$, that is $\lambda \subseteq \widehat{\lambda}$). (Indeed, this follows by the proof of the first part of Proposition 4.3, provided in [FS22, DS20a], and uses the fact that adding a ladder web $W_{\mathfrak{B}}$ to a rungless essential web $W_{\widehat{\mathfrak{T}}}$ preserves the tautness property.) Similarly, W' is in minimal position. Thus, applying the second part of Proposition 4.3, we gather that W can be taken to W' by a finite sequence of H-moves, global parallel-moves and generic isotopies. The result follows by the definition of good position and modified H-moves. \square



(a) Four times punctured sphere

(b) Ideal triangle

Figure 27. Dotted ideal triangulations.

5. Global coordinates for nonelliptic webs

Recall that $[\mathcal{W}_{\mathfrak{S}}]$ denotes the collection of parallel equivalence classes of nonelliptic webs on the surface \mathfrak{S} ; see just below Definition 2.5. Our goal in this section is to define a function $\Phi_{\lambda}^{\text{FG}} : [\mathcal{W}_{\mathfrak{S}}] \rightarrow \mathbb{Z}_{\geq 0}^N$ depending on the ideal triangulation λ , where $N = -8\chi(\mathfrak{S}) > 0$ is a positive integer depending only on the topology of \mathfrak{S} . In §6-8, we characterize the image of $\Phi_{\lambda}^{\text{FG}}$ and prove that it is injective. We think of $\Phi_{\lambda}^{\text{FG}}$ as putting global coordinates on $[\mathcal{W}_{\mathfrak{S}}]$.

5.1. Dotted ideal triangulations

Consider a surface $\widehat{\mathfrak{S}} = \mathfrak{S}$ or $= \mathfrak{T}$ equipped with an ideal triangulation λ , where, in this subsection, $\lambda = \mathfrak{T}$ when $\widehat{\mathfrak{S}} = \mathfrak{T}$. The associated *dotted ideal triangulation* is the pair consisting of λ together with $N' = N$ or $= 7$ distinct *dots* attached to the one- and two-cells of λ , where there are two *edge-dots* attached to each one-cell and there is one *triangle-dot* attached to each two-cell; see Figure 27. Given a triangle \mathfrak{T} of λ and an edge E of \mathfrak{T} , it makes sense to talk about the *left-edge-dot* and *right-edge-dot* as viewed from \mathfrak{T} ; see Figure 27b. Choosing an ordering for the N' dots lying on the dotted ideal triangulation λ defines a one-to-one correspondence between functions $\{\text{dots}\} \rightarrow \mathbb{Z}$ and elements of $\mathbb{Z}^{N'}$. We always assume that such an ordering has been chosen.

5.2. Local coordinate functions

Consider a dotted ideal triangle \mathfrak{T} ; see Figure 27b. Recall (Definition 3.19) that $\mathcal{W}_{\mathfrak{T}}$ denotes the collection of rungless essential local webs $W_{\mathfrak{T}}$ in \mathfrak{T} and that $[\mathcal{W}_{\mathfrak{T}}]$ denotes the set of corner-ambiguity classes $[W_{\mathfrak{T}}]$ of local webs $W_{\mathfrak{T}}$ in $\mathcal{W}_{\mathfrak{T}}$.

Definition 5.1. An *integer local coordinate function* or just *local coordinate function*,

$$\Phi_{\mathfrak{T}} : \mathcal{W}_{\mathfrak{T}} \longrightarrow \mathbb{Z}^7$$

is a function assigning to each local web $W_{\mathfrak{T}}$ in $\mathcal{W}_{\mathfrak{T}}$ one integer coordinate per dot lying on the dotted triangle \mathfrak{T} , satisfying the following properties:

1. if a local web $W_{\mathfrak{T}}$ in $\mathcal{W}_{\mathfrak{T}}$ can be written $W_{\mathfrak{T}} = W'_{\mathfrak{T}} \sqcup W''_{\mathfrak{T}}$ as the disjoint union of two local webs, each in $\mathcal{W}_{\mathfrak{T}}$, then

$$\Phi_{\mathfrak{T}}(W_{\mathfrak{T}}) = \Phi_{\mathfrak{T}}(W'_{\mathfrak{T}}) + \Phi_{\mathfrak{T}}(W''_{\mathfrak{T}}) \in \mathbb{Z}^7;$$

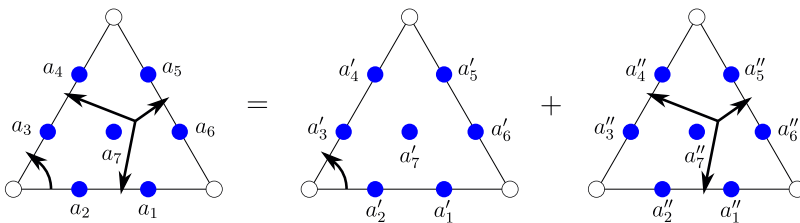


Figure 28. Property (1): $a_i = a'_i + a''_i$.



Figure 29. Properties (2) and (3).

2. for an edge E of \mathfrak{T} , the ordered pair of coordinates (a_E^L, a_E^R) of the function $\Phi_{\mathfrak{T}}$ assigned to the left- and right-edge-dots lying on E , respectively, depends only on the pair $(n_E^{\text{in}}, n_E^{\text{out}})$ of numbers of in- and out-strands of the local web $W_{\mathfrak{T}}$ on the edge E ; moreover, different pairs $(n_E^{\text{in}}, n_E^{\text{out}})$ yield different pairs of coordinates (a_E^L, a_E^R) ;
3. there are two symmetries; the first is that $\Phi_{\mathfrak{T}}$ respects the rotational symmetry of the triangle (see Remark 5.2 below for a more precise statement), and the second is that if the numbers n_E^{in} and n_E^{out} of in- and out-strands on an edge E are exchanged, then the coordinates a_E^L and a_E^R are exchanged as well;
4. observe, by property (1), the function $\Phi_{\mathfrak{T}}(W_{\mathfrak{T}}) = \Phi_{\mathfrak{T}}(W'_{\mathfrak{T}})$ agrees on local webs $W_{\mathfrak{T}}$ and $W'_{\mathfrak{T}}$ in $\mathscr{W}_{\mathfrak{T}}$ representing the same corner-ambiguity class $[W_{\mathfrak{T}}] = [W'_{\mathfrak{T}}]$ in $[\mathscr{W}_{\mathfrak{T}}]$ (because $W_{\mathfrak{T}}$ and $W'_{\mathfrak{T}}$ differ only by permutations of oriented corner arcs), thus inducing

$$\Phi_{\mathfrak{T}} : [\mathscr{W}_{\mathfrak{T}}] \longrightarrow \mathbb{Z}^7,$$

also called $\Phi_{\mathfrak{T}}$; we require that this induced function $\Phi_{\mathfrak{T}}$ is an injection.

The coordinates assigned by $\Phi_{\mathfrak{T}}$ to edge-dots (resp. triangle-dots) are called *edge-coordinates* (resp. *triangle-coordinates*).

We illustrate properties (1), (2), (3) in Figures 28 and 29.

Remark 5.2 (from pictures to coordinates). Let us be more precise about what we mean by the first symmetry of property (3), which will also allow us the opportunity to give a clearer explanation of the meaning of pictures such as those shown in the figures below. We will use the picture displayed on the left-hand side of Figure 28 as a reference. When we draw such a picture, we have implicitly selected a preferred vertex of the triangle \mathfrak{T} , say the vertex appearing at the top of the picture; write \mathfrak{T}_0 to indicate this extra data. A tuple $(a_1, a_2, \dots, a_7) \in \mathbb{Z}^7$ defines a function $\{\text{dots of } \mathfrak{T}_0\} \rightarrow \mathbb{Z}$ by sending the i -th dot to a_i , as indicated in the picture. If this tuple is associated to a local web $W_{\mathfrak{T}_0}$, then we say this tuple is the value $\Phi_{\mathfrak{T}_0}(W_{\mathfrak{T}_0})$ of the local coordinate function evaluated on the web $W_{\mathfrak{T}_0}$. The rotational symmetry of property (3) says that if $W'_{\mathfrak{T}_0}$ is the different local web obtained by rotating $W_{\mathfrak{T}_0}$ by $2\pi/3$ radians clockwise, with coordinates $\Phi_{\mathfrak{T}_0}(W'_{\mathfrak{T}_0}) = (a'_1, a'_2, \dots, a'_7)$, then $a'_1 = a_5, a'_2 = a_6, a'_3 = a_1, a'_4 = a_2, a'_5 = a_3, a'_6 = a_4$ and $a'_7 = a_7$. Lastly, we define $\Phi_{\mathfrak{T}}(W_{\mathfrak{T}}) = \Phi_{\mathfrak{T}_0}(W_{\mathfrak{T}_0})$, and the rotational symmetry implies that this is independent of the choice of preferred vertex.

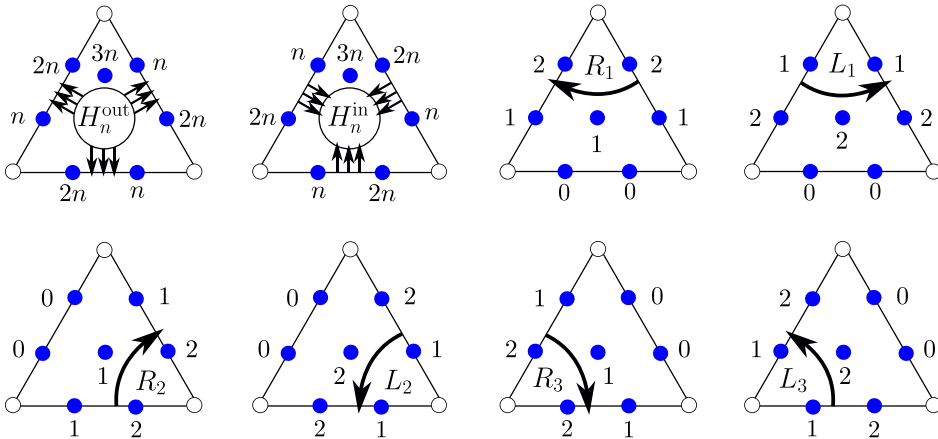


Figure 30. Fock–Goncharov local coordinate function $\Phi_{\mathfrak{T}}^{\text{FG}}$.

5.3. Local coordinates from Fock–Goncharov theory

We define an explicit Fock–Goncharov local coordinate function $\Phi_{\mathfrak{T}}^{\text{FG}} : \mathcal{W}_{\mathfrak{T}} \rightarrow \mathbb{Z}_{\geq 0}^7$ valued in nonnegative integers.

By property (1) in Definition 5.1, it suffices to define $\Phi_{\mathfrak{T}}^{\text{FG}}$ on connected local webs in $\mathcal{W}_{\mathfrak{T}}$. By Proposition 3.18, these come in one of exactly eight types $H_n^{\text{out}}, H_n^{\text{in}}, R_1, L_1, R_2, L_2, R_3, L_3$ illustrated in Figure 30. In the figure, note that in the two top left triangles we have, for visibility, drawn the local pictures $\langle H_n^{\text{out}} \rangle$ and $\langle H_n^{\text{in}} \rangle$ as a shorthand for the actual n -out-honeycomb-web H_n^{out} and n -in-honeycomb-web H_n^{in} , respectively; see Definition 3.20. It is immediate that $\Phi_{\mathfrak{T}}^{\text{FG}}$ satisfies property (3) and the first part of (2). The second part of (2) follows by the invertibility of the matrix $\begin{pmatrix} 2 & 1 \\ 1 & 2 \end{pmatrix}$. We will check property (4) in §6.

Remark 5.3.

1. Xie [Xie13] writes down the same local coordinates (up to a multiplicative factor of 3) for $R_1, L_1, R_2, L_2, R_3, L_3$ as well as the one-honeycomb-webs H_1^{out} and H_1^{in} .
2. The definition of these local coordinates can be checked experimentally by studying the highest terms of the Fock–Goncharov SL_3 -trace polynomials; see the introduction as well as [Kim20, Proposition 5.80] (and [Kim21, Proposition 3.15]). Moreover, it appears that these coordinates fit into a broader geometric context [SWZZ20, Theorem 8.22(2)].
3. The coordinates in the SL_2 -setting are geometric intersection numbers; see the introduction. In contrast, the SL_3 -coordinates depend on the choice of orientation of \mathfrak{S} .

5.4. Global coordinates from local coordinate functions

Assume that, for an abstract dotted triangle \mathfrak{T} , we have chosen an arbitrary local coordinate function $\Phi_{\mathfrak{T}} : \mathcal{W}_{\mathfrak{T}} \rightarrow \mathbb{Z}^7$. We show that this induces a global coordinate function $\Phi_{\lambda} : [\mathcal{W}_{\mathfrak{S}}] \rightarrow \mathbb{Z}^N$ that is well adapted to the choice of $\Phi_{\mathfrak{T}}$. The argument uses only properties (1), the first part of (2) and (3) of $\Phi_{\mathfrak{T}}$.

As a guiding example of the construction to come, reference Figure 33, which uses the Fock–Goncharov local coordinate function $\Phi_{\mathfrak{T}}^{\text{FG}}$. This is an example on the once punctured torus \mathfrak{S} . Note that the web W in the example has one hexagon-face. All of the other components of W^c are not contractible. So W is nonelliptic.

Step 1. Consider the split ideal triangulation $\widehat{\lambda}$ (§4.3). We put dots on each triangle \mathfrak{T} of $\widehat{\lambda}$. The chosen local coordinate function $\Phi_{\mathfrak{T}}$ can be associated to each of these dotted triangles \mathfrak{T} ; see the left-hand side of Figure 31.

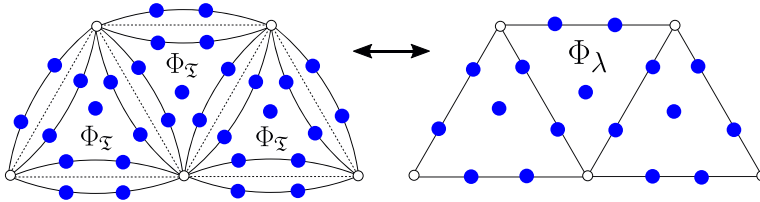


Figure 31. Local coordinates $\Phi_{\mathfrak{T}}$ attached to the triangles \mathfrak{T} of $\widehat{\lambda}$ (left), and the corresponding global coordinates Φ_{λ} attached to λ (right).

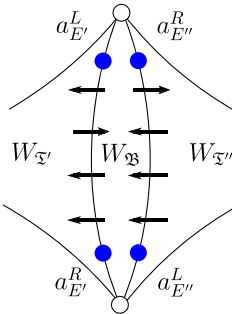


Figure 32. Local coordinates attached to a biangle: $a_{E'}^L = a_{E''}^R$, and $a_{E'}^R = a_{E''}^L$.

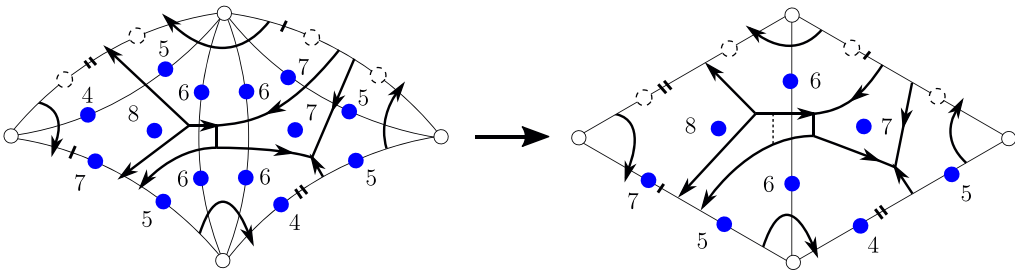


Figure 33. Tropical Fock–Goncharov \mathcal{A} -coordinates for a nonelliptic web.

Step 2. Fix a nonelliptic web W on \mathfrak{S} that is in good position (Definition 4.5) with respect to the split ideal triangulation $\widehat{\lambda}$. We assign to W one integer coordinate per dot lying on the dotted ideal triangulation λ , namely an element $\Phi_{\lambda}(W)$ in \mathbb{Z}^N .

By good position, the local web restriction $W_{\mathfrak{T}} = W \cap \mathfrak{T}$ is in $\mathcal{W}_{\mathfrak{T}}$ for each triangle \mathfrak{T} of $\widehat{\lambda}$. So, we may evaluate the local coordinate function $\Phi_{\mathfrak{T}}$ on $W_{\mathfrak{T}}$, obtaining coordinates for each of the seven dots lying on the dotted triangle \mathfrak{T} of $\widehat{\lambda}$. For instance, in this way we assign coordinates to all of the dots shown on the left-hand side of Figure 31 above. We claim that these coordinates glue together along each biangle \mathfrak{B} of $\widehat{\lambda}$ in such a way that we obtain one coordinate per dot lying on the dotted ideal triangulation λ ; see Figure 31.

Indeed, suppose \mathfrak{B} is a biangle between two triangles \mathfrak{T}' and \mathfrak{T}'' of $\widehat{\lambda}$. Let E' and E'' be the corresponding boundary edges of \mathfrak{B} , and let $a_{E'}^L$ and $a_{E'}^R$, (resp. $a_{E''}^L$ and $a_{E''}^R$) be the coordinates assigned by $\Phi_{\mathfrak{T}'}$ (resp. $\Phi_{\mathfrak{T}''}$) to the left- and right-edge-dots, respectively, lying on E' (resp. E'') as viewed from \mathfrak{T}' (resp. \mathfrak{T}''). Also, denote by $n_{E'}^{\text{in}}$ and $n_{E'}^{\text{out}}$ (resp. $n_{E''}^{\text{in}}$ and $n_{E''}^{\text{out}}$) the numbers of in- and out-strands of the local web restriction $W_{\mathfrak{T}'}$ (resp. $W_{\mathfrak{T}''}$) lying on the edge E' (resp. E''); see Figure 32.

Since, by good position, the restriction $W_{\mathfrak{B}} = W \cap \mathfrak{B}$ is a ladder-web, we have $n_{E'}^{\text{out}} = n_{E''}^{\text{in}}$ and $n_{E'}^{\text{in}} = n_{E''}^{\text{out}}$. It follows immediately from properties (3) and the first part of (2) that the coordinates across from each other agree $a_{E'}^L = a_{E''}^R$ and $a_{E'}^R = a_{E''}^L$. So, we may glue together the two pairs of coordinates into two coordinates lying on the edge E of λ , as desired.

Step 3. For a general nonelliptic web W' on \mathfrak{S} , by the first part of Proposition 4.7 there exists a nonelliptic web W that is parallel equivalent to W' and that is in good position with respect to the split ideal triangulation $\widehat{\lambda}$. Define $\Phi_\lambda(W') = \Phi_\lambda(W)$ in \mathbb{Z}^N .

To show $\Phi_\lambda(W')$ is well defined, suppose W_2 is another web as W . By the second part of Proposition 4.7, the nonelliptic webs W and W_2 are related by a sequence of modified H-moves and global parallel-moves. The effect of either of these moves on a web in good position is to swap, possibly many, parallel oppositely oriented corner arcs in the triangles \mathfrak{T} of $\widehat{\lambda}$; recall Figures 25 and 3 above, respectively. By property (1) of $\Phi_{\mathfrak{T}}$, we have $\Phi_\lambda(W) = \Phi_\lambda(W_2)$.

From this point on, our approach diverges from that in [FS22]. In particular, our coordinates are different from theirs.

Definition 5.4. The *Fock–Goncharov global coordinate function*

$$\Phi_\lambda^{\text{FG}} : [\mathcal{W}_\mathfrak{S}] \longrightarrow \mathbb{Z}_{\geq 0}^N$$

is the well defined global coordinate function on $[\mathcal{W}_\mathfrak{S}]$, valued in nonnegative integers, induced by the Fock–Goncharov local coordinate function $\Phi_{\mathfrak{T}}^{\text{FG}}$. In §7-8, we prove:

Proposition 5.5. *The Fock–Goncharov global coordinate function Φ_λ^{FG} is an injection of sets.*

Remark 5.6. Proposition 5.5 is valid for any global coordinate function $\Phi_\lambda : [\mathcal{W}_\mathfrak{S}] \rightarrow \mathbb{Z}^N$ induced by a local coordinate function $\Phi_{\mathfrak{T}} : [\mathcal{W}_\mathfrak{T}] \rightarrow \mathbb{Z}^7$. The proof is the same as the one we will give for Φ_λ^{FG} and uses properties (4) and the second part of (2) in Definition 5.1.

Remark 5.7 (relation to Fock–Goncharov theory; see [DS20b] for a more detailed discussion). To a surface-with-boundary $\widehat{\mathfrak{S}}$ (see §9 below), Fock–Goncharov/Goncharov–Shen [FG06, GS15] associated two dual moduli spaces $\mathcal{A}_{\text{PGL}_3, \widehat{\mathfrak{S}}}$ and $\mathcal{R}_{\text{SL}_n, \widehat{\mathfrak{S}}}$, both of which are certain generalizations of the character variety. They are dual in the sense of Fock–Goncharov–Shen duality, which in particular says that the positive tropical integer points $\mathcal{A}_{\text{PGL}_3, \widehat{\mathfrak{S}}}^+(\mathbb{Z}^I)$ of the \mathcal{A} -moduli space index a natural linear basis for the ring $\mathcal{O}(\mathcal{R}_{\text{SL}_n, \widehat{\mathfrak{S}}})$ of regular functions on the generalized character variety. Here, the positivity is taken with respect to the tropicalized Goncharov–Shen potential.

An ideal triangulation λ determines a coordinate chart $\mathcal{A}_{\text{PGL}_3, \widehat{\mathfrak{S}}}^+(\mathbb{Z}^I)_\lambda$ of $\mathcal{A}_{\text{PGL}_3, \widehat{\mathfrak{S}}}^+(\mathbb{Z}^I)$. More concretely, in coordinates the positivity condition with respect to the tropicalized Goncharov–Shen potential translates to the Knutson–Tao rhombus inequalities (see §6 below), and in this way the coordinate chart $\mathcal{A}_{\text{PGL}_3, \widehat{\mathfrak{S}}}^+(\mathbb{Z}^I)_\lambda \cong \mathcal{C}_\lambda^+$ becomes identified with the Knutson–Tao cone \mathcal{C}_λ^+ . If λ' is another ideal triangulation, the coordinate change map $\mathcal{A}_{\text{PGL}_3, \widehat{\mathfrak{S}}}^+(\mathbb{Z}^I)_\lambda \rightarrow \mathcal{A}_{\text{PGL}_3, \widehat{\mathfrak{S}}}^+(\mathbb{Z}^I)_{\lambda'}$ takes the form of a tropicalized \mathcal{A} -coordinate cluster transformation. For these reasons, Theorems 1.1 and 1.2 can be interpreted as saying that the web coordinates constructed above provide a natural identification between the set $[\mathcal{W}_\mathfrak{S}]$ of parallel equivalence classes of rungless essential webs (see §9 below) and the positive tropical integer points $\mathcal{A}_{\text{PGL}_3, \widehat{\mathfrak{S}}}^+(\mathbb{Z}^I)$.

As another concrete manifestation of Fock–Goncharov duality, when the trace function Tr_W on the SL_3 -character variety associated to a basis web W is written as a polynomial in the Fock–Goncharov \mathcal{A} -coordinates, then this polynomial has a unique highest term, whose exponents are precisely the tropical \mathcal{A} -coordinates assigned to the web W ; see §9.3 below for more precise statements.

For a discussion of previous works motivating our construction, see the introduction as well as Remarks 3.10(2), 4.4, 5.3(1, 2), 6.5(1), 9.2, 9.12(2).

6. Knutson–Tao cone

For $N = -8\chi(\mathfrak{S}) > 0$, we construct a subset $\mathcal{E}_\lambda^+ \subseteq \mathbb{Z}_{\geq 0}^N$ that we will show, in §7-8, is the image $\mathcal{E}_\lambda^+ = \Phi_\lambda^{\text{FG}}([\mathcal{W}_\mathfrak{S}])$ of the mapping $\Phi_\lambda^{\text{FG}} : [\mathcal{W}_\mathfrak{S}] \rightarrow \mathbb{Z}_{\geq 0}^N$ constructed in §5. The subset \mathcal{E}_λ^+ is called the

Knutson–Tao cone associated to the ideal triangulation λ , and is defined by finitely many Knutson–Tao rhombus inequalities and modulo 3 congruence conditions.

6.1. Integer cones

Definition 6.1. An *integer cone*, or just *cone*, \mathcal{C} is a submonoid of \mathbb{Z}^n for some positive integer n . In other words, $\mathcal{C} \subseteq \mathbb{Z}^n$ is a subset that contains 0 and is closed under addition.

A *partition* of \mathcal{C} is a decomposition $\mathcal{C} = \mathcal{C}_1 \sqcup \mathcal{C}_2 \sqcup \dots \sqcup \mathcal{C}_k$ as a disjoint union of subsets.

A *positive integer cone*, or just *positive cone*, \mathcal{C}^+ is a cone that is contained in $\mathbb{Z}_{\geq 0}^n$.

We define notions of independence for cones.

Definition 6.2. Let $\mathcal{C} \subseteq \mathbb{Z}^n \subseteq \mathbb{Q}^n$ be a cone, and let $\Omega \subseteq \mathbb{Q}$ be a subset such that $0 \in \Omega$. Let c_1, c_2, \dots, c_k be a collection of cone points in \mathcal{C} . We say that the cone points $\{c_i\}$

1. *span* the cone \mathcal{C} if every cone point $c \in \mathcal{C}$ can be written as a $\mathbb{Z}_{\geq 0}$ -linear combination of the cone points $\{c_i\}$;
2. are *weakly independent* over Ω if

$$\omega_1 c_1 + \dots + \omega_k c_k = 0 \in \mathbb{Q}^n \implies \omega_1 = \dots = \omega_k = 0 \quad (\omega_1, \dots, \omega_k \in \Omega);$$

3. form a *weak basis* of \mathcal{C} if they span \mathcal{C} and are weakly independent over $\Omega = \mathbb{Z}_{\geq 0} \subseteq \mathbb{Q}$;
4. are *strongly independent* over Ω if

$$\omega_1 c_1 + \dots + \omega_k c_k = \omega'_1 c_1 + \dots + \omega'_k c_k \in \mathbb{Q}^n \implies \omega_1 = \omega'_1, \dots, \omega_k = \omega'_k \quad (\omega_i, \omega'_j \in \Omega).$$

Note:

- o strongly independent over $\Omega \implies$ weakly independent over Ω ;
- o strongly independent over $\mathbb{Z}_{\geq 0} \iff$ weakly independent over $\mathbb{Z} \iff$ linearly independent over \mathbb{Q} (the usual definition from linear algebra).

The following technical fact is immediate from the definitions.

Lemma 6.3. Let $\mathcal{C}, \mathcal{C}' \subseteq \mathbb{Z}^n$ be two cones. Consider a $\mathbb{Z}_{\geq 0}$ -linear bijection $\psi : \mathcal{C}' \rightarrow \mathcal{C}$ that extends to a \mathbb{Q} -linear isomorphism $\tilde{\psi} : \mathbb{Q}^n \rightarrow \mathbb{Q}^n$. Let $\{c_i\}$ be cone points of \mathcal{C} , and let $\{c'_i\}$ be cone points of \mathcal{C}' , such that $\psi(c'_i) = c_i$. Then,

1. if the cone points $\{c'_i\}$ span \mathcal{C}' , then the cone points $\{c_i\}$ span \mathcal{C} ;
2. if the $\{c'_i\}$ are weakly independent over $\mathbb{Z}_{\geq 0}$, then so are the $\{c_i\}$;
3. therefore, if the $\{c'_i\}$ form a weak basis of \mathcal{C}' , then the $\{c_i\}$ form a weak basis of \mathcal{C} ;
4. if the $\{c'_i\}$ are strongly independent over $\mathbb{Z}_{\geq 0}$, then so are the $\{c_i\}$;
5. the function ψ sends partitions of \mathcal{C}' to partitions of \mathcal{C} . □

6.2. Local Knutson–Tao cone

Let \mathfrak{X} be a dotted ideal triangle (§5.1); recall Figure 27b above. In this section, we are going to order the dots on \mathfrak{X} so that if the dots are labeled as in the left-hand side of Figure 34, then a point $c \in \mathbb{Z}^7$ will be written

$$c = (a_{11}, a_{12}, a_{21}, a_{22}, a_{31}, a_{32}, a) \in \mathbb{Z}^7. \tag{*}$$

Let $\mathbb{Z}/3 \subseteq \mathbb{Q}$ denote the set of integer thirds within the rational numbers, namely $\mathbb{Z}/3$ is the image of the map $\mathbb{Z} \rightarrow \mathbb{Q}$ sending $n \mapsto n/3$. Note that $\mathbb{Z} \subseteq \mathbb{Z}/3$.

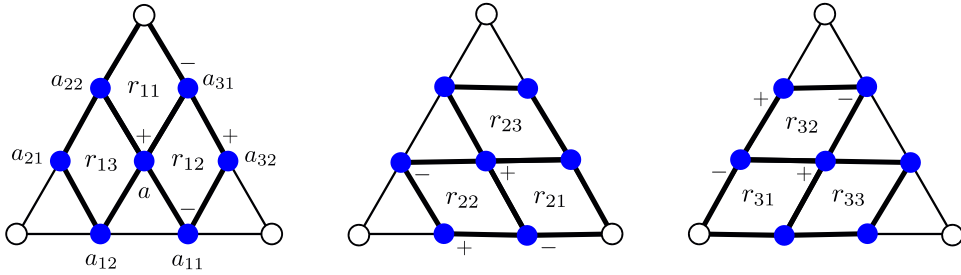


Figure 34. Rhombus numbers.

To each point $c \in \mathbb{Z}^7$, as in Equation (*), associate a nine-tuple of *rhombus numbers*

$$r(c) = (r_{11}, r_{12}, r_{13}, r_{21}, r_{22}, r_{23}, r_{31}, r_{32}, r_{33}) \in (\mathbb{Z}/3)^9$$

by the linear equations (see Figure 34 above)

$$\begin{aligned} r_{12} &= (a + a_{32} - a_{11} - a_{31})/3, & r_{11} &= (a_{22} + a_{31} - a - 0)/3, \\ r_{13} &= (a_{21} + a - a_{12} - a_{22})/3; \\ r_{22} &= (a + a_{12} - a_{21} - a_{11})/3, & r_{21} &= (a_{32} + a_{11} - a - 0)/3, \\ r_{23} &= (a_{31} + a - a_{22} - a_{32})/3; \\ r_{32} &= (a + a_{22} - a_{31} - a_{21})/3, & r_{31} &= (a_{12} + a_{21} - a - 0)/3, \\ r_{33} &= (a_{11} + a - a_{32} - a_{12})/3. \end{aligned}$$

Definition 6.4. The *local Knutson–Tao positive cone*, or just *local Knutson–Tao cone* or *local cone*, $\mathcal{C}_{\mathfrak{X}}^+$ associated to the dotted ideal triangle \mathfrak{X} is defined by

$$\mathcal{C}_{\mathfrak{X}}^+ = \{c \in \mathbb{Z}^7; \quad r(c) = (r_{11}, r_{12}, r_{13}, r_{21}, r_{22}, r_{23}, r_{31}, r_{32}, r_{33}) \in \mathbb{Z}_{\geq 0}^9 \subseteq (\mathbb{Z}/3)^9\}.$$

By linearity, this indeed defines a cone contained in \mathbb{Z}^7 . We will prove below in this subsection that $\mathcal{C}_{\mathfrak{X}}^+ \subseteq \mathbb{Z}_{\geq 0}^7$ is, in fact, a positive cone.

Remark 6.5.

1. The inequalities $3r_{ij} \geq 0$ are known as the Knutson–Tao rhombus inequalities; see [KT99, Appendix 2] and [GS15, §3.1]. Note that $3r_{ij}$ is always in \mathbb{Z} by definition. We impose the additional modulo 3 congruence condition that the r_{ij} are integers. This is analogous to the parity condition imposed in [Foc97, §3.1] in the case of SL_2 .
2. By the proof of Proposition 6.6 below, we could just as well have taken rational coefficients $c \in \mathbb{Q}^7$ in Definition 6.4 without changing the resulting cone $\mathcal{C}_{\mathfrak{X}}^+ \subseteq \mathbb{Z}_{\geq 0}^7 \subseteq \mathbb{Q}^7$. That is, any rational solution to $r(c) \in \mathbb{Z}_{\geq 0}^9$ is, in fact, a nonnegative integer solution.

To see that $\mathcal{C}_{\mathfrak{X}}^+$ is nontrivial, one checks that the image $\Phi_{\mathfrak{X}}^{\text{FG}}(\mathcal{W}_{\mathfrak{X}})$ of the Fock-Goncharov local coordinate function $\Phi_{\mathfrak{X}}^{\text{FG}} : \mathcal{W}_{\mathfrak{X}} \rightarrow \mathbb{Z}_{\geq 0}^7$ (§5.3) lies in the local cone $\Phi_{\mathfrak{X}}^{\text{FG}}(\mathcal{W}_{\mathfrak{X}}) \subseteq \mathcal{C}_{\mathfrak{X}}^+$. By property (1)

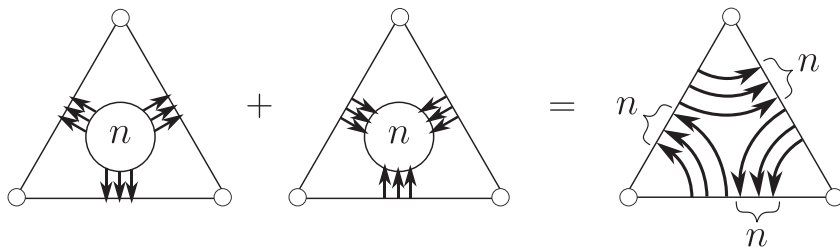


Figure 35. Linear dependence relation over \mathbb{Z} .

in Definition 5.1, it suffices to check this on the connected local webs in $\mathcal{W}_{\mathfrak{X}}$; recall Figure 30 above. Specifically, using the convention in Equation (*), we have

$$\begin{aligned}
 c(R_1) &= \Phi_{\mathfrak{X}}^{\text{FG}}(R_1) = (0, 0, 1, 2, 2, 1, 1), & c(L_1) &= \Phi_{\mathfrak{X}}^{\text{FG}}(L_1) = (0, 0, 2, 1, 1, 2, 2), \\
 c(R_2) &= \Phi_{\mathfrak{X}}^{\text{FG}}(R_2) = (2, 1, 0, 0, 1, 2, 1), & c(L_2) &= \Phi_{\mathfrak{X}}^{\text{FG}}(L_2) = (1, 2, 0, 0, 2, 1, 2), \\
 c(R_3) &= \Phi_{\mathfrak{X}}^{\text{FG}}(R_3) = (1, 2, 2, 1, 0, 0, 1), & c(L_3) &= \Phi_{\mathfrak{X}}^{\text{FG}}(L_3) = (2, 1, 1, 2, 0, 0, 2), \\
 c(H_n^{\text{in}}) &= \Phi_{\mathfrak{X}}^{\text{FG}}(H_n^{\text{in}}) = (2n, n, 2n, n, 2n, n, 3n), \\
 c(H_n^{\text{out}}) &= \Phi_{\mathfrak{X}}^{\text{FG}}(H_n^{\text{out}}) = (n, 2n, n, 2n, n, 2n, 3n).
 \end{aligned}$$

The associated nine-tuples of rhombus numbers are

$$\begin{aligned}
 r(c(R_1)) &= (1, 0, 0, 0, 0, 0, 0, 0, 0), & r(c(L_1)) &= (0, 1, 1, 0, 0, 0, 0, 0, 0), \\
 r(c(R_2)) &= (0, 0, 0, 1, 0, 0, 0, 0, 0), & r(c(L_2)) &= (0, 0, 0, 0, 1, 1, 0, 0, 0), \\
 r(c(R_3)) &= (0, 0, 0, 0, 0, 0, 1, 0, 0), & r(c(L_3)) &= (0, 0, 0, 0, 0, 0, 0, 1, 1), \\
 r(c(H_n^{\text{in}})) &= (0, 0, n, 0, 0, n, 0, 0, n), \\
 r(c(H_n^{\text{out}})) &= (0, n, 0, 0, 0, n, 0, 0, n).
 \end{aligned}$$

By rank considerations, the eight cone points $c(R_1), c(L_1), c(R_2), c(L_2), c(R_3), c(L_3), c(H_n^{\text{in}}), c(H_n^{\text{out}})$ have a linear dependence relation over \mathbb{Z} . For instance (see Figure 35),

$$c(H_n^{\text{out}}) + c(H_n^{\text{in}}) = n(c(L_1) + c(L_2) + c(L_3)) \in \mathcal{C}_{\mathfrak{X}}^+.$$

Nevertheless, we can say the following:

Proposition 6.6. *The collection of eight cone points*

$$c(R_1), c(L_1), c(R_2), c(L_2), c(R_3), c(L_3), c(H_1^{\text{in}}), c(H_1^{\text{out}}) \in \Phi_{\mathfrak{X}}^{\text{FG}}(\mathcal{W}_{\mathfrak{X}}) \subseteq \mathcal{C}_{\mathfrak{X}}^+$$

forms a weak basis of the Knutson–Tao local cone $\mathcal{C}_{\mathfrak{X}}^+$.

Among these eight cone points, the seven points

$$c(R_1), c(L_1), c(R_2), c(L_2), c(R_3), c(L_3), c(H_1^{\text{in}})$$

are strongly independent over $\mathbb{Z}_{\geq 0}$, and the seven points

$$c(R_1), c(L_1), c(R_2), c(L_2), c(R_3), c(L_3), c(H_1^{\text{out}})$$

are strongly independent over $\mathbb{Z}_{\geq 0}$. Moreover, each cone point c in $\mathcal{C}_{\mathfrak{X}}^+$ can be uniquely expressed in exactly one of the following three forms:

$$\begin{aligned} c &= n_1c(R_1) + n_2c(L_1) + \cdots + n_6c(L_3), \\ c &= n_1c(R_1) + n_2c(L_1) + \cdots + n_6c(L_3) + nc(H_1^{\text{in}}), \\ c &= n_1c(R_1) + n_2c(L_1) + \cdots + n_6c(L_3) + nc(H_1^{\text{out}}), \quad (n_i \in \mathbb{Z}_{\geq 0}, \quad n \in \mathbb{Z}_{>0}). \end{aligned}$$

Because the spanning set $c(R_1), c(L_1), c(R_2), c(L_2), c(R_3), c(L_3), c(H_1^{\text{in}}), c(H_1^{\text{out}})$ consists of positive points, we immediately obtain:

Corollary 6.7. *The local Knutson–Tao cone satisfies the property that $\mathcal{C}_{\mathfrak{X}}^+ = \Phi_{\mathfrak{X}}^{\text{FG}}(\mathcal{W}_{\mathfrak{X}}) \subseteq \mathbb{Z}_{\geq 0}^7$. In particular, $\mathcal{C}_{\mathfrak{X}}^+$ is a positive cone. \square*

Corollary 6.8. *The Fock–Goncharov local coordinate function $\Phi_{\mathfrak{X}}^{\text{FG}} : \mathcal{W}_{\mathfrak{X}} \rightarrow \mathcal{C}_{\mathfrak{X}}^+$ satisfies property (4) in Definition 5.1, namely, the induced function $\Phi_{\mathfrak{X}}^{\text{FG}} : [\mathcal{W}_{\mathfrak{X}}] \hookrightarrow \mathcal{C}_{\mathfrak{X}}^+$, defined on the collection of corner-ambiguity classes $[W_{\mathfrak{X}}]$ of local webs $W_{\mathfrak{X}}$ in $\mathcal{W}_{\mathfrak{X}}$, is an injection.*

Proof. Assume $\Phi_{\mathfrak{X}}^{\text{FG}}(W_{\mathfrak{X}}) = \Phi_{\mathfrak{X}}^{\text{FG}}(W'_{\mathfrak{X}}) \in \mathcal{C}_{\mathfrak{X}}^+$. This cone point falls into one of the three families in Proposition 6.6. For the sake of argument, suppose

$$\Phi_{\mathfrak{X}}^{\text{FG}}(W_{\mathfrak{X}}) = \Phi_{\mathfrak{X}}^{\text{FG}}(W'_{\mathfrak{X}}) = n_1c(R_1) + n_2c(L_1) + \cdots + n_6c(L_3) + nc(H_1^{\text{in}}) \quad (n_i \in \mathbb{Z}_{\geq 0}, \quad n \in \mathbb{Z}_{>0}).$$

Note that $nc(H_1^{\text{in}}) = c(H_n^{\text{in}})$ in $\mathcal{C}_{\mathfrak{X}}^+$; see Figure 30. By the uniqueness property in Proposition 6.6 together with property (1) in Definition 5.1, we gather that $W_{\mathfrak{X}}$ and $W'_{\mathfrak{X}}$ have $1 + \sum_{i=1}^6 n_i$ connected components, one of which is a n -in-honeycomb H_n^{in} , and n_1 (resp. n_2, n_3, n_4, n_5, n_6) of which are corner arcs R_1 (resp. L_1, R_2, L_2, R_3, L_3). The only ambiguity is how these corner arcs are permuted on their respective corners, that is $[W_{\mathfrak{X}}] = [W'_{\mathfrak{X}}]$ in $[\mathcal{W}_{\mathfrak{X}}]$. \square

Proof of Proposition 6.6. Define two subsets $\overline{(\mathcal{C}_{\mathfrak{X}}^+)^{\text{in}}}$ and $(\mathcal{C}_{\mathfrak{X}}^+)^{\text{out}}$ of $\mathcal{C}_{\mathfrak{X}}^+$ by

$$\overline{(\mathcal{C}_{\mathfrak{X}}^+)^{\text{in}}} = \text{Span}_{\mathbb{Z}_{\geq 0}}(c(R_1), c(L_1), c(R_2), c(L_2), c(R_3), c(L_3)) + \mathbb{Z}_{\geq 0} \cdot c(H_1^{\text{in}}), \tag{\#}$$

$$(\mathcal{C}_{\mathfrak{X}}^+)^{\text{out}} = \text{Span}_{\mathbb{Z}_{\geq 0}}(c(R_1), c(L_1), c(R_2), c(L_2), c(R_3), c(L_3)) + \mathbb{Z}_{>0} \cdot c(H_1^{\text{out}}). \tag{\#\#}$$

(Here, $A + B = \{a + b; \quad a \in A \text{ and } b \in B\}$.) Put

$$\begin{aligned} c_1 &= c(R_1), & c_2 &= c(L_1), & c_3 &= c(R_2), & c_4 &= c(L_2), \\ c_5 &= c(R_3), & c_6 &= c(L_3), & c_7 &= c(H_1^{\text{in}}), & c_8 &= c(H_1^{\text{out}}). \end{aligned}$$

By Lemma 6.3, with $\mathcal{C} = \mathcal{C}_{\mathfrak{X}}^+$, in order to prove Proposition 6.6 it suffices to establish:

Claim 6.9. *There exists*

1. a cone $\mathcal{C}' \subseteq \mathbb{Z}^7$;
2. a collection of cone points c'_1, \dots, c'_8 in \mathcal{C}' ;
3. a partition $\mathcal{C}' = \overline{(\mathcal{C}')^{>0}} \sqcup (\mathcal{C}')^{<0}$;
4. a $\mathbb{Z}_{>0}$ -linear bijection $\psi : \mathcal{C}' \rightarrow \mathcal{C}_{\mathfrak{X}}^+$;
5. an extension $\tilde{\psi}$ of ψ to a \mathbb{Q} -linear isomorphism $\tilde{\psi} : \mathbb{Q}^7 \rightarrow \mathbb{Q}^7$;

such that

1. we have $\psi(c'_i) = c_i$;
2. we have $\psi((\mathcal{C}')^{>0}) = \overline{(\mathcal{C}_{\mathfrak{X}}^+)^{\text{in}}}$ and $\psi((\mathcal{C}')^{<0}) = (\mathcal{C}_{\mathfrak{X}}^+)^{\text{out}}$;
3. the eight cone points $c'_1, \dots, c'_6, c'_7, c'_8$ form a weak basis of the cone \mathcal{C}' ;

- 4. the seven cone points c'_1, \dots, c'_6, c'_7 are strongly independent over $\mathbb{Z}_{\geq 0}$;
- 5. the seven cone points c'_1, \dots, c'_6, c'_8 are strongly independent over $\mathbb{Z}_{> 0}$.

We prove the claim. Define $\mathcal{C}' \subseteq \mathbb{Z}_{\geq 0}^6 \times \mathbb{Z} \subseteq \mathbb{Z}^7$ by

$$\mathcal{C}' = \{(r_{11}, r_{12}, r_{21}, r_{22}, r_{31}, r_{32}, x) \in \mathbb{Z}_{\geq 0}^6 \times \mathbb{Z}; \quad -x \leq \min(r_{12}, r_{22}, r_{32})\}. \tag{**}$$

It follows from the definition that \mathcal{C}' is a cone. Put

$$\begin{aligned} c'_1 &= (1, 0, 0, 0, 0, 0, 0), & c'_2 &= (0, 1, 0, 0, 0, 0, 0), \\ c'_3 &= (0, 0, 1, 0, 0, 0, 0), & c'_4 &= (0, 0, 0, 1, 0, 0, 0), \\ c'_5 &= (0, 0, 0, 0, 1, 0, 0), & c'_6 &= (0, 0, 0, 0, 0, 1, 0), \\ c'_7 &= (0, 0, 0, 0, 0, 0, 1), & c'_8 &= (0, 1, 0, 1, 0, 1, -1). \end{aligned}$$

One checks that c'_1, \dots, c'_8 are in \mathcal{C}' . Define

$$\overline{(\mathcal{C}')^{>0}} = \mathcal{C}' \cap (\mathbb{Z}_{\geq 0}^6 \times \mathbb{Z}_{\geq 0}), \quad (\mathcal{C}')^{<0} = \mathcal{C}' \cap (\mathbb{Z}_{\geq 0}^6 \times \mathbb{Z}_{< 0}).$$

Then $\mathcal{C}' = \overline{(\mathcal{C}')^{>0}} \sqcup (\mathcal{C}')^{<0}$ is a partition.

First, we show $c'_1, \dots, c'_6, c'_7, c'_8$ spans \mathcal{C}' . We see that

$$\overline{(\mathcal{C}')^{>0}} = \text{Span}_{\mathbb{Z}_{\geq 0}}(c'_1, \dots, c'_6) + \mathbb{Z}_{\geq 0} \cdot c'_7 \quad (= \mathbb{Z}_{\geq 0}^6 \times \mathbb{Z}_{\geq 0}). \tag{\dagger}$$

If $c' \in (\mathcal{C}')^{<0}$, then its last coordinate is $x \leq -1$. Since $-x > 0$ and $-x \leq \min(r_{12}, r_{22}, r_{32})$,

$$c' = (r_{11}, -x + r'_{12}, r_{21}, -x + r'_{22}, r_{31}, -x + r'_{32}, -x \cdot -1)$$

for some $r_{11}, r'_{12}, r_{21}, r'_{22}, r_{31}, r'_{32} \in \mathbb{Z}_{\geq 0}$ and $-x \in \mathbb{Z}_{> 0}$. That is,

$$c' = r_{11}c'_1 + r'_{12}c'_2 + r_{21}c'_3 + r'_{22}c'_4 + r_{31}c'_5 + r'_{32}c'_6 + (-x)c'_8 \in \text{Span}_{\mathbb{Z}_{\geq 0}}(c'_1, \dots, c'_6) + \mathbb{Z}_{> 0} \cdot c'_8.$$

Thus,

$$(\mathcal{C}')^{<0} = \text{Span}_{\mathbb{Z}_{\geq 0}}(c'_1, \dots, c'_6) + \mathbb{Z}_{> 0} \cdot c'_8, \tag{\dagger\dagger}$$

where the \supseteq containment follows since $\text{Span}_{\mathbb{Z}_{\geq 0}}(c'_1, \dots, c'_6) + \mathbb{Z}_{> 0} \cdot c'_8 \subseteq \mathbb{Z}_{\geq 0}^6 \times \mathbb{Z}_{< 0}$.

Next, we show $c'_1, \dots, c'_6, c'_7, c'_8$ are weakly independent over $\mathbb{Z}_{\geq 0}$. Indeed, if $n_1c'_1 + \dots + n_7c'_7 + n_8c'_8 = 0$, then $n_1 = n_3 = n_5 = 0$ and $n_2 + n_8, n_4 + n_8, n_6 + n_8, n_7 - n_8 = 0$. Since all $n_i \in \mathbb{Z}_{\geq 0}$, it follows that $n_2 = n_4 = n_6 = n_8 = 0$, and so $n_7 = n_8 = 0$, as desired.

We gather that $c'_1, \dots, c'_6, c'_7, c'_8$ form a weak basis of \mathcal{C}' .

Next, we show c'_1, \dots, c'_6, c'_7 are strongly independent over $\mathbb{Z}_{\geq 0}$. This is equivalent to being linearly independent over \mathbb{Q} , which follows from the definitions. Similarly, it follows from the definitions that c'_1, \dots, c'_6, c'_8 are strongly independent over $\mathbb{Z}_{\geq 0}$.

We now define a $\mathbb{Z}_{\geq 0}$ -linear bijection $\varphi: \mathcal{C}'_{\mathbb{Z}}^+ \rightarrow \mathcal{C}'$. Its inverse will be the desired $\mathbb{Z}_{\geq 0}$ -linear bijection $\psi = \varphi^{-1}: \mathcal{C}' \rightarrow \mathcal{C}'_{\mathbb{Z}}^+$. Let c be a cone point in $\mathcal{C}'_{\mathbb{Z}}^+$, written as in Equation (*). Put

$$\begin{aligned} x &= (a_{11} - a_{12} + a_{21} - a_{22} + a_{31} - a_{32})/3 \\ &= r_{13} - r_{12} = r_{23} - r_{22} = r_{33} - r_{32} \\ &\geq -r_{12} \text{ and } -r_{22} \text{ and } -r_{32}, \end{aligned}$$

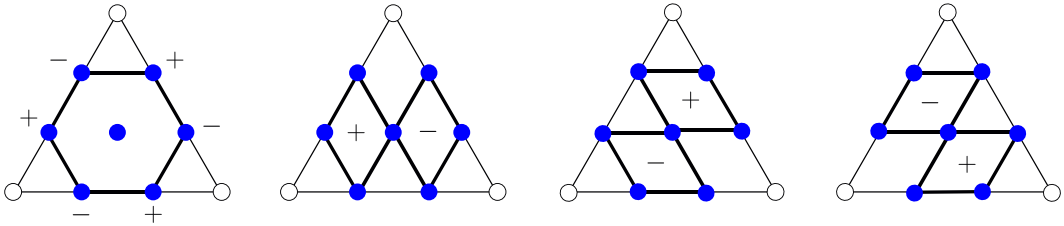


Figure 36. Four ways to view the tropical Fock–Goncharov \mathcal{X} -coordinate.

where the rhombus numbers r_{ij} are in $\mathbb{Z}_{\geq 0}$ since $c \in \mathcal{E}_{\mathfrak{T}}^+$; see Figure 36 (we think of x as the tropical Fock–Goncharov \mathcal{X} -coordinate for the triangle). Thus,

$$x \geq \max(-r_{12}, -r_{22}, -r_{32}) = -\min(r_{12}, r_{22}, r_{32}).$$

Therefore, recalling $\mathcal{E}' \subseteq \mathbb{Z}_{\geq 0}^6 \times \mathbb{Z}$ (Equation (**)), we may define the function $\varphi: \mathcal{E}_{\mathfrak{T}}^+ \rightarrow \mathcal{E}'$ by

$$\varphi(c) = (r_{11}, r_{12}, r_{21}, r_{22}, r_{31}, r_{32}, x).$$

It follows from the definition that $\varphi: \mathcal{E}_{\mathfrak{T}}^+ \rightarrow \mathcal{E}'$ is $\mathbb{Z}_{\geq 0}$ -linear. One checks that $\varphi(c_i) = c'_i$. Since the c'_i span \mathcal{E}' , we have φ is surjective. In particular, by Equations (#),(##),(†),(††),

$$\varphi(\overline{(\mathcal{E}_{\mathfrak{T}}^+)^{\text{in}}}) = \overline{(\mathcal{E}')^{>0}} \quad \text{and} \quad \varphi((\mathcal{E}_{\mathfrak{T}}^+)^{\text{out}}) = (\mathcal{E}')^{<0}.$$

The formula for φ extends to define a \mathbb{Q} -linear isomorphism $\tilde{\varphi}: \mathbb{Q}^7 \rightarrow \mathbb{Q}^7$, and its inverse is the desired \mathbb{Q} -linear isomorphism $\tilde{\psi} = (\tilde{\varphi})^{-1}: \mathbb{Q}^7 \rightarrow \mathbb{Q}^7$. Indeed, the bijectivity of $\tilde{\varphi}$ follows by computing the values on the standard column basis of \mathbb{Q}^7 , giving the invertible matrix

$$\tilde{\varphi}(\vec{e}_1, \vec{e}_2, \vec{e}_3, \vec{e}_4, \vec{e}_5, \vec{e}_6, \vec{e}_7) = \frac{1}{3} \begin{pmatrix} 0 & 0 & 0 & 1 & 1 & 0 & -1 \\ -1 & 0 & 0 & 0 & -1 & 1 & 1 \\ 1 & 0 & 0 & 0 & 0 & 1 & -1 \\ -1 & 1 & -1 & 0 & 0 & 0 & 1 \\ 0 & 1 & 1 & 0 & 0 & 0 & -1 \\ 0 & 0 & -1 & 1 & -1 & 0 & 1 \\ 1 & -1 & 1 & -1 & 1 & -1 & 0 \end{pmatrix}.$$

So $\tilde{\psi} = (\tilde{\varphi})^{-1}$ is defined. Since $\tilde{\varphi}$ is an injection so is its restriction $\varphi: \mathcal{E}_{\mathfrak{T}}^+ \rightarrow \mathcal{E}'$. Also, since, as we argued above, φ is a surjection, we gather φ is a bijection. Thus, $\psi = \varphi^{-1}: \mathcal{E}' \rightarrow \mathcal{E}_{\mathfrak{T}}^+$ is defined. This completes the proof of the claim, thereby establishing the proposition. \square

6.3. Global Knutson–Tao cone

Given the dotted ideal triangulation λ on the surface \mathfrak{S} , an element c of \mathbb{Z}^N corresponds to a function {dots on λ } $\rightarrow \mathbb{Z}$; see §5.1. If \mathfrak{T} is a dotted triangle of λ , then an element c of \mathbb{Z}^N induces a function {dots on \mathfrak{T} } $\rightarrow \mathbb{Z}$, which likewise corresponds to an element $c_{\mathfrak{T}}$ of \mathbb{Z}^7 .

Definition 6.10. The global Knutson–Tao positive cone, or just Knutson–Tao cone or global cone, $\mathcal{E}_{\lambda}^+ \subseteq \mathbb{Z}_{\geq 0}^N$ is defined by

$$\mathcal{E}_{\lambda}^+ = \{c \in \mathbb{Z}^N; \quad c_{\mathfrak{T}} \text{ is in } \mathcal{E}_{\mathfrak{T}}^+ \text{ for all triangles } \mathfrak{T} \text{ of } \lambda\}.$$

It follows from Corollary 6.7 that $\mathcal{E}_{\lambda}^+ \subseteq \mathbb{Z}_{\geq 0}^N$ is indeed a positive cone.

In §5, we defined the global coordinate function $\Phi_{\lambda}^{\text{FG}}: [\mathcal{W}_{\mathfrak{S}}] \rightarrow \mathbb{Z}_{\geq 0}^N$; see Definition 5.4. Since the image $\Phi_{\lambda}^{\text{FG}}([\mathcal{W}_{\mathfrak{T}}]) \subseteq \mathcal{E}_{\mathfrak{T}}^+$ (which is, in fact, an equality by Corollary 6.7), it follows by the construction of $\Phi_{\lambda}^{\text{FG}}$ that the image $\Phi_{\lambda}^{\text{FG}}([\mathcal{W}_{\mathfrak{S}}]) \subseteq \mathcal{E}_{\lambda}^+$; recall, for instance, Figure 33.

Proposition 6.11. *Moreover, we have (see §7-8 for a proof)*

$$\Phi_\lambda^{\text{FG}}([\mathcal{W}_\mathfrak{S}]) = \mathcal{C}_\lambda^+.$$

7. Main result: global coordinates

We summarize what we have done so far. Consider a punctured surface \mathfrak{S} with empty boundary; see §2. Let $[\mathcal{W}_\mathfrak{S}]$ denote the collection of parallel equivalence classes of global nonelliptic webs on \mathfrak{S} . Assume that \mathfrak{S} is equipped with an ideal triangulation λ . For $N = -8\chi(\mathfrak{S})$, in §5 we defined the Fock–Goncharov global coordinate function $\Phi_\lambda^{\text{FG}} : [\mathcal{W}_\mathfrak{S}] \rightarrow \mathbb{Z}_{\geq 0}^N$, depending on the choice of the ideal triangulation λ . Proposition 5.5, which still needs to be proved, says that the mapping Φ_λ^{FG} is injective. In §6, we defined the global Knutson–Tao positive cone $\mathcal{C}_\lambda^+ \subseteq \mathbb{Z}_{\geq 0}^N$, which also depends on the ideal triangulation λ . By construction, the image $\Phi_\lambda^{\text{FG}}([\mathcal{W}_\mathfrak{S}]) \subseteq \mathcal{C}_\lambda^+$. According to Proposition 6.11, which also still needs to be proved, Φ_λ^{FG} maps $[\mathcal{W}_\mathfrak{S}]$ onto \mathcal{C}_λ^+ . Therefore, assuming Propositions 5.5 and 6.11, we have proved:

Theorem 7.1. *The Fock–Goncharov global coordinate function*

$$\Phi_\lambda^{\text{FG}} : [\mathcal{W}_\mathfrak{S}] \xrightarrow{\sim} \mathcal{C}_\lambda^+ \subseteq \mathbb{Z}_{\geq 0}^N$$

is a bijection of sets. □

Remark 7.2. In §9, we generalize Theorem 7.1 to the setting of surfaces-with-boundary $\widehat{\mathfrak{S}}$.

7.1. Inverse mapping

Our strategy for proving Propositions 5.5 and 6.11 (equivalently, Theorem 7.1) is to construct an explicit inverse mapping

$$\Psi_\lambda^{\text{FG}} : \mathcal{C}_\lambda^+ \longrightarrow [\mathcal{W}_\mathfrak{S}],$$

namely a function that is both a left and a right inverse for the function Φ_λ^{FG} . The definition of the mapping Ψ_λ^{FG} is relatively straightforward, and it will be automatic that it is an inverse for Φ_λ^{FG} . The more challenging part will be to show that Ψ_λ^{FG} is well defined.

7.2. Inverse mapping: ladder gluing construction

Recall that for a triangle \mathfrak{T} we denote by $\mathcal{W}_\mathfrak{T}$ the collection of rungless essential local webs $W_\mathfrak{T}$ in \mathfrak{T} ; see Definition 3.19. We will once again make use of the split ideal triangulation $\widehat{\lambda}$; see §4.3.

Definition 7.3. A collection $\{W_\mathfrak{T}\}_{\mathfrak{T} \in \widehat{\lambda}}$ of local webs $W_\mathfrak{T} \in \mathcal{W}_\mathfrak{T}$, varying over the triangles \mathfrak{T} of $\widehat{\lambda}$, is *compatible* if for each biangle \mathfrak{B} , with boundary edges E' and E'' , sitting between two triangles \mathfrak{T}' and \mathfrak{T}'' , respectively, the number of out-strands (resp. in-strands) of $W_{\mathfrak{T}'}$ on E' is equal to the number of in-strands (resp. out-strands) of $W_{\mathfrak{T}''}$ on E'' .

For example, see the third row of Figure 37, an example on a once-punctured torus.

To a compatible collection $\{W_\mathfrak{T}\}_{\mathfrak{T} \in \widehat{\lambda}}$ of local webs, we will associate a global web W on \mathfrak{S} that need not be nonelliptic and that is in good position with respect to $\widehat{\lambda}$; recall Definition 4.5. The global web W is well defined up to ambient isotopy of \mathfrak{S} respecting $\widehat{\lambda}$.

Construction of W . Consider a biangle \mathfrak{B} sitting between two triangles \mathfrak{T}' and \mathfrak{T}'' . The local webs $W_{\mathfrak{T}'}$ and $W_{\mathfrak{T}''}$ determine strand sets S' and S'' on the boundary edges E' and E'' , respectively. By the compatibility property, the strand-set pair $S = (S', S'')$ is symmetric; see Definition 3.12. Let $W_\mathfrak{B} = W_\mathfrak{B}(S)$ be the induced ladder-web in \mathfrak{B} ; see Definition 3.14.

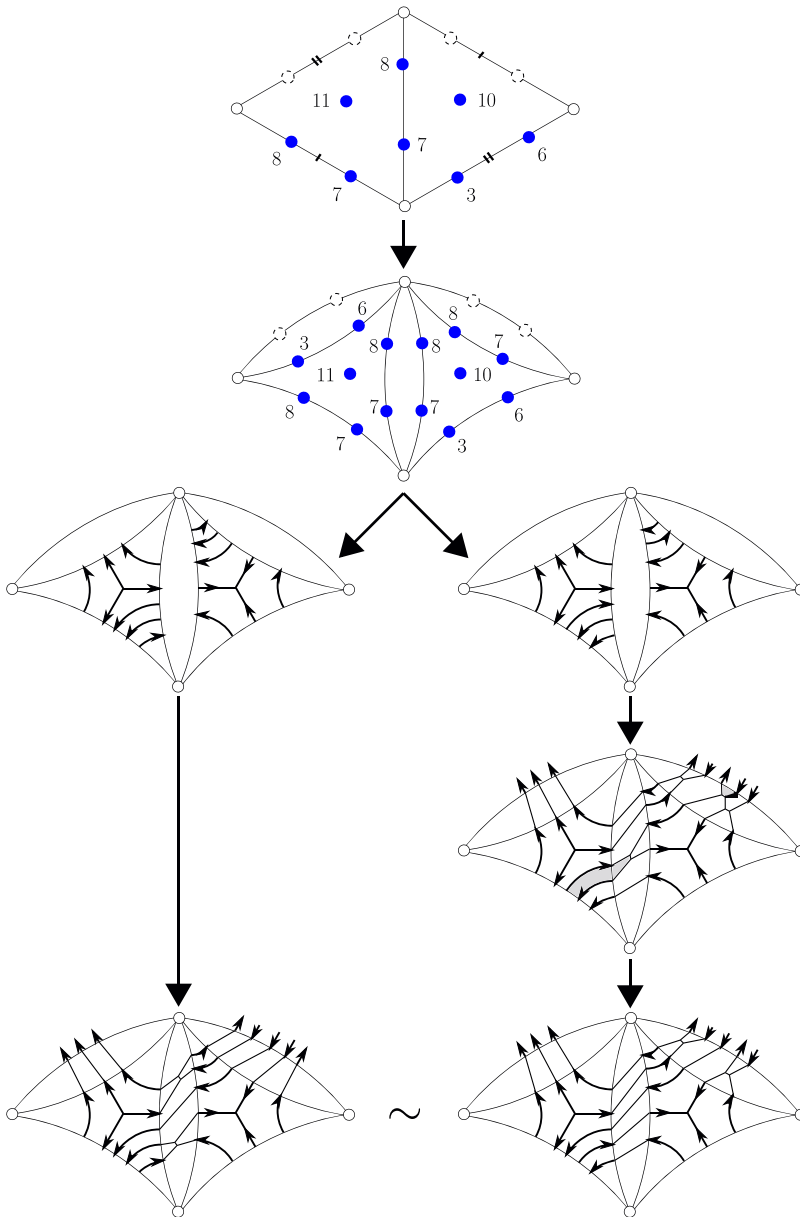


Figure 37. Ladder gluing construction (on the once-punctured torus). Shown are two different ways of assigning the local webs, differing by permutations of corner arcs. On the left, the result of the gluing is a nonelliptic web. On the right, the result is an elliptic web, which has to be resolved by removing a square before becoming a nonelliptic web. The two nonelliptic webs obtained in this way are equivalent.

Define W to be the global web obtained by gluing together the local webs $\{W_{\mathfrak{I}}\}_{\mathfrak{I} \in \hat{\lambda}}$ and $\{W_{\mathfrak{B}}\}_{\mathfrak{B} \in \hat{\lambda}}$ in the obvious way; see the fourth row and the left side of the fifth row of Figure 37.

Definition 7.4. We say that the global web W has been obtained from the compatible collection $\{W_{\mathfrak{I}}\}_{\mathfrak{I} \in \hat{\lambda}}$ of local webs by applying the ladder gluing construction.

The following statement is immediate.

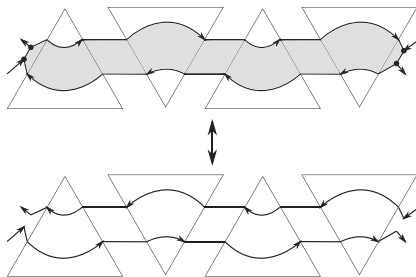


Figure 38. Resolving a square-face.

Lemma 7.5. *A global web W obtained via the ladder gluing construction is in good position with respect to $\widehat{\lambda}$. Conversely, if W is a global web in good position, then W can be recovered as the result of applying the ladder gluing construction to $\{W_{\mathfrak{T}} = W \cap \mathfrak{T}\}_{\mathfrak{T} \in \widehat{\lambda}}$. \square*

If the global web W is obtained via the ladder gluing construction, then W could be (1) nonelliptic, for example, see the left side of the fifth row of Figure 37, or (2) elliptic, for example, see the fourth row of Figure 37.

7.3. Inverse mapping: resolving an elliptic web

Recall the notion of a local parallel-move; see Figure 21. Note that if $\{W'_{\mathfrak{T}}\}_{\mathfrak{T} \in \widehat{\lambda}}$ is a compatible collection of local webs and if $W_{\mathfrak{T}}$ is related to $W'_{\mathfrak{T}}$ by a sequence of local parallel-moves, then $\{W_{\mathfrak{T}}\}_{\mathfrak{T} \in \widehat{\lambda}}$ is also compatible.

Lemma 7.6. *Given a compatible collection $\{W'_{\mathfrak{T}}\}_{\mathfrak{T} \in \widehat{\lambda}}$ of local webs, there exist local webs $\{W_{\mathfrak{T}}\}_{\mathfrak{T} \in \widehat{\lambda}}$ such that $W_{\mathfrak{T}}$ is related to $W'_{\mathfrak{T}}$ by a sequence of local parallel-moves and the global web W obtained by applying the ladder gluing construction to $\{W_{\mathfrak{T}}\}_{\mathfrak{T} \in \widehat{\lambda}}$ is nonelliptic.*

Proof. Suppose that the global web W' obtained by applying the ladder gluing construction to the local webs $\{W'_{\mathfrak{T}}\}_{\mathfrak{T} \in \widehat{\lambda}}$ is elliptic.

Step 1. We show that the elliptic global web W' has no disk- or bigon-faces. If there were a disk- or bigon-face, then it could not lie completely in a triangle \mathfrak{T} or biangle \mathfrak{B} of $\widehat{\lambda}$, for this would violate that the local web restriction $W'_{\mathfrak{T}}$ or $W'_{\mathfrak{B}}$ is essential (in particular, nonelliptic) by Lemma 7.5. Consequently, there is a cap- or fork-face lying in some \mathfrak{T} or \mathfrak{B} , contradicting that the local web restriction $W'_{\mathfrak{T}}$ or $W'_{\mathfrak{B}}$ is essential (in particular, taut).

Step 2. We consider the possible positions of square-faces relative to the split ideal triangulation $\widehat{\lambda}$. We claim that a square-face can only appear as demonstrated at the top of Figure 38, namely having two H-faces in two (possibly identical) biangles \mathfrak{B} and, in between, having opposite sides traveling parallel through the intermediate triangles \mathfrak{T} and biangles \mathfrak{B} . Indeed, otherwise there would be a square-, cap-, or fork-face, similar to Step 1.

Step 3. We remove a square-face. Since the square-faces are positioned in this way, given a fixed square-face there is a well defined *state* into which the square-face can be resolved, illustrated in Figure 38. The resulting global web W_1 is in good position with respect to $\widehat{\lambda}$. Also, W_1 is less complex than W' , where the *complexity* of a global web in good position is measured by the total number of vertices lying in the union $\cup_{\mathfrak{B}} \mathfrak{B}$ of all of the biangles \mathfrak{B} . Note that resolving a square-face decreases the complexity by four.

The effect of resolving a square-face is to perform, in each triangle \mathfrak{T} , some number (possibly zero) of local parallel-moves, replacing the original local webs $\{W'_{\mathfrak{T}}\}_{\mathfrak{T} \in \widehat{\lambda}}$ with new local webs $\{(W_1)_{\mathfrak{T}}\}_{\mathfrak{T} \in \widehat{\lambda}}$ such that $(W_1)_{\mathfrak{T}}$ is equivalent to $W'_{\mathfrak{T}}$ up to corner-ambiguity; see Figure 38.

Step 4. By a complexity argument, we can repeat the previous step until we obtain a sequence $W' = W_0, W_1, W_2, \dots, W_n = W$ of global webs in good position such that $\{(W_{i+1})_{\mathfrak{T}}\}_{\mathfrak{T} \in \widehat{\lambda}}$ is related to

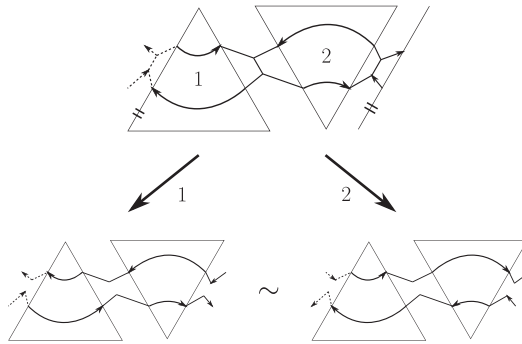


Figure 39. Elliptic web resulting from the ladder gluing construction (top) and two different applications of the square removing algorithm, yielding different, but parallel equivalent, nonelliptic webs (bottom).

$\{(W_i)_{\mathfrak{T}}\}_{\mathfrak{T} \in \widehat{\lambda}}$ by a sequence of local parallel-moves and such that W has no square-faces. By Lemma 7.5, W is recovered by applying the ladder gluing construction to $\{W_{\mathfrak{T}}\}_{\mathfrak{T} \in \widehat{\lambda}}$. By Step 1, W has no disk- or bigon-faces. Thus, W is nonelliptic. \square

We refer to the algorithm used in the proof of Lemma 7.6 as the *square removing algorithm*. For example, see the fourth row and the right side of the fifth row of Figure 37.

Note that the algorithm removes the square-faces at random, thus the local webs $\{W_{\mathfrak{T}}\}_{\mathfrak{T} \in \widehat{\lambda}}$ satisfying the conclusion of Lemma 7.6 are not necessarily unique. For example, see Figure 39.

7.4. Inverse mapping: definition

Let c be a point in the global cone \mathcal{C}_{λ}^+ ; see Definition 6.10. Our goal is to associate to c a parallel equivalence class $\Psi_{\lambda}^{\text{FG}}(c) \in [\mathcal{W}_{\mathfrak{S}}]$ of global nonelliptic webs on \mathfrak{S} . Equivalently, we want to associate to c a nonelliptic web $\widetilde{\Psi}_{\lambda}^{\text{FG}}(c)$ on \mathfrak{S} well defined up to parallel equivalence; see Definition 2.3. Recall that we identify the triangles \mathfrak{T} of the ideal triangulation λ with the triangles \mathfrak{T} of the split ideal triangulation $\widehat{\lambda}$.

Construction of $\widetilde{\Psi}_{\lambda}^{\text{FG}}(c)$. The global cone point c determines a local cone point $c_{\mathfrak{T}}$ in the local cone $\mathcal{C}_{\mathfrak{T}}^+$ for each triangle \mathfrak{T} of λ ; see just before Definition 6.10. By the triangle identifications between λ and $\widehat{\lambda}$, the local cone point $c_{\mathfrak{T}} \in \mathcal{C}_{\mathfrak{T}}^+$ is assigned to each triangle \mathfrak{T} of $\widehat{\lambda}$; see the first and second rows of Figure 37.

Note, by construction, corresponding edge-coordinates located across a biangle \mathfrak{B} take the same value. More precisely, if \mathfrak{B} sits between two triangles \mathfrak{T}' and \mathfrak{T}'' and if the boundary edges of \mathfrak{B} are E' and E'' , respectively, then the coordinate $a_{E'}^L$ (resp. $a_{E'}^R$) lying on the left-edge-dot (resp. right-edge-dot) as viewed from \mathfrak{T}' agrees with the coordinate $a_{E''}^R$ (resp. $a_{E''}^L$) lying on the right-edge-dot (resp. left-edge-dot) as viewed from \mathfrak{T}'' ; see Figure 37.

By Corollaries 6.7 and 6.8, for each local cone point $c_{\mathfrak{T}} \in \mathcal{C}_{\mathfrak{T}}^+$ assigned to a triangle \mathfrak{T} of $\widehat{\lambda}$, there exists a unique corner-ambiguity class $[W_{\mathfrak{T}}]$ of local webs $W_{\mathfrak{T}}$ in $\mathcal{W}_{\mathfrak{T}}$ such that $\Phi_{\mathfrak{T}}^{\text{FG}}(W_{\mathfrak{T}}) = c_{\mathfrak{T}}$ for any representative $W_{\mathfrak{T}}$ of $[W_{\mathfrak{T}}]$.

We now make a choice of such a representative $W_{\mathfrak{T}}$ for each \mathfrak{T} . Two different choices $W_{\mathfrak{T}}$ and $W'_{\mathfrak{T}}$ of local webs representing $[W_{\mathfrak{T}}] = [W'_{\mathfrak{T}}]$ are, by definition, related by local parallel-moves; see the third row of Figure 37.

Since corresponding edge-coordinates across biangles agree, the collection $\{W_{\mathfrak{T}}\}_{\mathfrak{T} \in \widehat{\lambda}}$ of local webs is compatible (Definition 7.3). This follows by Figure 30. (There is also a general argument, by properties (2) and (3) in Definition 5.1, which uses the fact that if $W_{\mathfrak{T}} \in \mathcal{W}_{\mathfrak{T}}$, then the opposite web $W_{\mathfrak{T}}^{\text{op}}$ obtained by reversing all of the orientations of $W_{\mathfrak{T}}$ is also in $\mathcal{W}_{\mathfrak{T}}$).

By Lemma 7.6, this choice of a compatible collection $\{W_{\mathfrak{T}}\}_{\mathfrak{T} \in \widehat{\lambda}}$ of local webs can be made (in a nonunique way) such that the global web W on \mathfrak{S} obtained by applying the ladder gluing construction to $\{W_{\mathfrak{T}}\}_{\mathfrak{T} \in \widehat{\lambda}}$ is nonelliptic. Finally, we define $\widetilde{\Psi}_{\lambda}^{\text{FG}}(c) = W$. In order for the global web $\widetilde{\Psi}_{\lambda}^{\text{FG}}(c)$ to be well defined up to parallel equivalence, we require:

Main Lemma 7.7. *Assume that each of $\{W_{\mathfrak{T}}\}_{\mathfrak{T} \in \widehat{\lambda}}$ and $\{W'_{\mathfrak{T}}\}_{\mathfrak{T} \in \widehat{\lambda}}$ is a compatible collection of rungless essential webs in the $\mathcal{W}_{\mathfrak{T}}$, satisfying*

1. *for each triangle \mathfrak{T} , the local webs $W_{\mathfrak{T}}$ and $W'_{\mathfrak{T}}$ are equivalent up to corner-ambiguity;*
2. *both global webs W and W' , obtained from the compatible collections $\{W_{\mathfrak{T}}\}_{\mathfrak{T} \in \widehat{\lambda}}$ and $\{W'_{\mathfrak{T}}\}_{\mathfrak{T} \in \widehat{\lambda}}$, respectively, by applying the ladder gluing construction, are nonelliptic.*

Then, the nonelliptic webs W and W' represent the same parallel equivalence class in $[\mathcal{W}_{\mathfrak{S}}]$.

Definition 7.8. *The inverse mapping*

$$\Psi_{\lambda}^{\text{FG}} : \mathcal{C}_{\lambda}^{+} \longrightarrow [\mathcal{W}_{\mathfrak{S}}]$$

is defined by sending a cone point c in the global Knutson–Tao cone $\mathcal{C}_{\lambda}^{+}$ to the parallel equivalence class in $[\mathcal{W}_{\mathfrak{S}}]$ of the global nonelliptic web $\widetilde{\Psi}_{\lambda}^{\text{FG}}(c)$ on \mathfrak{S} .

Proof of Propositions 5.5 and 6.11. Assuming Main Lemma 7.7 to be true, it follows immediately from the constructions that the well defined mapping $\Psi_{\lambda}^{\text{FG}} : \mathcal{C}_{\lambda}^{+} \rightarrow [\mathcal{W}_{\mathfrak{S}}]$ is the set-functional inverse of the Fock–Goncharov global coordinate function $\Phi_{\lambda}^{\text{FG}} : [\mathcal{W}_{\mathfrak{S}}] \rightarrow \mathcal{C}_{\lambda}^{+}$. □

In summary, we have reduced the proof of Theorem 7.1 to proving the main lemma.

8. Proof of the main lemma

In this section, we prove the main Lemma 7.7. In particular, we provide an explicit algorithm taking one web to the other by a sequence of modified H-moves and global parallel-moves.

The strategy of the proof is simple, whereas its implementation is more complicated due to the combinatorics. The key idea is to think of a web W not as a graph, but as a multicurve $\langle W \rangle$, which we call a *web picture*; see Figure 40. We have already previewed web pictures at the local level, in Definitions 3.16 and 3.20 (see also the second paragraph of §5.3).

If W and W' are two nonelliptic webs as in the main Lemma 7.7, we show that their associated multicurves $\langle W \rangle$ and $\langle W' \rangle$ satisfy a fellow traveler property; see Lemma 8.3. As a consequence of this fellow traveler lemma, the intersection points $\mathcal{P} \subseteq \langle W \rangle$ are in natural bijection with those $\mathcal{P}' \subseteq \langle W' \rangle$; here, the nonelliptic hypothesis is necessary. To finish, we can use modified H-moves (Figures 25 and 41) to push around these intersection points in both webs until they are in the same configuration, establishing that W and W' are equivalent.

8.1. Preparation: web pictures on the surface

For a web W on \mathfrak{S} in good position with respect to the split ideal triangulation $\widehat{\lambda}$, the restrictions $W_{\mathfrak{B}} = W \cap \mathfrak{B}$ and $W_{\mathfrak{T}} = W \cap \mathfrak{T}$ in the biangles \mathfrak{B} and triangles \mathfrak{T} of $\widehat{\lambda}$ are essential and rungless essential local webs, respectively. By Definitions 3.16 and 3.20, we may consider the corresponding local pictures $\langle W_{\mathfrak{B}} \rangle$ and $\langle W_{\mathfrak{T}} \rangle$, which are in particular immersed multicurves in the biangle \mathfrak{B} and the holed triangle \mathfrak{T}^0 , respectively; see Definition 3.11 and Figures 15 and 18.

Definition 8.1. The *holed surface* \mathfrak{S}^0 is the surface \mathfrak{S} minus one open disk per triangle \mathfrak{T} of $\widehat{\lambda}$. The *global picture* $\langle W \rangle$ corresponding to a web W in good position with respect to $\widehat{\lambda}$ is the multicurve on the holed surface \mathfrak{S}^0 obtained by gluing together in the obvious way the collection of local pictures $\{\langle W_{\mathfrak{B}} \rangle\}_{\mathfrak{B} \in \widehat{\lambda}}$ and $\{\langle W_{\mathfrak{T}} \rangle\}_{\mathfrak{T} \in \widehat{\lambda}}$ associated to the biangles \mathfrak{B} and triangles \mathfrak{T} of $\widehat{\lambda}$, well defined up to ambient isotopy of \mathfrak{S}^0 respecting $\widehat{\lambda}$. See Figure 40.

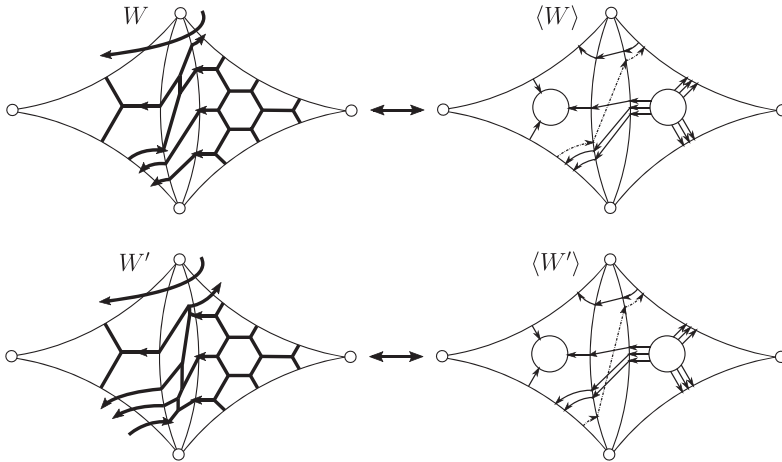


Figure 40. (Parts of) two webs W and W' in good position on the surface, and their corresponding global pictures $\langle W \rangle$ and $\langle W' \rangle$ on the holed surface. Note that, over triangles, W and W' differ by a permutation of corner arcs.

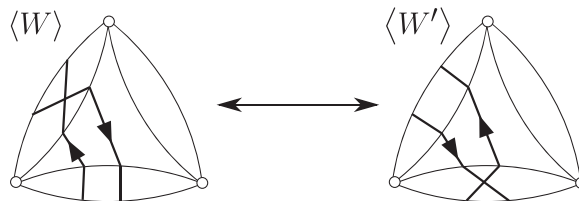


Figure 41. Modified H-move from the perspective of web pictures.

Figure 41 depicts how a modified H-move between webs W and W' in good position looks when viewed from the perspective of the global pictures $\langle W \rangle$ and $\langle W' \rangle$; see Figure 25.

Note the global picture $\langle W \rangle$ has no U-turns on any edge of $\widehat{\lambda}$, meaning there are no bigons formed between a component γ of $\langle W \rangle$ and $\widehat{\lambda}$. We call this the *no-switchbacks property*.

Definition 8.2. A based multicurve $(\Gamma, \{x_0^j\})$ on the holed surface \mathfrak{S}^0 is a multicurve $\Gamma = \{\gamma_i\}$ equipped with a base point $x_0^j \in \gamma_j$ for each loop component γ_j of Γ such that the base points x_0^j do not lie on any edges of the split ideal triangulation $\widehat{\lambda}$; see Definition 3.11.

8.2. Preparation: sequences

A convex subset $I \subseteq \mathbb{Z}$ of the integers is a subset such that if $n, m \in I$ are integers, then all the integers between n and m are in I .

A sequence $(a_i)_{i \in I}$ valued in a set \mathcal{A} is a function $I \rightarrow \mathcal{A}, i \mapsto a_i$, where $I \subseteq \mathbb{Z}$ is a convex subset of the integers.

Given a sequence $(a_i)_{i \in I}$, a subsequence $(a_{i_k})_{k \in K}$ is the sequence $K \rightarrow \mathcal{A}$ determined by a convex subset $K \subseteq \mathbb{Z}$ together with an order-preserving injective function $K \rightarrow I, k \mapsto i_k$.

Given a sequence $(a_i)_{i \in I}$, a convex subsequence $(a_{i_k})_{k \in K}$ is a subsequence such that the image I' of K in I under the function $K \rightarrow I$ is a convex subset of \mathbb{Z} .

Given two sequences $(a_i)_{i \in I}$ and $(b_j)_{j \in J}$ taking values in the same set, a common subsequence $\{(a_{i_k})_{k \in K}, (b_{j_k})_{k \in K}\}$ is a pair of subsequences having the same indexing set K such that $a_{i_k} = b_{j_k}$ for all $k \in K$.

A convex common subsequence $\{(a_{i_k})_{k \in K}, (b_{j_k})_{k \in K}\}$ is a common subsequence such that both subsequences $(a_{i_k})_{k \in K}$ and $(b_{j_k})_{k \in K}$ are convex.

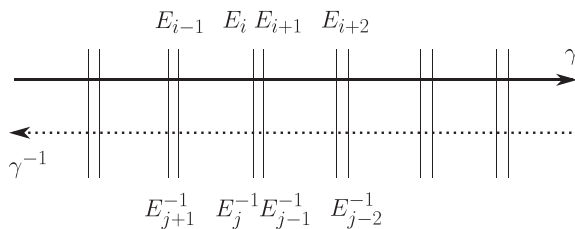


Figure 42. Route and past-route.

A maximal convex common subsequence $\{(a_{i_k})_{k \in K}, (b_{j_k})_{k \in K}\}$ is a convex common subsequence such that there does not exist: $K \subsetneq K'$ and a convex common subsequence $\{(a_{i'_k})_{k \in K'}, (b_{j'_k})_{k \in K'}\}$, satisfying $i'_k = i_k$ and $j'_k = j_k$ for all $k \in K$.

8.3. Preparation: edge-sequences and the fellow traveler lemma

Let W be a web on \mathfrak{S} in good position with respect to $\widehat{\lambda}$ such that its global picture $(\langle W \rangle, \{x_0^j\})$ is based.

Let γ be a loop or arc in $\langle W \rangle$. Associated to the component γ is an edge-sequence $(E_i)_{i \in I}$, where E_i is an edge of the split ideal triangulation $\widehat{\lambda}$. More precisely, the sequence $(E_i)_{i \in I}$ describes the i -th edge crossed by γ listed in order according to γ 's orientation. In the case where γ is an arc, we put $I = \{0, 1, \dots, n\} \subseteq \mathbb{Z}$, and the edge-sequence is well defined. In the case where γ is a loop with base point x_0 , we put $I = \mathbb{Z}$, and the edge-sequence is well defined by sending 0 to the first edge E_0 encountered by γ after passing x_0 .

We also associate an inverse edge-sequence $(E_i^{-1})_{i \in I^{-1}}$ to the inverse curve γ^{-1} , defined as follows. In the case of an arc put $I^{-1} = \{-n, \dots, 1, 0\}$, and in the case of a loop put $I^{-1} = \mathbb{Z}$. Then the inverse edge-sequence is defined by $E_i^{-1} = E_{-i}$ for all $i \in I^{-1}$.

Another name for a loop or arc γ in the global picture $\langle W \rangle$ is a traveler. Another name for an inverse curve γ^{-1} is a past-traveler. The edge-sequence $(E_i)_{i \in I}$ associated to a traveler γ is called its route, and the edge-sequence $(E_i^{-1})_{i \in I^{-1}}$ associated to a past-traveler γ^{-1} is called its past-route; see Figure 42. Two travelers γ in $\langle W \rangle$ and γ' in $\langle W' \rangle$ are called fellow travelers if they have the same routes $(E_i)_{i \in I} = (E'_i)_{i \in I'}$, $I = I'$. In particular, if γ is a loop (resp. arc), then γ' is also a loop (resp. arc of the same length).

The following statement is the key to proving the main lemma.

Lemma 8.3 (Fellow traveler lemma). Fix compatible local webs $\{W_{\mathfrak{T}}\}_{\mathfrak{T} \in \widehat{\lambda}}$ and $\{W'_{\mathfrak{T}}\}_{\mathfrak{T} \in \widehat{\lambda}}$ in the $\mathcal{W}_{\widehat{\lambda}}$ satisfying hypothesis (1) of the main Lemma 7.7, and let W and W' be the induced global webs obtained by the ladder gluing construction. Then, there exists a natural one-to-one correspondence

$$\gamma \longleftrightarrow \gamma' = \varphi(\gamma)$$

between the collection of travelers γ in the global picture $\langle W \rangle$ and the collection of travelers $\gamma' = \varphi(\gamma)$ in $\langle W' \rangle$, and there exists a choice of base points x_0 and x'_0 for the loops γ and γ' in $\langle W \rangle$ and $\langle W' \rangle$, respectively, such that γ and $\gamma' = \varphi(\gamma)$ are fellow travelers for all travelers γ .

For an example of the fellow traveler lemma on the once punctured torus, see Figure 43.

Proof of Lemma 8.3. Let E be an edge of $\widehat{\lambda}$. This is associated to a unique triangle \mathfrak{T} of $\widehat{\lambda}$ containing E in its boundary. Let $S^{(E)\text{out}} = (s_i^{(E)\text{out}})_{i=1, \dots, n_E^{\text{out}}}$ (resp. $S'^{(E)\text{out}} = (s'_i^{(E)\text{out}})_{i=1, \dots, n_E^{\text{out}'}}$) denote the sequence of out-strands of the global picture $\langle W \rangle$ (resp. $\langle W' \rangle$) lying on the edge E , ordered, say, from left to right as viewed from \mathfrak{T} . By hypothesis (1) of the main lemma, $n_E^{\text{out}} = n_E^{\text{out}'}$. Let $\gamma_i^{(E)}$ denote the unique

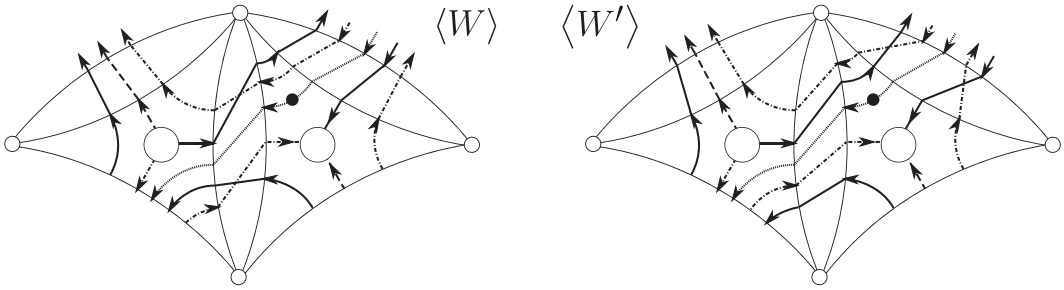


Figure 43. Fellow traveler lemma.

traveler in $\langle W \rangle$ containing the strand $s_i^{(E)\text{out}}$. Similarly, define travelers $\gamma_i'^{(E)}$ with respect to $\langle W' \rangle$. The mapping φ is defined by

$$\varphi\left(\gamma_i^{(E)}\right) = \gamma_i'^{(E)} \quad (i = 1, 2, \dots, n_E^{\text{out}} = n_{E'}^{\text{out}}).$$

Note every traveler γ in $\langle W \rangle$ (resp. γ' in $\langle W' \rangle$) is of the form $\gamma_i^{(E)}$ (resp. $\gamma_i'^{(E)}$) for some E .

To establish that φ is well defined, we show that $\gamma_{i_1}^{(E_1)} = \gamma_{i_2}^{(E_2)}$ implies $\gamma_{i_1}'^{(E_1)} = \gamma_{i_2}'^{(E_2)}$. This property follows immediately from:

Claim 8.4. For some $k \in \{1, 2, \dots, n_E^{\text{out}} = n_{E'}^{\text{out}}\}$, let $s_k^{(E)\text{out}} \in S^{(E)\text{out}}$ and $s_k'^{(E)\text{out}} \in S'^{(E)\text{out}}$ be out-strands of $\langle W \rangle$ and $\langle W' \rangle$, respectively, lying on an edge E of a triangle \mathfrak{T} of $\widehat{\lambda}$. Note that each of these strands, according to its orientation, enters via the edge E into a biangle \mathfrak{B} , exits via an edge E_2 into a triangle \mathfrak{T}_2 and then either

1. turns left in \mathfrak{T}_2 , ending as a strand s or s' , respectively, lying on an edge E_3 ;
2. turns right in \mathfrak{T}_2 , ending as a strand s or s' , respectively, lying on an edge E_3 ;
3. terminates in a honeycomb H_n .

The claim is that if the forward motion of the strand $s_k^{(E)\text{out}}$ is described by item (i) above for $i \in \{1, 2, 3\}$, then the forward motion of the strand $s_k'^{(E)\text{out}}$ is also described by item (i). Consequently, in cases (1) or (2), there exists some $k_3 \in \{1, 2, \dots, n_{E_3}^{\text{out}} = n_{E_3'}^{\text{out}}\}$ such that

$$s = s_{k_3}^{(E_3)\text{out}} \in S^{(E_3)\text{out}} \quad \text{and} \quad s' = s_{k_3}'^{(E_3)\text{out}} \in S'^{(E_3)\text{out}}.$$

The claim is true since, by hypothesis, on each corner of each triangle, $\langle W \rangle$ and $\langle W' \rangle$ have the same number of clockwise-oriented (resp. counterclockwise-oriented) corner arcs, together with the fact that only oppositely oriented arcs cross in the biangles; see Figure 44.

Having established that φ is well defined, it follows by the definition that φ is a bijection. Another consequence of Claim 8.4 is that if γ is an arc, then $\gamma' = \varphi(\gamma)$ is an arc such that γ and γ' are fellow travelers. Also, if $\gamma = \gamma_i^{(E)}$ is a loop, then $\gamma' = \varphi(\gamma) = \gamma_i'^{(E)}$ is a loop. Choosing base points x_0 and x_0' on the out-strands $s_i^{(E)\text{out}}$ and $s_i'^{(E)\text{out}}$, respectively, just before, say, the strands cross the edge E makes the loops γ and γ' into fellow travelers. \square

8.4. Preparation: shared-routes

As in the previous subsection, let W be a web on \mathfrak{S} in good position with respect to $\widehat{\lambda}$ such that its global picture $(\langle W \rangle, \{x_0^j\})$ is based.

Let γ be a traveler in $\langle W \rangle$ having route $(E_i)_{i \in I}$. For some $i \in I$ indexing an edge E_i , by definition of the route there is a corresponding point y_i of γ lying on E_i . Consider the associated segment $\bar{\gamma}_i$ of γ

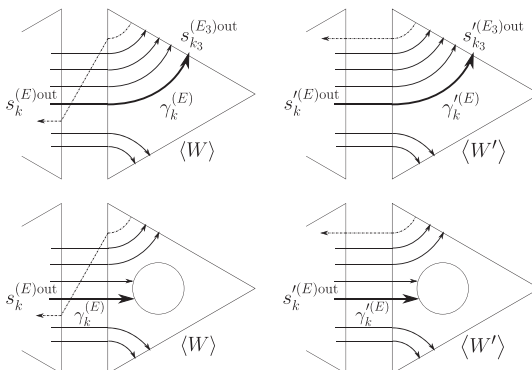


Figure 44. Cases (1) (top) and (3) (bottom) in Claim 8.4.

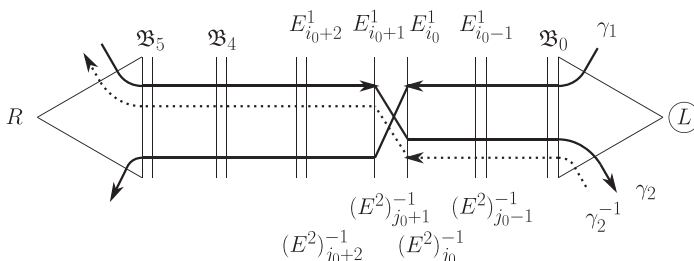


Figure 45. Crossing shared-route.

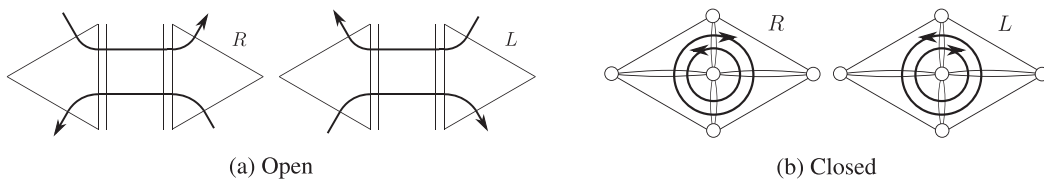


Figure 46. Noncrossing shared-routes.

lying between the points y_i and y_{i+1} . Similarly, define segments $\overline{(\gamma^{-1})_i}$ associated to the past-traveler γ^{-1} with respect to its past-route $(E^{-1}_i)_{i \in I-1}$.

Definition 8.5. Let γ_1, γ_2 be travelers in $\langle W \rangle$ and $\gamma_1^{-1}, \gamma_2^{-1}$ the corresponding past travelers, with routes $(E^1_i)_{i \in I}$ and $(E^2_j)_{j \in J}$ and past routes $((E^1_i)^{-1})_{i \in I-1}$ and $((E^2_j)^{-1})_{j \in J-1}$.

An *oppositely oriented shared-route*, or just *shared-route*, for the ordered pair (γ_1, γ_2) of travelers is a maximal convex common subsequence (§8.2) $SR = \{(E^1_k)_{k \in K}, ((E^2_j)^{-1})_{j \in K}\}$ for the route $(E^1_i)_{i \in I}$ of γ_1 and the past-route $((E^2_j)^{-1})_{j \in J-1}$ of γ_2^{-1} .

A shared-route is *open* (resp. *closed*) if its domain K is not equal to (resp. equal to) \mathbb{Z} .

A shared-route is *crossing* if there exists an index $k \in K$ such that the associated segments $\overline{(\gamma_1)_{i_k}}$ and $\overline{(\gamma_2)^{-1}_{j_k}}$ intersect, say at a point p_k . We call p_k an *intersection point* of the crossing shared-route. Note that an intersection point must lie inside a biangle \mathfrak{B} of $\widehat{\lambda}$. A shared-route is *noncrossing* if it has no intersection points.

For some examples, see Figures 45 and 46. Our pictures for shared-routes are only schematics, since the actual shared-routes on \mathfrak{S}^0 might cross the same edge multiple times. That is, there might exist $k \neq k'$ such that $E^1_{i_k} = (E^2)^{-1}_{j_k} = E^1_{i_{k'}} = (E^2)^{-1}_{j_{k'}}$. Alternatively, one could think of these pictures at the level of the universal cover $\widetilde{\mathfrak{S}^0}$. Note that travelers in open shared-routes may end in honeycombs (Figure 44), but this will not affect our arguments.

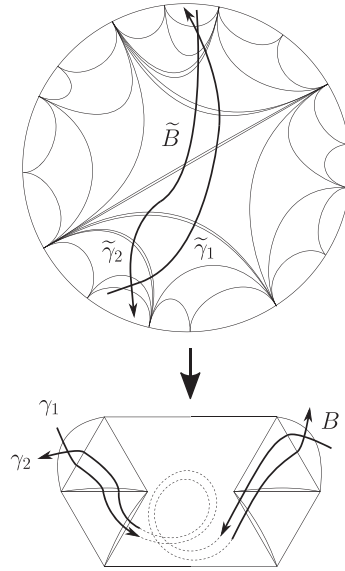


Figure 47. Immersed bigons do not exist: 1 of 2.

Lemma 8.6. Assume in addition that W is nonelliptic. Then any shared-route SR has at most one intersection point p . In particular, a crossing shared-route is necessarily open.

Proof. The second statement follows from the first since otherwise the oriented holed surface \mathfrak{S}^0 would contain a Möbius strip.

Suppose, for an ordered pair (γ_1, γ_2) of travelers, there were a crossing shared-route $\{(E^1_{ik})_{k \in K}, ((E^2)_{jk}^{-1})_{k \in K}\}$ that has more than one intersection point. There are only finitely many intersection points, denoted $p_{k_1}, p_{k_2}, \dots, p_{k_m}$ with $k_i < k_{i+1}$. The intersection points p_{k_1} and p_{k_2} form the tips of an immersed bigon B , which we formalize as the convex common subsequence $B = \{(E^1_{ik})_{k_1 \leq k \leq k_2+1}, ((E^2)_{jk}^{-1})_{k_1 \leq k \leq k_2+1}\}$; see the bottom of Figure 47. Alternatively, we think of B as bounded by the segments of γ_1 and γ_2 between p_{k_1} and p_{k_2} .

Let π be the projection map from the universal cover \mathfrak{S}^0 to the holed surface \mathfrak{S}^0 . Equip \mathfrak{S}^0 with the lifted split ideal triangulation $\tilde{\lambda} = \pi^{-1}(\hat{\lambda})$. For a traveler γ , consider one of its lifts $\tilde{\gamma}$ in \mathfrak{S}^0 . By the no-switchbacks property (§8.1), and the fact that the dual graph of $\tilde{\lambda}$ in \mathfrak{S}^0 is a tree, the lifted curve $\tilde{\gamma}$ does not cross the same edge \tilde{E} in the universal cover \mathfrak{S}^0 more than once. Therefore, the immersed bigon B lifts to an embedded topological bigon \tilde{B} in \mathfrak{S}^0 , bounded by segments of lifts $\tilde{\gamma}_1$ and $\tilde{\gamma}_2$ of the curves γ_1 and γ_2 ; see Figure 47.

The preimage $\tilde{W} = \pi^{-1}(W)$ of the web W is an (infinite) web in \mathfrak{S}^0 . Moreover, \tilde{W} is in good position with respect to $\tilde{\lambda}$. Since W is nonelliptic, so is \tilde{W} (compare the proof of Lemma 7.6). Let $\langle \tilde{W} \rangle$ be the global picture associated to \tilde{W} . Note that the lifted curves $\tilde{\gamma}_1$ and $\tilde{\gamma}_2$ are in $\langle \tilde{W} \rangle$. Observe that it is possible for $\text{int}(\tilde{B}) \cap \langle \tilde{W} \rangle \neq \emptyset$ to be nonempty; see Figure 48. However, by the no-switchbacks property, there are no closed curves of $\langle \tilde{W} \rangle$ in this interior.

The rest of the proof is similar to the proof of Proposition 3.15; see Figure 16. Here, the web orientation is important. Specifically, since only (locally) oppositely oriented (with respect to bigons) curves in the global picture $\langle \tilde{W} \rangle$ can intersect, it follows by the no-switchbacks property that if a curve $\tilde{\gamma}$ enters the embedded bigon \tilde{B} via a boundary edge \tilde{E} , then $\tilde{\gamma}$ must leave through \tilde{E} as well. Consequently, there exists an innermost embedded bigon $\tilde{B}' \subseteq \tilde{B}$ whose interior does not intersect $\langle \tilde{W} \rangle$; see Figure 48. But then \tilde{B}' corresponds to a square-face \tilde{D} in the lifted nonelliptic web \tilde{W} , which is a contradiction. \square

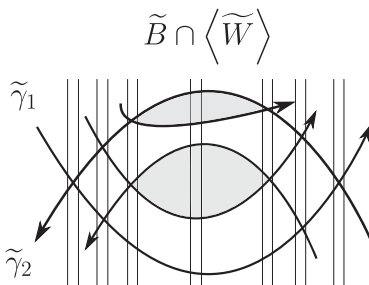


Figure 48. Immersed bigons do not exist: 2 of 2.

Lemma 8.7. *If the web W is nonelliptic, then there are no intersection points of $\langle W \rangle$ along any closed noncrossing shared-route (as opposed to open noncrossing shared-routes). In particular, each closed noncrossing shared-route SR is embedded, namely its travelers γ_1 and γ_2 bound an embedded annulus $A \subseteq \mathfrak{S}$; see Figure 46b.*

Proof. If there were an intersection point of $\langle W \rangle$ along either traveler, then an argument similar to that depicted in Figure 48 implies there would exist an immersed bigon in $\langle W \rangle$. □

Definition 8.8. Consider an open shared-route SR for an ordered pair (γ_1, γ_2) of travelers in $\langle W \rangle$. We say that the *source-end* \mathcal{E} of the open shared-route SR is the unique end \mathcal{E} of SR such that the traveler γ_1 enters the shared-route SR through the end \mathcal{E} .

Assuming W is nonelliptic, we say that the unique intersection point p in a crossing shared-route SR , which is necessarily open by Lemma 8.6, lies in the i -th shared-route-biangle \mathfrak{B}_i , denoted $p \in_{SR} \mathfrak{B}_i$, $i \geq 0$, if γ_1 crosses γ_2^{-1} (at the point p) inside the i -th biangle through which γ_1 travels after entering SR through the source-end \mathcal{E} .

For example, in Figure 45, the source-end \mathcal{E} of SR is the end labeled L .

Also, in Figure 45, p is in the shared-route-biangle $p \in_{SR} \mathfrak{B}_2$. Note that there is a unique index i such that $p \in_{SR} \mathfrak{B}_i$. This definition is specially designed to circumvent the situation where \mathfrak{B}_i and \mathfrak{B}_j represent the same biangle \mathfrak{B} on the surface for different indices $i \neq j$. For example, in Figure 45, even if, say, \mathfrak{B}_5 represented the same biangle \mathfrak{B} as \mathfrak{B}_2 , we would say $p \in_{SR} \mathfrak{B}_2$ and $p \notin_{SR} \mathfrak{B}_5$. Alternatively, one could think of this distinction at the level of the universal cover.

8.5. Preparation: oriented shared-routes

As previously, let W be a web on \mathfrak{S} in good position with respect to $\hat{\lambda}$ such that its global picture $(\langle W \rangle, \{x_0^j\})$ is based.

Definition 8.9. We say that a noncrossing shared-route SR for an ordered pair (γ_1, γ_2) of travelers in $\langle W \rangle$ is *left-oriented* (resp. *right-oriented*) if for either of the travelers γ_1 or γ_2 , call it γ , the other traveler appears on the left (resp. right) of γ with respect to γ 's orientation; see Figure 46.

The web W is *closed-left-oriented* (resp. *closed-right-oriented*) if all of $\langle W \rangle$'s closed noncrossing shared-routes are left-oriented (resp. right-oriented); see Figure 46b.

Note, by Lemma 8.7, a nonelliptic web W can always be replaced with a closed-left-oriented or closed-right-oriented nonelliptic web by performing global parallel-moves (Definition 2.3); see Figure 3.

We also want to define a notion of orientation for crossing shared-routes. Unlike for noncrossing shared-routes, this will depend on the ordering of the pair (γ_1, γ_2) . Since we will be dealing with nonelliptic webs, by Lemma 8.6 it suffices to think about open shared-routes.

Definition 8.10. We say that an end \mathcal{E} of an open shared-route SR is *left-oriented* or *right-oriented* in the same way as in Definition 8.9 for noncrossing shared routes.

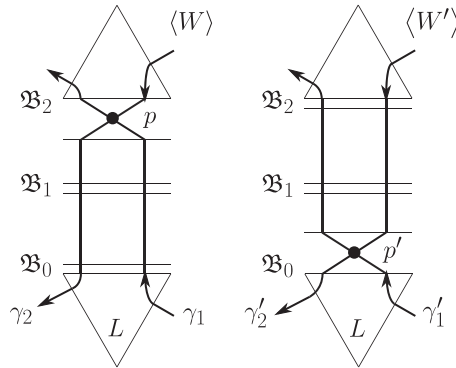


Figure 49. Natural one-to-one correspondence between intersection points.

Assuming W is nonelliptic, a crossing shared-route SR for an ordered pair (γ_1, γ_2) of travelers in $\langle W \rangle$, which is necessarily open by Lemma 8.6, is *left-oriented* (resp. *right-oriented*) if its source-end \mathcal{E} (Definition 8.8) is left-oriented (resp. right-oriented).

For example, the crossing shared-route shown in Figure 45 is left-oriented.

8.6. Proof of the main lemma: intersection points

We now begin the formal proof of the main Lemma 7.7. Fix local webs $\{W_{\mathfrak{X}}\}_{\mathfrak{X} \in \hat{\lambda}}$ and $\{W'_{\mathfrak{X}}\}_{\mathfrak{X} \in \hat{\lambda}}$ in the $\mathscr{W}_{\hat{\lambda}}$ satisfying the hypotheses of the main lemma, and let W and W' be the induced nonelliptic global webs obtained by the ladder gluing construction. By applying global parallel-moves, we may assume that both W and W' are closed-left-oriented, say (Definition 8.9). Assume that the global pictures $(\langle W \rangle, \{x_0^j\})$ and $(\langle W' \rangle, \{x_0^j\})$ are based and that the base points x_0^j and x_0^j satisfy the conclusion of the fellow traveler Lemma 8.3. Throughout, for each traveler γ in $\langle W \rangle$ we denote by γ' the corresponding traveler in $\langle W' \rangle$ as provided by the fellow traveler lemma.

Let \mathcal{P} (resp. \mathcal{P}') denote the set of intersection points p of all travelers in $\langle W \rangle$ (resp. $\langle W' \rangle$).

Corollary 8.11. *There is a natural bijection $\varphi : \mathcal{P} \xrightarrow{\sim} \mathcal{P}'$. We write $p' = \varphi(p)$.*

For the proof, we will need the following notion.

Definition 8.12. Let $p \in \mathcal{P}$. We define the *left-oriented crossing shared-route generated by p* , denoted $SR(p)$, to be the unique left-oriented crossing shared-route (Definition 8.10) in $\langle W \rangle$ whose intersection point is p . Note, in particular, that the left-orientation condition determines the order (γ_1, γ_2) of the involved travelers. (Technically speaking, we choose K starting at 0, and then the shared-route $SR(p) = \{(E^1_{i_k})_{k \in K}, ((E^2)^{-1}_{j_k})_{k \in K}\}$ is only uniquely determined after choosing the two indices i_0 and j_0 assigned by $0 \in K$; this ambiguity only occurs when the shared-route has – part of – a loop traveler.)

Proof of Corollary 8.11. Consider the left-oriented crossing shared-route $SR(p)$ in $\langle W \rangle$ with travelers (γ_1, γ_2) generated by the intersection point p . By the fellow traveler lemma, there is a corresponding shared-route SR' in $\langle W' \rangle$ with the travelers (γ'_1, γ'_2) , which must also be open; see Figures 45 and 46a. Moreover, the ends \mathcal{E}' of SR' have orientations (Definition 8.10) matching those of the ends \mathcal{E} of $SR(p)$. It follows that SR' is crossing. Its unique intersection point p' is the desired image of p ; see Figure 49. (Note for later that since $SR(p)$ is left-oriented, so is SR' , thus $SR' = SR'(p')$.) \square

Recall that a crossing shared-route SR for the ordered pair (γ_1, γ_2) comes with an ordering of the shared-route-biangles \mathfrak{B}_i appearing along γ_1 's route, starting from the source-end \mathcal{E} ; see Definition 8.8. If p and p' are intersection points as in Corollary 8.11 and its proof, then the left-oriented crossing shared-routes $SR(p)$ and $SR'(p')$ have the same associated sequence of shared-route-biangles \mathfrak{B}_i . However, if $p \in_{SR(p)} \mathfrak{B}_i$ and $p' \in_{SR'(p')} \mathfrak{B}_j$ (see again Definition 8.8), it need not be true that $i = j$; see Figure 49.

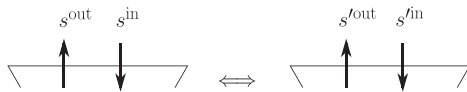


Figure 50. Identical oriented strand-sequences on each edge E .

Definition 8.13. We say that two corresponding intersection points p and p' , as in Corollary 8.11, lie in the same shared-route-biangle if there is an index i such that $p \in_{SR(p)} \mathfrak{B}_i \ni_{SR'(p')} p'$, where the sequence of shared-route-biangles $\{\mathfrak{B}_i\}$ is defined with respect to the left-oriented crossing shared-routes $SR(p)$ and $SR'(p')$ generated by p and p' , respectively.

For example, in Figure 49, even if it were true that \mathfrak{B}_0 and \mathfrak{B}_2 represented the same biangle \mathfrak{B} on the surface, we would not say that p and p' lie in the same shared-route-biangle.

Lemma 8.14. There is a sequence of modified H -moves (Figure 41) applicable to the web W and a sequence of modified H -moves applicable to W' , after which the bijection $\mathcal{P} \leftrightarrow \mathcal{P}'$ from Corollary 8.11 satisfies the property that each intersection point p in the global picture $\langle W \rangle$ and its corresponding intersection point p' in $\langle W' \rangle$ lie in the same shared-route-biangle \mathfrak{B}_i .

Before giving a proof (§8.8), we reduce the proof of the main lemma to that of Lemma 8.14.

8.7. Proof of the main lemma: finishing the argument

Assuming corresponding intersection points lie in the same shared-route-biangle, we claim that we are done, $W = W'$.

By the proof of the fellow traveler lemma, not only is there a natural bijection of travelers $\gamma \leftrightarrow \gamma'$, moreover for each edge E of $\tilde{\lambda}$ there is a natural bijection of oriented strands $s \leftrightarrow s'$ of $\langle W \rangle$ and $\langle W' \rangle$, respectively, on E . Namely, the k -th out-strand (resp. in-strand) s , measured from left to right, say, with respect to \mathfrak{Z} , is matched with the k -th out-strand (resp. in-strand) s' . This satisfies that s lies in γ if and only if s' lies in γ' .

Fix an edge E adjacent to a triangle \mathfrak{Z} . Let $S = (s_i)$ (resp. $S' = (s'_i)$) be the full sequence of oriented strands for $\langle W \rangle$ (resp. $\langle W' \rangle$) on the edge E , measured from left to right. In particular, both in- and out-strands occur in S (resp. S').

Lemma 8.15. Assuming corresponding intersection points lie in the same shared-route-biangle, we have that $S = S'$, for every edge E of $\tilde{\lambda}$; see Definition 8.13. (That is, $s_i^* = s'_i$ for all i .)

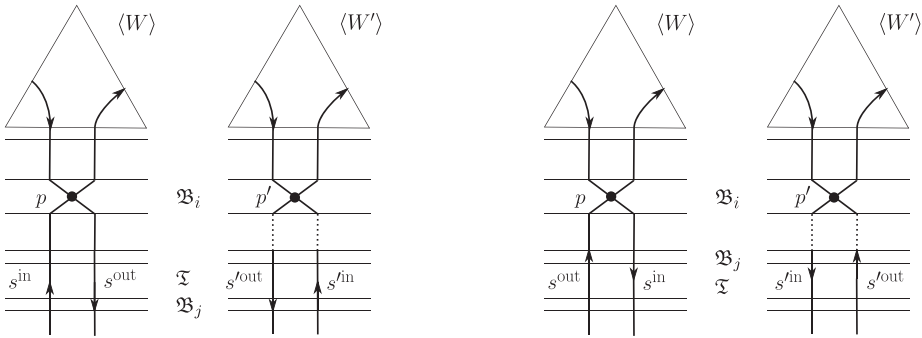
Proof. It suffices to prove the following statement.

Claim 8.16. If s^{out} is an out-strand of S and if s^{in} is an in-strand of S , then

$$s^{\text{out}} \text{ lies to the left of } s^{\text{in}} \iff s'^{\text{out}} \text{ lies to the left of } s'^{\text{in}}.$$

See Figure 50. To prove the forward direction of the claim, suppose otherwise, that is suppose s'^{out} lies to the right of s'^{in} . Let SR (resp. SR') be a shared-route containing s^{out} and s^{in} (resp. s'^{out} and s'^{in}) (there are two possibilities for each, determined by the order of the pair of involved travelers). By the fellow traveler lemma, SR is crossing (resp. open/closed noncrossing) if and only if SR' is crossing (resp. open/closed noncrossing).

Suppose SR and SR' are crossing. Then we may assume that $SR = SR(p)$ and $SR' = SR'(p')$ have been chosen as the left-oriented crossing shared-routes generated by their unique intersection points p and p' , respectively; see Definition 8.12. By hypothesis, p and p' lie in the same shared-route-biangle, call it \mathfrak{B}_i , that is $p \in_{SR(p)} \mathfrak{B}_i \ni_{SR'(p')} p'$. Letting \mathfrak{B}_j denote the shared-route-biangle containing the edge E with the strands s^{out} and s^{in} (and s'^{in} and s'^{out}), let us say that *the strands are on the close (resp. far) side* if they are on the first (resp. last) edge of \mathfrak{B}_j hit while traveling from the source-end of the shared-route. Similarly, it makes sense to say that *the crossing comes before (resp. after) the strands*



(a) Case 1: crossing before the strands, and strands on the close side of the biangle \mathfrak{B}_i (b) Case 2: crossing before the strands, and strands on the far side of the biangle \mathfrak{B}_i

Figure 51. Proof of Claim 8.16, by contradiction.

with respect to the source-end. Our first observation is that since the source-end is left-oriented, and since s^{out} lies to the left of s^{in} , it cannot be true that the crossing comes after the strands. So let Case 1 (resp. Case 2) be the case that the crossing comes before the strands and that the strands are on the close (resp. far) side. Since s^{in} lies to the left of s^{out} (by contradiction hypothesis), both Case 1 and Case 2 lead to a contradiction, namely that both ends of the crossing shared-route SR' are left-oriented (Definition 8.10); see Figure 51.

Similarly, if SR and SR' are noncrossing, the contradiction is that one of the shared-routes is left-oriented, and the other is right-oriented; see Definition 8.9. Indeed, in the open case (Figure 46a), this violates their matching end orientations (by the fellow traveler lemma), and in the closed case (Figure 46b), this violates that both W and W' are closed-left-oriented; see the beginning of §8.6.

The backward direction of the claim is proved by symmetry. □

Proof of main Lemma 7.7. By Lemma 8.14, we may assume that corresponding intersection points lie in the same shared-route-biangle. By hypothesis, the webs W and W' may differ over triangles \mathfrak{T} by permutations of corner arcs. However, we gather from Lemma 8.15 that they in fact have the same orderings of corner arcs in each triangle \mathfrak{T} . Also, since the ladder-webs in the biangles \mathfrak{B} are uniquely determined by their boundary-edge sequences, it follows that W and W' have the same ladder-web in each biangle \mathfrak{B} ; see Proposition 3.15. □

8.8. Proof of the main lemma: proof of Lemma 8.14

We have reduced the proof of the main lemma to proving Lemma 8.14. We begin by laying some groundwork.

Let \mathfrak{B} be a biangle, and let $\mathcal{P}_{\mathfrak{B}} = \mathcal{P} \cap \mathfrak{B}$ be the set of intersection points of $\langle W \rangle$ in \mathfrak{B} . Let E be a boundary edge of the biangle \mathfrak{B} , and let \mathfrak{B}_1 and \mathfrak{B}_2 be the two biangles opposite \mathfrak{B} across the triangle \mathfrak{T} adjacent to the edge E ; see Figure 52.

Definition 8.17. Let $p \in \mathcal{P}_{\mathfrak{B}}$ be an intersection point in \mathfrak{B} of two travelers γ_1 and γ_2 in $\langle W \rangle$. We denote by $\bar{\gamma}_1(p, E)$ the half-segment of γ_1 connecting p to E . Define similarly $\bar{\gamma}_2(p, E)$. The *pyramid* $\Delta(p, E)$ bounded by p and E is the triangular subset of the biangle \mathfrak{B} bordered by the boundary edge E and the two half-segments $\bar{\gamma}_1(p, E)$ and $\bar{\gamma}_2(p, E)$; see Figure 52.

Let $P \subseteq \mathcal{P}_{\mathfrak{B}}$ be a subset of intersection points. We call P *saturated with respect to E* if

$$\mathcal{P}_{\mathfrak{B}} \cap \left(\bigcup_{p \in P} \Delta(p, E) \right) = P.$$

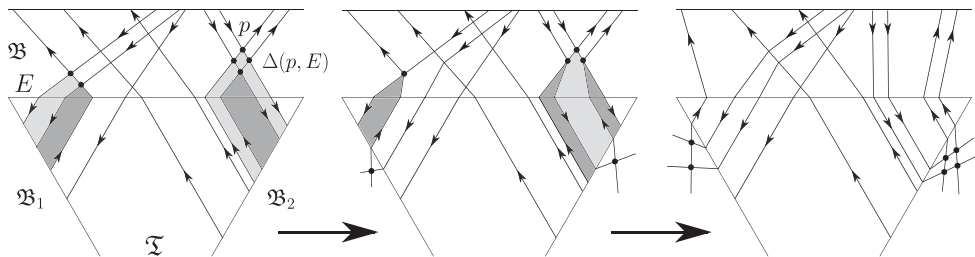


Figure 52. Pushing a saturated movable subset P into adjacent biangles. (Two rounds of pushes are required to go from the second to third picture.)

In other words, there are no intersection points in the pyramids $\Delta(p, E)$, $p \in P$, that are not already in P .

An intersection point $p \in \mathcal{P}_{\mathfrak{B}}$ is *movable with respect to E* if, after crossing E , the half-segments $\bar{\gamma}_1(p, E)$ and $\bar{\gamma}_2(p, E)$ extend parallel to each other across the adjacent triangle \mathfrak{T} , thus landing in the same opposite biangle, either \mathfrak{B}_1 or \mathfrak{B}_2 ; see Figure 52, where on the left, six points are movable; in the middle, four points are movable and on the right, none are movable. We say a subset $P \subseteq \mathcal{P}_{\mathfrak{B}}$ is *movable with respect to E* if each $p \in P$ is movable.

Claim 8.18. *Let $P \subseteq \mathcal{P}_{\mathfrak{B}}$ be a subset of intersection points that is saturated and movable with respect to E . Then, there exists a sequence $W = W_0, W_1, \dots, W_n$ of webs and a sequence $P_{-1} = \emptyset \subsetneq P_0 \subsetneq P_1 \subsetneq \dots \subsetneq P_{n-1} = P \subseteq \mathcal{P}_{\mathfrak{B}}$ of intersection points of $\langle W \rangle$ in the biangle \mathfrak{B} , such that W_{i+1} is obtained from W_i by a finite number of modified H-moves (Figure 41) in such a way that the points $P_i - P_{i-1}$ are carried into the two biangles $\mathfrak{B}_1 \cup \mathfrak{B}_2$ and no other intersection points are moved. After this process is complete, P has been moved into $\mathfrak{B}_1 \cup \mathfrak{B}_2$ and all the other intersection points $\mathcal{P} - P$ remain unmoved in their original biangles.*

Claim 8.18 will first be used in the proof of Claim 8.22. We now prepare to prove Claim 8.18.

We say that $p \in \mathcal{P}_{\mathfrak{B}}$ is *immediately movable with respect to E* if it is movable and there are no other intersection points in the pyramid $\Delta(p, E)$, that is $\Delta(p, E) \cap \mathcal{P}_{\mathfrak{B}} = \{p\}$. Equivalently, $\text{Int}(\Delta(p, E)) \cap \langle W \rangle = \emptyset$, hence a modified H-move can be applied to carry p across the edge E , across the adjacent triangle \mathfrak{T} and into one of the opposite biangles \mathfrak{B}_1 or \mathfrak{B}_2 ; see Figure 52, where on the left and in the middle, two and three points are immediately movable.

The following statement is evident from the ladder-web structure in the biangle \mathfrak{B} .

Fact 8.19 (Nested pyramids). *If $q \in \mathcal{P}_{\mathfrak{B}} \cap \Delta(p, E)$ is an intersection point in the pyramid $\Delta(p, E)$, then $\Delta(q, E) \subseteq \Delta(p, E)$. Consequently, if p is movable, then so is q . Therefore, if p is movable, then there exists an innermost q in $\Delta(p, E)$ that is immediately movable. \square*

Proof of Claim 8.18. By induction, assume W_i and P_{i-1} are given. At this stage, the intersection points P_{i-1} have been moved into $\mathfrak{B}_1 \cup \mathfrak{B}_2$, and the intersection points $P - P_{i-1} \neq \emptyset$ are still in \mathfrak{B} . Note that, since P is saturated in $\langle W \rangle$, $P - P_{i-1}$ is saturated in $\langle W_i \rangle$, that is,

$$P - P_{i-1} = \mathcal{P}_{\mathfrak{B}}^{(i)} \cap \left(\bigcup_{p \in P - P_{i-1}} \Delta^{(i)}(p, E) \right) \subseteq \langle W_i \rangle.$$

Since by hypothesis each $p \in P - P_{i-1}$ is movable, by Fact 8.19 the subset

$$Q_i = \{q \in \mathcal{P}_{\mathfrak{B}}^{(i)} \cap \left(\bigcup_{p \in P - P_{i-1}} \Delta^{(i)}(p, E) \right); \quad q \text{ is immediately movable} \} \neq \emptyset,$$

is nonempty. In particular, $Q_i \subseteq P - P_{i-1}$. We can thus apply modified H-moves to W_i to move the intersection points Q_i from the biangle \mathfrak{B} into the two biangles $\mathfrak{B}_1 \cup \mathfrak{B}_2$, yielding the new web W_{i+1} . Putting $P_i = P_{i-1} \cup Q_i$ finishes the induction step; see Figure 52, where $n = 3$. \square

The following statement is immediate from Fact 8.19.

Fact 8.20 (Saturation of a subset of intersection points). *For any subset $Q \subseteq \mathcal{P}_{\mathfrak{B}}$, the set*

$$P = \mathcal{P}_{\mathfrak{B}} \cap \left(\bigcup_{q \in Q} \Delta(q, E) \right) \subseteq \mathcal{P}_{\mathfrak{B}}$$

is saturated with respect to E . □

We continue moving toward the proof of Lemma 8.14. We are now dealing with two webs W and W' . Let $E, \mathfrak{I}, \mathfrak{B}, \mathfrak{B}_1, \mathfrak{B}_2$ be as before. We begin by setting some notation.

Given a subset $P \subseteq \mathcal{P}_{\mathfrak{B}}$, put

$$P'(P, E) = \mathcal{P}'_{\mathfrak{B}} \cap \left(\bigcup_{\{p \in P; \quad p \text{ and } p' \text{ lie in the same shared-route-biangle}\}} \Delta(p', E) \right) \subseteq \mathcal{P}'_{\mathfrak{B}}.$$

In other words, $P'(P, E)$ consists of the points in $\mathcal{P}'_{\mathfrak{B}}$ lying in the pyramids $\Delta(p', E)$ generated by those intersection points p' in $\mathcal{P}'_{\mathfrak{B}}$ whose corresponding intersection point p lies in the same shared-route-biangle as p' and satisfies $p \in P$. Symmetrically, given a subset $P' \subseteq \mathcal{P}'_{\mathfrak{B}}$, put

$$P(P', E) = \mathcal{P}_{\mathfrak{B}} \cap \left(\bigcup_{\{p' \in P'; \quad p' \text{ and } p \text{ lie in the same shared-route-biangle}\}} \Delta(p, E) \right) \subseteq \mathcal{P}_{\mathfrak{B}}.$$

Note that (1) the above shared-route-biangles necessarily coincide with the biangle \mathfrak{B} , and (2) generally, either of the sets $P'(P, E)$ or $P(P', E)$ may be empty.

Fact 8.21. *The union of movable sets is movable. Let $P \subseteq \mathcal{P}_{\mathfrak{B}}$ (resp. $P' \subseteq \mathcal{P}'_{\mathfrak{B}}$) be movable with respect to E . Then $P'(P, E) \subseteq \mathcal{P}'_{\mathfrak{B}}$ (resp. $P(P', E) \subseteq \mathcal{P}_{\mathfrak{B}}$) is movable with respect to E .*

Proof. The first statement is obvious. For the second, if $p \in P$ is movable and if p' lies in the same shared-route-biangle as p , then, by the fellow traveler Lemma 8.3, p' is movable. By Fact 8.19, $\mathcal{P}'_{\mathfrak{B}} \cap \Delta(p', E) \subseteq \mathcal{P}'_{\mathfrak{B}}$ is movable. By the first statement, $P'(P, E)$ is movable. □

We are now prepared to prove Lemma 8.14, which we restate here for convenience.

Lemma 8.14. *There is a sequence of modified H-moves (Figure 41) applicable to the web W and a sequence of modified H-moves applicable to W' , after which the bijection $\mathcal{P} \leftrightarrow \mathcal{P}'$ from Corollary 8.11 satisfies the property that each intersection point p in the global picture $\langle W \rangle$ and its corresponding intersection point p' in $\langle W' \rangle$ lie in the same shared-route-biangle.*

Proof. *Step 1.* Let N equal the cardinality $N = |\mathcal{P}| = |\mathcal{P}'|$. Define

$$N(W, W') = |\{p \in \mathcal{P}; \quad p \text{ and } p' \text{ lie in the same shared-route-biangle}\}| \in \mathbb{Z}_{\geq 0}.$$

If $N(W, W') = N$, then we are done. So assume $N(W, W') < N$.

The strategy is simple. If two intersection points $p \in \mathcal{P}_{\mathfrak{B}}$ and $p' \in \mathcal{P}'_{\mathfrak{B}}$ do not lie in the same shared-route-biangle, then we choose sufficiently large saturated movable sets $p \in P \subseteq \mathcal{P}_{\mathfrak{B}}$ and $p' \in P' \subseteq \mathcal{P}'_{\mathfrak{B}}$ such that pushing P and P' into adjacent biangles via Claim 8.18 does not decrease $N(W, W')$. This can be done in a controlled way so that eventually $N(W, W')$ increases.

Step 2. Let $E, \mathfrak{I}, \mathfrak{B}, \mathfrak{B}_1, \mathfrak{B}_2$ be as above.

Claim 8.22. Let $p_0 \in \mathcal{P}_{\mathfrak{B}}$ be movable with respect to E . Then, there exist subsets $p_0 \in P(p_0) \subseteq \mathcal{P}_{\mathfrak{B}}$ and $P'(p_0) \subseteq \mathcal{P}'_{\mathfrak{B}}$, and webs W_1 and W'_1 obtained by applying finitely many modified H-moves to W and W' , respectively, such that: in $\langle W_1 \rangle$ and $\langle W'_1 \rangle$ the subsets $P(p_0)$ and $P'(p_0)$ have been moved into $\mathfrak{B}_1 \cup \mathfrak{B}_2$; also $\mathcal{P} - P(p_0)$ and $\mathcal{P}' - P'(p_0)$ are unmoved; and

$$N \geq N(W_1, W'_1) \geq N(W, W') \in \mathbb{Z}_{\geq 0}. \tag{*}$$

We prove the claim. Our main task is to define two subsets $p_0 \in P(p_0) \subseteq \mathcal{P}_{\mathfrak{B}}$ and $P'(p_0) \subseteq \mathcal{P}'_{\mathfrak{B}}$ that are saturated and movable with respect to E , satisfying the property that

$$\begin{aligned} p \in P(p_0), \quad p \text{ and } p' \text{ lie in the same shared-route-biangle} \\ \iff \\ p' \in P'(p_0), \quad p' \text{ and } p \text{ lie in the same shared-route-biangle.} \end{aligned} \tag{**}$$

We do this simultaneously by a ping-pong procedure.

Put $P_1 = \mathcal{P}_{\mathfrak{B}} \cap \Delta(p_0, E)$ and $P'_1 = P'(P_1, E) \subseteq \mathcal{P}'_{\mathfrak{B}}$. Having defined $P_i \subseteq \mathcal{P}_{\mathfrak{B}}$ and $P'_i \subseteq \mathcal{P}'_{\mathfrak{B}}$, put $P_{i+1} = P_i \cup P(P'_i, E)$ and $P'_{i+1} = P'_i \cup P'(P_{i+1}, E)$. This defines two nested infinite sequences $P_1 \subseteq P_2 \subseteq \dots \subseteq \mathcal{P}_{\mathfrak{B}}$ and $P'_1 \subseteq P'_2 \subseteq \dots \subseteq \mathcal{P}'_{\mathfrak{B}}$. Since $\mathcal{P}_{\mathfrak{B}}$ and $\mathcal{P}'_{\mathfrak{B}}$ are finite, these sequences stabilize: $P_i = P_{i+1}$ and $P'_i = P'_{i+1}$ for all $i \geq i_0$. Set $P(p_0) = P_{i_0} \ni p_0$ and $P'(p_0) = P'_{i_0}$.

Note that, by construction, there exists $Q \subseteq \mathcal{P}_{\mathfrak{B}}$ and $Q' \subseteq \mathcal{P}'_{\mathfrak{B}}$ such that

$$P(p_0) = \mathcal{P}_{\mathfrak{B}} \cap \left(\bigcup_{q \in Q} \Delta(q, E) \right) \quad \text{and} \quad P'(p_0) = \mathcal{P}'_{\mathfrak{B}} \cap \left(\bigcup_{q' \in Q'} \Delta(q', E) \right).$$

By Fact 8.20, $P(p_0)$ and $P'(p_0)$ are saturated with respect to E .

Observe also that since $p_0 \in \mathcal{P}_{\mathfrak{B}}$ is movable by hypothesis, $P_1 = \mathcal{P}_{\mathfrak{B}} \cap \Delta(p_0, E)$ is movable by Fact 8.19, hence $P(p_0) \subseteq \mathcal{P}_{\mathfrak{B}}$ and $P'(p_0) \subseteq \mathcal{P}'_{\mathfrak{B}}$ are movable by Fact 8.21.

To check Equation (**), by symmetry it suffices to check one direction. Assume $p \in P(p_0)$ and that p and p' lie in the same shared-route-biangle. Let i be such that $p \in P_i$. Then

$$p' \in \mathcal{P}'_{\mathfrak{B}} \cap \Delta(p', E) \subseteq P'(P_i, E) \subseteq P'_i \subseteq P'(p_0).$$

To prove Equation (*), we use Claim 8.18 to move the saturated and movable sets $P(p_0)$ and $P'(p_0)$, and only these sets, into the opposite biantles $\mathfrak{B}_1 \cup \mathfrak{B}_2$ via finitely many modified H-moves applied to W and W' , yielding the desired webs W_1 and W'_1 (note what we are here calling W_1 was called W_n in the statement of Claim 8.18). If $p \in P(p_0)$ moves into the biangle \mathfrak{B}_1 (resp. \mathfrak{B}_2), and if p' lies in the same shared-route-biangle as p so that $p' \in P'(p_0)$ by Equation (**), then by the fellow traveler Lemma 8.3 p' also moves into the biangle \mathfrak{B}_1 (resp. \mathfrak{B}_2) and similarly if the roles of p and p' are reversed.

Step 3. To finish the proof, assume that p and p' do not lie in the same shared-route-biangle. Then it makes sense to talk about which of p or p' is farther away from the source-end \mathcal{E} or \mathcal{E}' of the left-oriented crossing shared-route $SR(p)$ or $SR'(p')$ which it generates, respectively. More precisely, if $p \in_{SR(p)} \mathfrak{B}_i$ and $p' \in_{SR'(p')} \mathfrak{B}_j$, $i, j \geq 0$, then $i \neq j$ and p being farther away is equivalent to $i > j$.

Assume p is farther away, so $i > j$. By Claim 8.22, we can push p one step closer to the source-end \mathcal{E} , that is we can push p into \mathfrak{B}_{i-1} . For this step, p' either (1) stays in \mathfrak{B}_j , (2) is pushed into \mathfrak{B}_{j-1} , or (3) is pushed into \mathfrak{B}_{j+1} ; see Figure 53. Notice since no two adjacent edges in a shared-route can represent the same edge in the split ideal triangulation $\widehat{\lambda}$ (by the no-switchbacks property), case (3) can only happen if $j < i - 1$. Also, again by Claim 8.22, as a result of this step the number $N(W, W')$ only increases or stays the same.

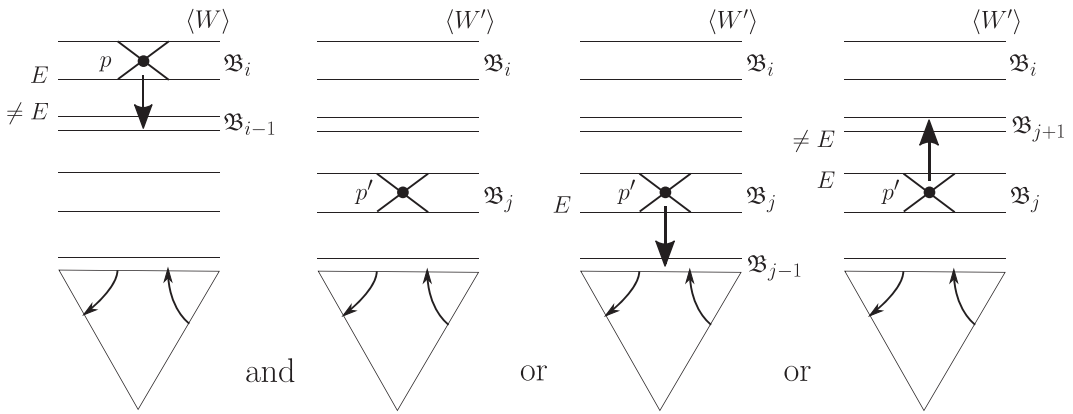


Figure 53. Moving intersection points into the same shared-route-biangle.

Since the indices i, j are bounded below, after multiple applications of this step eventually p and p' fall into the same shared-route-biangle, at which point $N(W, W')$ strictly increases. Repeating this procedure for each pair p and p' completes the proof of Lemma 8.14. \square

9. Webs on surfaces-with-boundary

We generalize Theorem 7.1 to the case of surfaces-with-boundary $\widehat{\mathfrak{S}}$. More precisely, we give two distinct, but complementary, versions of the result. The first version, where we think of the surface $\widehat{\mathfrak{S}}$ as generalizing punctured surfaces \mathfrak{S} , originates in the geometry and topology of $SL_3(\mathbb{C})$ -character varieties. The second version, where we think of the surface $\widehat{\mathfrak{S}}$ as generalizing ideal polygons \mathfrak{D}_k , originates in the representation theory of the Lie group $SL_3(\mathbb{C})$. The proof of either statement is essentially the same as in the empty boundary case.

9.1. Essential webs

9.1.1. Surfaces-with-boundary

Our surfaces, now denoted $\widehat{\mathfrak{S}} = \overline{\mathfrak{S}} - P$, are obtained by removing a finite set P of punctures from a compact oriented surface $\overline{\mathfrak{S}}$. We require that there is at least one puncture, that each boundary component of $\overline{\mathfrak{S}}$ contains a puncture, and that the resulting punctured surface $\widehat{\mathfrak{S}}$ admits an ideal triangulation λ ; this last property is equivalent to the Euler characteristic condition $\chi(\widehat{\mathfrak{S}}) < d/2$, where d is the number of components of $\partial\widehat{\mathfrak{S}}$. The boundary edges of $\widehat{\mathfrak{S}}$ count as edges in an ideal triangulation λ .

Once again, for simplicity, we assume that λ does not contain any self-folded triangles; however, our results should extend to this setting essentially without change.

The split ideal triangulation $\widehat{\lambda}$ associated to an ideal triangulation λ is defined as in §4.3. In particular, the boundary edges of $\widehat{\mathfrak{S}}$ are split as well.

9.1.2. Essential webs

A *global web*, or just *web*, W on the surface $\widehat{\mathfrak{S}}$ is defined as in Definition 3.1, except ‘ \mathfrak{D}_k ’ is replaced by ‘ $\widehat{\mathfrak{S}}$ ’ and ‘local’ is replaced by ‘global’.

The internal and external faces of a web W on $\widehat{\mathfrak{S}}$ are defined as in Definition 3.2, except with the appropriate replacements as above. As usual, a web W on $\widehat{\mathfrak{S}}$ is nonelliptic if all of its internal faces have at least six sides; compare Definition 3.4.

An *essential web* W on $\widehat{\mathfrak{S}}$ is defined as in Definition 3.8, where in addition the arc α needs to be isotopic (respecting boundary) in $\widehat{\mathfrak{S}}$ to the segment \overline{E} .

The good position of a web W with respect to a split ideal triangulation $\widehat{\lambda}$ is defined exactly as in Definition 4.5, without change.

9.2. Rungless essential webs; first version of the boundary result

9.2.1. Rungless essential webs

As usual, a *rungless* web W on the surface $\widehat{\mathfrak{S}}$ is a web that does not have any H-faces; compare Definition 3.9.

The *parallel equivalence class* of a *rungless* web W is defined as in Definition 2.3, except we have to include another global parallel-move exchanging two arcs that together with segments in $\partial\widehat{\mathfrak{S}}$ form the boundary of an embedded rectangle R in the surface $\widehat{\mathfrak{S}}$; for instance, this would be the case in Figure 3 had we not identified the top and bottom edges of the surface.

The property of being essential is preserved by parallel equivalence. The collection of parallel equivalence classes of *rungless* essential webs is denoted by $[\mathcal{W}_{\widehat{\mathfrak{S}}}]$. (Note, by definition, the empty class $[W] = [\emptyset]$ is in $[\mathcal{W}_{\widehat{\mathfrak{S}}}]$.)

9.2.2. Knutson–Tao cone associated to an ideal triangulation

To an ideal triangulation λ of the surface $\widehat{\mathfrak{S}}$ we associate a dotted ideal triangulation, also denoted λ , as in §5.1. In particular, there are dots located on the boundary edges of $\widehat{\mathfrak{S}}$, as, for example, in Figure 27b, where $\widehat{\mathfrak{S}} = \mathfrak{T}$ is an ideal triangle. The number N of dots in the dotted triangulation λ can be computed as $N = 2 * \#\{\text{edges } E \text{ of } \lambda\} + \#\{\text{triangles } \mathfrak{T} \text{ of } \lambda\}$. (Since each ideal triangulation λ has $-3\chi(\widehat{\mathfrak{S}}) + 2d$ edges and $-2\chi(\widehat{\mathfrak{S}}) + d$ triangles, note N is independent of λ .)

To the dotted triangulation λ we associate the *Knutson–Tao cone* $\mathcal{C}_{\lambda}^+ \subseteq \mathbb{Z}_{\geq 0}^N$, as in §6.3.

9.2.3. Coordinates for rungless essential webs

The minimal position of a *rungless* web W with respect to an ideal triangulation λ is defined as in Definition 4.2. Then, Proposition 4.3 holds word for word, except ‘nonelliptic’ is replaced by ‘*rungless essential*’.

Modified H-moves take *rungless* essential webs in good position to webs of the same type. Proposition 4.7 holds verbatim, except ‘nonelliptic’ is replaced by ‘*rungless essential*’.

Given an ideal triangulation λ , we define the Fock–Goncharov global coordinate function $\Phi_{\lambda}^{\text{FG}} : [\mathcal{W}_{\widehat{\mathfrak{S}}}] \rightarrow \mathcal{C}_{\lambda}^+$ as in §5.4; see Definition 5.4.

Theorem 9.1 (First boundary result). *The Fock–Goncharov global coordinate function*

$$\Phi_{\lambda}^{\text{FG}} : [\mathcal{W}_{\widehat{\mathfrak{S}}}] \xrightarrow{\sim} \mathcal{C}_{\lambda}^+ \subseteq \mathbb{Z}_{\geq 0}^N$$

is a bijection of sets, identifying parallel equivalence classes of *rungless* essential webs on the surface $\widehat{\mathfrak{S}}$ with points of the *Knutson–Tao cone* associated to the ideal triangulation λ .

Proof. As in the proof of Theorem 7.1, the strategy is to construct an explicit inverse

$$\Psi_{\lambda}^{\text{FG}} : \mathcal{C}_{\lambda}^+ \longrightarrow [\mathcal{W}_{\widehat{\mathfrak{S}}}] .$$

The mapping $\Psi_{\lambda}^{\text{FG}}$ is defined via the ladder gluing construction followed by removing internal elliptic faces, as explained in §7.2-7.3. Because of the *rungless* condition, we also need to remove external H-faces, which can be done at the cost of swapping two strands of the web lying on the boundary $\partial\widehat{\mathfrak{S}}$. For two examples of this procedure, see Figures 54 and 55 (compare Figures 37 and 39). As before, the resulting *rungless* essential web is not unique in general.

In order to deal with this ambiguity, we need the analogue of the main Lemma 7.7, saying that two *rungless* essential webs resulting from the ladder gluing construction are parallel equivalent. The proof of the main lemma is essentially unchanged from §8. To say a word about it, the proof of Corollary 8.11 requires the fact that there are no crossing shared-routes terminating on the boundary $\partial\widehat{\mathfrak{S}}$. This follows from the *rungless* condition. □

Remark 9.2. Theorem 9.1 is closely related to [Kim20, Proposition 1.12].

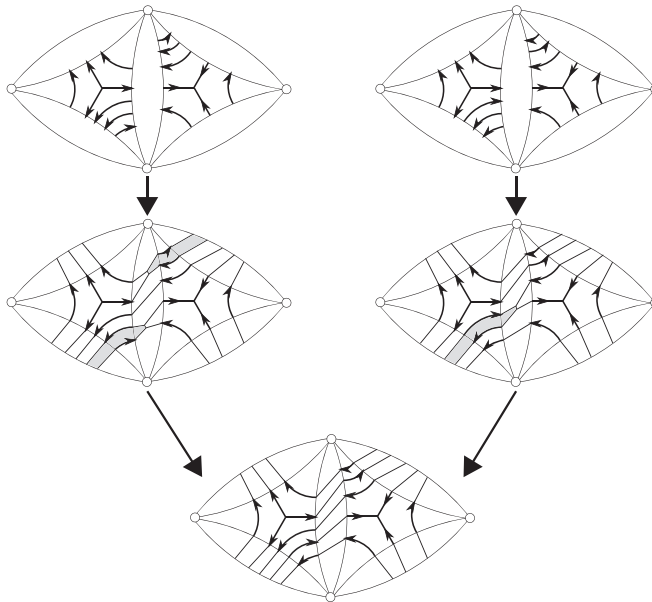


Figure 54. Ladder gluing construction for rungless essential webs: 1 of 2 (on the ideal square).

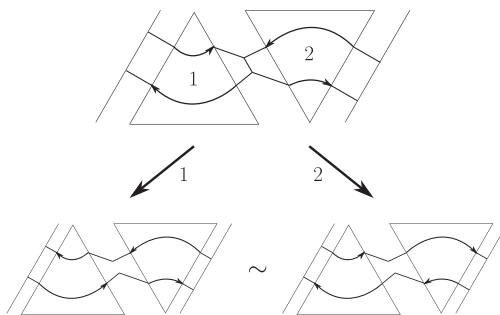


Figure 55. Ladder gluing construction for rungless essential webs: 2 of 2.

9.3. Application: geometry and topology of $SL_3(\mathbb{C})$ -character varieties

As a consequence of the first version of the result, Theorem 9.1, we give an alternative geometric proof of the Sikora–Westbury theorem [SW07, Theorem 9.5] (see also [FS22, Proposition 4]), whose original proof in [SW07] assumes the diamond lemma from noncommutative algebra.

Corollary 9.3 (Application of the first boundary result). *The collection $[\mathcal{W}_{\widehat{\mathfrak{S}}}]$ of parallel equivalence classes of rungless essential webs on the surface $\widehat{\mathfrak{S}}$ indexes a natural linear basis for the algebra $\mathbb{C}[\mathcal{R}_{SL_3(\mathbb{C})}(\widehat{\mathfrak{S}})]$ of regular functions on the $SL_3(\mathbb{C})$ -character variety.*

Here, the character variety $\mathcal{R}_{SL_n(\mathbb{C})}(\widehat{\mathfrak{S}})$, for general n , was discussed in the introduction for surfaces $\widehat{\mathfrak{S}} = \mathfrak{S}$ with empty boundary. When $\partial\widehat{\mathfrak{S}} \neq \emptyset$, there is not a mainstream definition for $\mathcal{R}_{SL_n(\mathbb{C})}(\widehat{\mathfrak{S}})$. Possible models may be found in [FP14, GS15, CL22, KQ19, FS22, Hig23]. In order for Corollary 9.3 to be well posed, we make use of a purely topological model, via *skein algebras*, which has the advantage of admitting a natural deformation quantization.

Definition 9.4. Following Frohman–Sikora [FS22, §1,12], for a surface-with-boundary $\widehat{\mathfrak{S}}$ we define the algebra $\mathbb{C}[\mathcal{R}_{SL_3(\mathbb{C})}(\widehat{\mathfrak{S}})]$ of regular functions on the $SL_3(\mathbb{C})$ -character variety to be the commutative

(reduced skein) algebra $\mathcal{S}^1(\widehat{\mathfrak{C}})$ of [FS22, §3], where we have taken the specialization $q = a = 1$ of their deformation parameters.

In particular, a web W on $\widehat{\mathfrak{C}}$ represents an element of $\mathcal{S}^1(\widehat{\mathfrak{C}})$.

Remark 9.5. When $\widehat{\mathfrak{C}} = \mathfrak{C}$, Sikora [Sik01] proved that the trace functions Tr_W on the character variety $\mathcal{R}_{\text{SL}_3(\mathbb{C})}(\mathfrak{C})$ furnish a natural isomorphism $\mathcal{S}^1(\mathfrak{C}) \cong \mathbb{C}[\mathcal{R}_{\text{SL}_3(\mathbb{C})}(\mathfrak{C})]$.

Proof of Corollary 9.3. We prove a more general statement. Let $\mathcal{S}^{q,a}(\widehat{\mathfrak{C}})$ be the *reduced* SL_3 -skein algebra of [FS22, §3] for deformation parameters $q, a \in \mathbb{C} - \{0\}$. So, $\mathcal{S}^1(\widehat{\mathfrak{C}}) = \mathcal{S}^{1,1}(\widehat{\mathfrak{C}})$.

Higgins [Hig23] defined a SL_3 -stated skein algebra $\mathcal{S}_{\text{st}}^q(\widehat{\mathfrak{C}})$ generalizing the SL_2 -stated skein algebra of [CL22]. More precisely, we define $\mathcal{S}_{\text{st}}^q(\widehat{\mathfrak{C}})$ to be Kim’s [Kim20, §5] adaptation of Higgins’ stated skein algebra.

When $a = 1$, inclusion provides a natural algebra homomorphism $\iota : \mathcal{S}^{q,1}(\widehat{\mathfrak{C}}) \rightarrow \mathcal{S}_{\text{st}}^q(\widehat{\mathfrak{C}})$ from the Frohman–Sikora reduced skein algebra to the Higgins stated skein algebra; in fact, the mapping ι is onto the subalgebra $\mathcal{S}_{\text{st=top}}^q(\widehat{\mathfrak{C}})$ generated by webs with all-top-states on the boundary $\partial\widehat{\mathfrak{C}}$. Put $\mathcal{S}^q(\widehat{\mathfrak{C}}) := \mathcal{S}^{q,1}(\widehat{\mathfrak{C}})$. In summary, $\iota : \mathcal{S}^q(\widehat{\mathfrak{C}}) \rightarrow \mathcal{S}_{\text{st=top}}^q(\widehat{\mathfrak{C}}) \subseteq \mathcal{S}_{\text{st}}^q(\widehat{\mathfrak{C}})$.

Using the boundary orientation of $\partial\widehat{\mathfrak{C}}$ induced by the orientation of $\widehat{\mathfrak{C}}$, a web W on $\widehat{\mathfrak{C}}$ lifts to an element of the skein algebra $\mathcal{S}^q(\widehat{\mathfrak{C}})$. Moreover, parallel equivalent rungless webs $W \sim W'$ determine the same element of $\mathcal{S}^q(\widehat{\mathfrak{C}})$ (by [FS22, Figure 6] since $a = 1$). We prove $[\mathcal{W}_{\widehat{\mathfrak{C}}}]$ forms a basis for $\mathcal{S}^q(\widehat{\mathfrak{C}})$. It is immediate by construction that $[\mathcal{W}_{\widehat{\mathfrak{C}}}]$ is spanning.

We mimic the strategy of [BW11, §8] in the SL_2 -case. Fix an ideal triangulation λ of $\widehat{\mathfrak{C}}$. Building on [Dou20, Dou21a, Dou21b], Kim [Kim20] defined a SL_3 -quantum trace map, which in particular is an algebra homomorphism $\text{Tr}_\lambda^q : \mathcal{S}_{\text{st}}^q(\widehat{\mathfrak{C}}) \rightarrow \mathcal{F}_\lambda^q$ from the stated skein algebra $\mathcal{S}_{\text{st}}^q(\widehat{\mathfrak{C}})$ to a quantum torus \mathcal{F}_λ^q depending on λ . More precisely, $\mathcal{F}_\lambda^q = \mathbb{C}[Z_1^{\pm 1}, Z_2^{\pm 1}, \dots, Z_N^{\pm 1}]^q$ is a noncommutative q -deformation of the algebra of Laurent polynomials in variables Z_i , which no longer commute but q -commute (according to a quiver drawn on the triangulated surface). Here, N is the number of coordinates in Theorem 9.1. (When $q = 1$, the variables $Z_i = X_i^{1/3}$ can be thought of as formal cube roots of the Fock–Goncharov coordinates X_i .)

By [Kim20, Proposition 5.80] (and [Kim21, Proposition 3.15]), the quantum trace map Tr_λ^q satisfies the property that the polynomial $\text{Tr}_\lambda^q(\iota(W))$, obtained by evaluating a rungless essential web W in $[\mathcal{W}_{\widehat{\mathfrak{C}}}]$, has a highest term $Z_1^{a_1} Z_2^{a_2} \dots Z_N^{a_N}$ (omitting the power of q coefficient) whose exponents are the coordinates $(a_1, a_2, \dots, a_N) = \Phi_\lambda^{\text{FG}}(W) \in \mathbb{Z}_{\geq 0}^N$ of Theorem 9.1. (Here, by highest term, we mean that if a monomial $Z_1^{a'_1} Z_2^{a'_2} \dots Z_N^{a'_N}$ also appears in $\text{Tr}_\lambda^q(\iota(W))$, then $a'_i \leq a_i$ for all $i = 1, 2, \dots, N$.)

It follows that each W is nonzero in $\mathcal{S}^q(\widehat{\mathfrak{C}})$, that ι is injective on $[\mathcal{W}_{\widehat{\mathfrak{C}}}]$, that $\iota([\mathcal{W}_{\widehat{\mathfrak{C}}}]$ is linearly independent in $\mathcal{S}_{\text{st}}^q(\widehat{\mathfrak{C}})$, and lastly that $\iota : \mathcal{S}^q(\widehat{\mathfrak{C}}) \xrightarrow{\sim} \mathcal{S}_{\text{st=top}}^q(\widehat{\mathfrak{C}}) \subseteq \mathcal{S}_{\text{st}}^q(\widehat{\mathfrak{C}})$ is an isomorphism. In particular, we gather $[\mathcal{W}_{\widehat{\mathfrak{C}}}]$ is independent, hence a basis of $\mathcal{S}^q(\widehat{\mathfrak{C}})$. □

9.4. Boundary-fixed essential webs; second version of the boundary result

9.4.1. Boundary-fixed essential webs

For a boundary edge E of the surface $\widehat{\mathfrak{C}}$, a *strand-set* S_E is a (possibly empty) set $S_E = \{s\}$ of disjoint oriented strands s located on E (compare Definition 3.12); see Figures 56 and 57, where the strands are indicated by white-headed arrows. A *strand-set* $S_{\partial\widehat{\mathfrak{C}}} = \{S_E\}$ for $\widehat{\mathfrak{C}}$ is a collection of strand-sets S_E varying over all $E \subseteq \partial\widehat{\mathfrak{C}}$.

Definition 9.6. A *boundary-fixed web* W with respect to a strand-set $S_{\partial\widehat{\mathfrak{C}}}$ for the surface $\widehat{\mathfrak{C}}$ is a web W whose end-strands match the strand-set $S_{\partial\widehat{\mathfrak{C}}}$; see Figures 56 and 57.

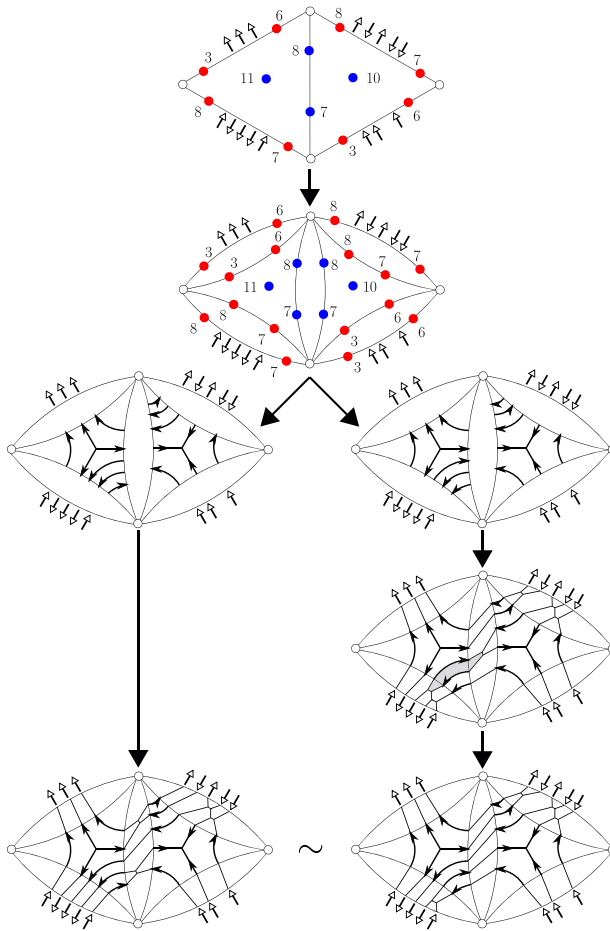


Figure 56. Ladder construction for boundary-fixed essential webs: 1 of 2 (on the ideal square).

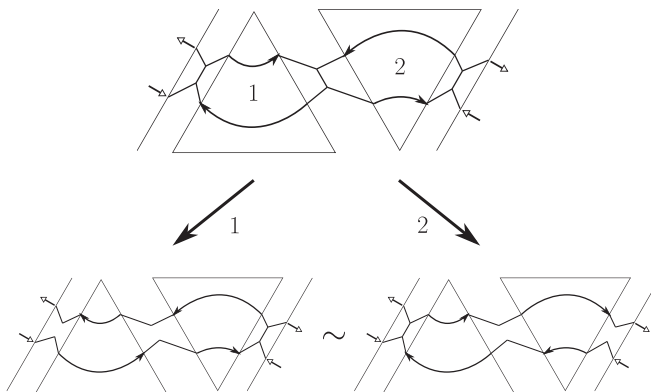


Figure 57. Ladder construction for boundary-fixed essential webs: 2 of 2.

If W is boundary-fixed for a strand-set $S_{\partial\tilde{\mathcal{E}}}$, then W is not boundary-fixed for any strand-set $S'_{\partial\tilde{\mathcal{E}}}$ obtained by swapping two oppositely oriented strands of $S_{\partial\tilde{\mathcal{E}}}$ on a boundary edge.

For boundary-fixed webs, global parallel-moves can only be performed across embedded annuli, in contrast to rungless webs (§9.2.1). Global parallel-moves preserve the property of being essential. We

denote by $[\mathcal{W}_{\widehat{\mathfrak{E}}}] (S_{\partial\widehat{\mathfrak{E}}})$ the collection of *parallel equivalence classes of boundary-fixed essential webs* for the strand-set $S_{\partial\widehat{\mathfrak{E}}}$. (Note, by definition, $[W] = [\emptyset] \in [\mathcal{W}_{\widehat{\mathfrak{E}}}] (S_{\partial\widehat{\mathfrak{E}}})$ if and only if $S_{\partial\widehat{\mathfrak{E}}} = \emptyset$.)

9.4.2. Boundary-fixed Knutson–Tao cone

By Figure 30 (recall also property (2) of Definition 5.1), a strand-set S_E determines two local coordinates on a boundary edge E of $\widehat{\mathfrak{E}}$. More generally, a strand-set $S_{\partial\widehat{\mathfrak{E}}}$ for the surface fixes $2 \cdot \#\{\text{boundary edges } E\}$ coordinates on the boundary $\partial\widehat{\mathfrak{E}}$. See Figure 56, for an example, where the fixed coordinates are colored red.

Definition 9.7. The *boundary-fixed Knutson–Tao cone* $\mathcal{C}_\lambda^+(S_{\partial\widehat{\mathfrak{E}}}) \subseteq \mathcal{C}_\lambda^+ \subseteq \mathbb{Z}_{\geq 0}^N$ with respect to a strand-set $S_{\partial\widehat{\mathfrak{E}}}$ is the subset of \mathcal{C}_λ^+ (as defined in §9.2.2) consisting of points whose boundary coordinates agree with those determined by $S_{\partial\widehat{\mathfrak{E}}}$.

Note that, in contrast to boundary-fixed webs (§9.4.1), the boundary-fixed Knutson–Tao cone $\mathcal{C}_\lambda^+(S_{\partial\widehat{\mathfrak{E}}}) \subseteq \mathcal{C}_\lambda^+$ is independent of permuting the boundary strands of $S_{\partial\widehat{\mathfrak{E}}}$. This is because the coordinates on a boundary component only depend on the number of in- and out-strands, not on their ordering along the edge (see property (2) in Definition 5.1).

9.4.3. Coordinates for boundary-fixed essential webs

The minimal position of a boundary-fixed web W with respect to an ideal triangulation λ is defined as in Definition 4.2. Proposition 4.3 holds word for word, except ‘nonelliptic’ is replaced by ‘boundary-fixed essential’.

Modified H-moves take boundary-fixed essential webs in good position to webs of the same type. Proposition 4.7 holds, except ‘nonelliptic’ is replaced by ‘boundary-fixed essential’.

Given a strand-set $S_{\partial\widehat{\mathfrak{E}}}$ and an ideal triangulation λ , we define the Fock–Goncharov global coordinate function $\Phi_\lambda^{\text{FG}}(S_{\partial\widehat{\mathfrak{E}}}) : [\mathcal{W}_{\widehat{\mathfrak{E}}}] (S_{\partial\widehat{\mathfrak{E}}}) \rightarrow \mathcal{C}_\lambda^+(S_{\partial\widehat{\mathfrak{E}}}) \subseteq \mathcal{C}_\lambda^+ \subseteq \mathbb{Z}_{>0}^N$ as in §5.4; see Definition 5.4.

Theorem 9.8 (Second boundary result). *The Fock–Goncharov global coordinate function*

$$\Phi_\lambda^{\text{FG}}(S_{\partial\widehat{\mathfrak{E}}}) : [\mathcal{W}_{\widehat{\mathfrak{E}}}] (S_{\partial\widehat{\mathfrak{E}}}) \xrightarrow{\sim} \mathcal{C}_\lambda^+(S_{\partial\widehat{\mathfrak{E}}}) \subseteq \mathcal{C}_\lambda^+ \subseteq \mathbb{Z}_{>0}^N$$

with respect to the strand-set $S_{\partial\widehat{\mathfrak{E}}}$ is a bijection of sets, identifying parallel equivalence classes of boundary-fixed essential webs with points of the boundary-fixed Knutson–Tao cone.

Proof. As in the proof of Theorem 7.1, the strategy is to construct an explicit inverse

$$\Psi_\lambda^{\text{FG}}(S_{\partial\widehat{\mathfrak{E}}}) : \mathcal{C}_\lambda^+(S_{\partial\widehat{\mathfrak{E}}}) \longrightarrow [\mathcal{W}_{\widehat{\mathfrak{E}}}] (S_{\partial\widehat{\mathfrak{E}}}).$$

The mapping $\Psi_\lambda^{\text{FG}}(S_{\partial\widehat{\mathfrak{E}}})$ is defined via the ladder gluing construction followed by removing internal elliptic faces, as explained in §7.2–7.3. In contrast to the rungless setting (§9.2.3), no new reductions are required. For examples, see Figures 56 and 57; compare the empty-boundary case, Figures 37 and 39, and the rungless boundary case, Figures 54 and 55.

We also need the analogue of the main Lemma 7.7, saying that two boundary-fixed essential webs resulting from the ladder gluing construction are parallel equivalent. The proof of the main lemma is essentially unchanged from §8. To say a word about it, for the proof of Corollary 8.11, if a shared-route for W ending on the boundary $\partial\widehat{\mathfrak{E}}$ is crossing, then the corresponding shared-route for W' is also crossing, by the boundary-fixed condition. □

Corollary 9.9. *Let two strand-sets $S_{\partial\widehat{\mathfrak{E}}}$ and $S'_{\partial\widehat{\mathfrak{E}}}$ be the same up to permuting strands lying on the same boundary edge. Then, there is a natural one-to-one correspondence*

$$\Phi_\lambda^{\text{FG}}(S'_{\partial\widehat{\mathfrak{E}}})^{-1} \circ \Phi_\lambda^{\text{FG}}(S_{\partial\widehat{\mathfrak{E}}}) : [\mathcal{W}_{\widehat{\mathfrak{E}}}] (S_{\partial\widehat{\mathfrak{E}}}) \xrightarrow{\sim} \mathcal{C}_\lambda^+(S_{\partial\widehat{\mathfrak{E}}}) = \mathcal{C}_\lambda^+(S'_{\partial\widehat{\mathfrak{E}}}) \xrightarrow{\sim} [\mathcal{W}_{\widehat{\mathfrak{E}}}] (S'_{\partial\widehat{\mathfrak{E}}})$$

sending parallel equivalence classes of boundary-fixed essential webs W for $S_{\partial\widehat{\mathfrak{E}}}$ to parallel equivalence classes of boundary-fixed essential webs W' for $S'_{\partial\widehat{\mathfrak{E}}}$. Here, natural means that the resulting bijection $[\mathscr{W}_{\widehat{\mathfrak{E}}}] (S_{\partial\widehat{\mathfrak{E}}}) \rightarrow [\mathscr{W}_{\widehat{\mathfrak{E}}}] (S'_{\partial\widehat{\mathfrak{E}}})$ is independent of the choice of triangulation λ .

Proof. Let W be a boundary-fixed essential web for $S_{\partial\widehat{\mathfrak{E}}}$, and let λ_1 and λ_2 be two ideal triangulations. We claim that there are webs W_{λ_1} and W_{λ_2} isotopic to W and in good position for the split ideal triangulation $\widehat{\lambda}_1$ and $\widehat{\lambda}_2$, respectively, such that W_{λ_1} and W_{λ_2} have the same ladders in the boundary biangles \mathfrak{B} facing $\partial\widehat{\mathfrak{E}}$.

Indeed, by pushing as many H's of W as possible into the boundary biangles \mathfrak{B} , we may assume that the web \widetilde{W} obtained from W by chopping off the boundary biangles \mathfrak{B} is rungless essential. By §9.2.3 there exist webs $\widetilde{W}_{\lambda_1}$ and $\widetilde{W}_{\lambda_2}$ isotopic to \widetilde{W} that are in good position for $\widehat{\lambda}_1$ and $\widehat{\lambda}_2$, respectively. Let W_{λ_1} and W_{λ_2} be obtained by reattaching the ladders from the cut-off boundary biangles \mathfrak{B} to $\widetilde{W}_{\lambda_1}$ and $\widetilde{W}_{\lambda_2}$, respectively. This proves the claim.

To finish, the map $[\mathscr{W}_{\widehat{\mathfrak{E}}}] (S_{\partial\widehat{\mathfrak{E}}}) \rightarrow [\mathscr{W}_{\widehat{\mathfrak{E}}}] (S'_{\partial\widehat{\mathfrak{E}}})$ for λ_1 is computed via the following steps: (1) erase the ladders of W_{λ_1} from the boundary biangles \mathfrak{B} ; (2) replace $S_{\partial\widehat{\mathfrak{E}}}$ with $S'_{\partial\widehat{\mathfrak{E}}}$ by permuting boundary strands; (3) insert the unique ladders into the boundary biangles \mathfrak{B} matching this new boundary data; (4) eliminate elliptic faces. A similar computation holds for the map with respect to λ_2 . By the claim, the webs for λ_1 and λ_2 resulting after step (3) are isotopic. \square

9.5. Application: representation theory of the Lie group $SL_3(\mathbb{C})$

As a consequence of the second version of the result, Theorem 9.8, we make a connection to Kuperberg's famous theorem relating webs in the disk to the representation theory of $SL_3(\mathbb{C})$.

The finite-dimensional irreducible representations of $SL_3(\mathbb{C})$ are in one-to-one correspondence with ordered pairs $(n^{\text{in}}, n^{\text{out}}) \in \mathbb{Z}_{\geq 0}^2$. For example, we may say that $(1, 0)$ corresponds to the defining vector representation V and $(0, 1)$ corresponds to its dual representation V^* .

We assign to each strand-set $S_{\partial\widehat{\mathfrak{E}}}$ a tensor product $V(S_{\partial\widehat{\mathfrak{E}}}) = \otimes_E V_E$ of finite-dimensional irreducible representations V_E of $SL_3(\mathbb{C})$, varying over boundary edges E of $\widehat{\mathfrak{E}}$, as follows. If n_E^{in} (resp. n_E^{out}) is the number of in-strands (resp. out-strands) of S_E , where $S_{\partial\widehat{\mathfrak{E}}} = \{S_E\}_E$, then we define V_E to be the irreducible representation corresponding to $(n_E^{\text{in}}, n_E^{\text{out}})$.

Note $V(S_{\partial\widehat{\mathfrak{E}}}) = V(S'_{\partial\widehat{\mathfrak{E}}})$ if $S_{\partial\widehat{\mathfrak{E}}}$ and $S'_{\partial\widehat{\mathfrak{E}}}$ are the same up to permuting strands on an E .

For a representation V of $SL_3(\mathbb{C})$, let $V^{\text{SL}_3(\mathbb{C})} \subseteq V$ be the subspace of invariant vectors.

Theorem 9.10 [Kup96, Theorem 6.1]. *For $\widehat{\mathfrak{E}} = \mathfrak{D}_k$ ($k \geq 1$) the ideal polygon with k boundary edges (§3.1), the collection $[\mathscr{W}_{\mathfrak{D}_k}] (S_{\partial\mathfrak{D}_k})$ of classes $[W]$ of boundary-fixed essential webs with respect to a strand-set $S_{\partial\mathfrak{D}_k}$ indexes a linear basis for the invariant space $V(S_{\partial\mathfrak{D}_k})^{\text{SL}_3(\mathbb{C})}$.*

Note that, for $\widehat{\mathfrak{E}} = \mathfrak{D}_k$, a parallel equivalence class $[W] \in [\mathscr{W}_{\mathfrak{D}_k}] (S_{\partial\mathfrak{D}_k})$ is an isotopy class.

From Kuperberg's theorem, together with Theorem 9.8, we immediately obtain:

Corollary 9.11 (Application of the second boundary result). *For $\widehat{\mathfrak{E}} = \mathfrak{D}_k$ ($k \geq 3$), a strand-set $S_{\partial\mathfrak{D}_k}$, and an ideal triangulation λ of \mathfrak{D}_k , the boundary-fixed Knutson–Tao cone $\mathcal{C}_{\lambda}^+(S_{\partial\mathfrak{D}_k}) \subseteq \mathcal{C}_{\lambda}^+ \subseteq \mathbb{Z}_{\geq 0}^N$ indexes a linear basis for the invariant space $V(S_{\partial\mathfrak{D}_k})^{\text{SL}_3(\mathbb{C})}$.* \square

Remark 9.12.

1. This corollary is reminiscent of results about the Knutson–Tao hive model [KT99, Buc00] for the general linear group $GL_n(\mathbb{C})$, where the Littlewood–Richardson coefficients $c_{\lambda\mu}^{\nu}$ associated to highest weights λ, μ, ν provide the multiplicities of irreducible representations V_{ν} in $V_{\lambda} \otimes V_{\mu}$. Certain multiplicities $c_{\lambda\mu}^{\nu}$ can be computed as the number of solutions of the Knutson–Tao rhombus inequalities, without n -congruence conditions (see Remark 6.5(1)), on the dotted n -triangle matching certain fixed boundary conditions determined by the weights λ, μ, ν . (Possibly related, see [Mag20].)

2. Corollary 9.11 was the result of Kuperberg’s theorem combined with Theorem 9.8. We would like to have gone in the other direction. That is, we would like to give an alternative geometric proof of Kuperberg’s theorem, as a consequence of Theorem 9.8 and Corollary 9.11. Indeed, this was the spirit of Kuperberg’s proof for the $SL_2(\mathbb{C})$ -version of his result [Kup96, Theorem 2.4], where the $SL_2(\mathbb{C})$ -analogue of Corollary 9.11 is a simple consequence of the Clebsch–Gordan theorem. It is natural then to ask:

Question 9.13. Is there an alternative purely representation theoretic proof of Corollary 9.11?

Question 9.14. Is there a representation theoretic interpretation of Theorem 9.8 for any surface-with-boundary $\widehat{\mathfrak{S}}$, generalizing Kuperberg’s theorem in the case $\widehat{\mathfrak{S}} = \mathfrak{D}_k$? (We ask this question also for $SL_2(\mathbb{C})$.) Possible clues may lie in [FP14, CL22, GS19].

Acknowledgements. This research would not have been possible without the help and support of many people, whose time and patience often seem limitless. In particular, we are profoundly grateful to Dylan Allegretti for his involvement during the early stages of this project; Charlie Frohman for his guidance from the very beginning; Francis Bonahon and Viktor Kleen for helping us refine our ideas and for technical assistance; Tommaso Cremaschi for his invaluable feedback after reading way too many drafts; as well as Vijay Higgins, Hyun Kyu Kim, Linhui Shen and Adam Sikora for helpful conversations. Much of this work was completed during very enjoyable visits to Tsinghua University in Beijing (supported by a GEAR graduate internship grant) and the University of Southern California in Los Angeles. We would like to take this opportunity to extend our enormous gratitude to these institutions for their warm hospitality and many tasty dinners (the first author was especially fond of the *sōngshū guiyú*).

Competing interest. The authors have no competing interests to declare.

Funding statement. This work was partially supported by the U.S. National Science Foundation grants DMS-1107452, 1107263, 1107367 ‘RNMS: GEometric structures And Representation varieties’ (the GEAR Network). The first author was also partially supported by the U.S. National Science Foundation grants DMS-1406559 and 1711297, and the second author by the China Postdoctoral Science Foundation grant 2018T110084, the FNR AFR Bilateral grant COALAS 11802479-2, and the Huawei Young Talents Program at IHES.

References

- [AK17] D. G. L. Allegretti and H. K. Kim, ‘A duality map for quantum cluster varieties from surfaces’, *Adv. Math.* **306** (2017), 1164–1208.
- [Buc00] A. S. Buch, ‘The saturation conjecture (after A. Knutson and T. Tao)’, *Enseign. Math.* **46** (2000), 43–60. With an appendix by William Fulton.
- [Bul97] D. Bullock, ‘Rings of $SL_2(\mathbb{C})$ -characters and the Kauffman bracket skein module’, *Comment. Math. Helv.* **72** (1997), 521–542.
- [BW11] F. Bonahon and H. Wong, ‘Quantum traces for representations of surface groups in $SL_2(\mathbb{C})$ ’, *Geom. Topol.* **15** (2011), 1569–1615.
- [CKM14] S. Cautis, J. Kamnitzer, and S. Morrison, ‘Webs and quantum skew Howe duality’, *Math. Ann.* **360** (2014), 351–390.
- [CL22] F. Costantino and T. T. Q. Lê, ‘Stated skein algebras of surfaces’, *J. Eur. Math. Soc.* **24** (2022), 4063–4142.
- [CTT20] A. Casella, D. Tate and S. Tillmann, ‘Moduli spaces of real projective structures on surfaces’, in *MSJ Memoirs*, vol. **38** (Mathematical Society of Japan, Tokyo, 2020).
- [Dou20] D. C. Douglas, ‘Classical and quantum traces coming from $SL_n(\mathbb{C})$ and $U_q(\mathfrak{sl}_n)$ ’, Ph.D. thesis, University of Southern California, 2020.
- [Dou21a] D. C. Douglas, ‘Points of quantum SL_n coming from quantum snakes’, *Algebr. Geom. Topol.* (to appear). <https://arxiv.org/abs/2103.04471>.
- [Dou21b] D. C. Douglas, ‘Quantum traces for $SL_n(\mathbb{C})$: the case $n = 3$ ’, 2021, <https://arxiv.org/abs/2101.06817>, 2021.
- [DS20a] D. C. Douglas and Z. Sun, ‘Tropical Fock–Goncharov coordinates for SL_3 -webs on surfaces I: construction’, 2020, <https://arxiv.org/abs/2011.01768>.
- [DS20b] D. C. Douglas and Z. Sun, ‘Tropical Fock–Goncharov coordinates for SL_3 -webs on surfaces II: naturality’, 2020, <https://arxiv.org/abs/2012.14202>.
- [FG06] V. V. Fock and A. B. Goncharov, ‘Moduli spaces of local systems and higher Teichmüller theory’, *Publ. Math. Inst. Hautes Études Sci.* **103** (2006), 1–211.
- [FG07a] V. V. Fock and A. B. Goncharov, ‘Dual Teichmüller and lamination spaces’, *Handbook of Teichmüller Theory* **1** (2007), 647–684.
- [FG07b] V. V. Fock and A. B. Goncharov, ‘Moduli spaces of convex projective structures on surfaces’, *Adv. Math.* **208** (2007), 249–273.

- [FKK13] B. Fontaine, J. Kamnitzer and G. Kuperberg, ‘Buildings, spiders, and geometric Satake’, *Compos. Math.* **149** (2013), 1871–1912.
- [Foc97] V. V. Fock, ‘Dual Teichmüller spaces’, 1997, <https://arxiv.org/abs/dg-ga/9702018>.
- [Fon12] B. Fontaine, ‘Generating basis webs for SL_n ’, *Adv. Math.* **229** (2012), 2792–2817.
- [FP14] S. Fomin and P. Pylyavskyy, ‘Webs on surfaces, rings of invariants, and clusters’, *Proc. Natl. Acad. Sci. USA* **111** (2014), 9680–9687.
- [FP16] S. Fomin and P. Pylyavskyy, ‘Tensor diagrams and cluster algebras’, *Adv. Math.* **300** (2016), 717–787.
- [FS22] C. Frohman and A. S. Sikora, ‘ $SU(3)$ -skein algebras and webs on surfaces’, *Math. Z.* **300** (2022), 33–56.
- [FZ02] S. Fomin and A. Zelevinsky, ‘Cluster algebras. I. Foundations’, *J. Amer. Math. Soc.* **15** (2002), 497–529.
- [GHKK18] M. Gross, P. Hacking, S. Keel and M. Kontsevich, ‘Canonical bases for cluster algebras’, *J. Amer. Math. Soc.* **31** (2018), 497–608.
- [GMN13] D. Gaiotto, G. W. Moore and A. Neitzke, ‘Spectral networks’, *Ann. Henri Poincaré* **14** (2013), 1643–1731.
- [GS15] A. B. Goncharov and L. Shen, ‘Geometry of canonical bases and mirror symmetry’, *Invent. Math.* **202** (2015), 487–633.
- [GS18] A. B. Goncharov and L. Shen, ‘Donaldson–Thomas transformations of moduli spaces of G -local systems’, *Adv. Math.* **327** (2018), 225–348.
- [GS19] A. B. Goncharov and L. Shen, ‘Quantum geometry of moduli spaces of local systems and representation theory’, 2019, <https://arxiv.org/abs/1904.10491>.
- [Hig23] V. Higgins, ‘Triangular decomposition of SL_3 skein algebras’, *Quantum Topol.* **14** (2023), 1–63.
- [Hit92] N. J. Hitchin, ‘Lie groups and Teichmüller space’, *Topology* **31** (1992), 449–473.
- [HP93] J. Hoste and J. H. Przytycki, ‘The $(2, \infty)$ -skein module of lens spaces; a generalization of the Jones polynomial’, *J. Knot Theory Ramifications* **2** (1993), 321–333.
- [HS23] Y. Huang and Z. Sun, ‘McShane identities for higher Teichmüller theory and the Goncharov–Shen potential’, *Mem. Amer. Math. Soc.* **286** (2023).
- [IK22] T. Ishibashi and S. Kano, ‘Unbounded sI_3 -laminations and their shear coordinates’, 2022, <https://arxiv.org/abs/2204.08947>.
- [IY23] T. Ishibashi and W. Yuasa, ‘Skein and cluster algebras of unpunctured surfaces for sI_3 ’, *Math. Z.* **303** (2023).
- [Kim20] H. K. Kim, ‘ SL_3 -laminations as bases for PGL_3 cluster varieties for surfaces’, *Mem. Amer. Math. Soc.* (to appear), 2020, <https://arxiv.org/abs/2011.14765>.
- [Kim21] H. K. Kim, ‘Naturality of SL_3 quantum trace maps for surfaces’, 2021, <https://arxiv.org/abs/2104.06286>.
- [KQ19] J. Korinman and A. Quesney, ‘Classical shadows of stated skein representations at roots of unity’, *Algebr. Geom. Topol.* (to appear), 2019, <https://arxiv.org/abs/1905.03441>.
- [KT99] A. Knutson and T. Tao, ‘The honeycomb model of $GL_n(\mathbb{C})$ tensor products. I. Proof of the saturation conjecture’, *J. Amer. Math. Soc.* **12** (1999), 1055–1090.
- [Kup96] G. Kuperberg, ‘Spiders for rank 2 Lie algebras’, *Comm. Math. Phys.* **180** (1996), 109–151.
- [Lab06] F. Labourie, ‘Anosov flows, surface groups and curves in projective space’, *Invent. Math.* **165** (2006), 51–114.
- [Le16] I. Le, ‘Higher laminations and affine buildings’, *Geom. Topol.* **20** (2016), 1673–1735.
- [Mag20] T. Magee, ‘Littlewood–Richardson coefficients via mirror symmetry for cluster varieties’, *Proc. Lond. Math. Soc.* **121** (2020), 463–512.
- [Mar19] G. Martone, ‘Positive configurations of flags in a building and limits of positive representations’, *Math. Z.* **293** (2019), 1337–1368.
- [MFK94] D. Mumford, J. Fogarty and F. Kirwan, *Geometric Invariant Theory*, Third ed. (Springer-Verlag, Berlin, 1994).
- [NY22] A. Neitzke and F. Yan, ‘The quantum UV-IR map for line defects in $gl(3)$ -type class S theories’, *J. High Energy Phys.* **2022** (2022), 1–51.
- [Pro76] C. Procesi, ‘The invariant theory of $n \times n$ matrices’, *Adv. Math.* **19** (1976), 306–381.
- [Sik01] A. S. Sikora, ‘ SL_n -character varieties as spaces of graphs’, *Trans. Amer. Math. Soc.* **353** (2001), 2773–2804.
- [Sik05] A. S. Sikora, ‘Skein theory for $SU(n)$ -quantum invariants’, *Algebr. Geom. Topol.* **5** (2005), 865–897.
- [SW07] A. S. Sikora and B. W. Westbury, ‘Confluence theory for graphs’, *Algebr. Geom. Topol.* **7** (2007), 439–478.
- [SWZ20] Z. Sun, A. Wienhard and T. Zhang, ‘Flows on the $PGL(V)$ -Hitchin component’, *Geom. Funct. Anal.* **30** (2020), 588–692.
- [Xie13] D. Xie, ‘Higher laminations, webs and $\mathcal{N} = 2$ line operators’, 2013, <https://arxiv.org/abs/1304.2390>.